

HADAMARD TRANSFORM AND PROGRAMMED SCAN
MULTIELEMENT ANALYSIS - MULTIPLEX VERSUS
SINGLE CHANNEL ATOMIC FLUORESCENCE SPECTROMETRY

By

FRANCIS WILLIAM PLANKEY, JR.

A DISSERTATION PRESENTED TO THE GRADUATE COUNCIL OF
THE UNIVERSITY OF FLORIDA
IN PARTIAL FULFILLMENT OF THE REQUIREMENTS FOR THE DEGREE OF
DOCTOR OF PHILOSOPHY

UNIVERSITY OF FLORIDA

1974

This work is dedicated to my wife, Bonnie, who encouraged and supported me in many, many ways and who spent lonely, patient hours in order to make this work and my graduate program a success.

ACKNOWLEDGMENTS

The author wishes to acknowledge the outstanding assistance of his teachers and associates, especially the help and guidance of Professor Sidney Siggia during the early years and Professor James D. Winefordner during Graduate School. The enthusiasm and encouragement of these latter two persons was the driving force of his academic work. Furthermore, he would like to thank Dr. Dave Johnson, Lucas Hart and Gail Pokrant for their help in many instances.

TABLE OF CONTENTS

| | Page |
|--|------|
| ACKNOWLEDGMENTS | iii |
| ABSTRACT | vi |
| Chapter | |
| I INTRODUCTION TO FLAME SPECTROMETRY AND MULTIELEMENT ANALYSIS | 1 |
| Atomic Methods of Analysis | 1 |
| Single Element Analysis | 2 |
| Multielement Analysis | 3 |
| II MULTIPLEX SPECTROMETRY SYSTEMS | 5 |
| Types of Multiplex Spectrometry | 5 |
| Previous Spectroscopic Studies with Multiplex Methods. | 6 |
| Signal-to-Noise Relationships for UV-Visible HTS | 8 |
| III ATOMIC FLUORESCENCE COMPONENTS COMMON TO THE SYSTEMS STUDIED | 15 |
| The Atomic Fluorescence Excitation Source | 15 |
| The Atomization Cell | 16 |
| The Optical System | 20 |
| IV THE HADAMARD TRANSFORM SPECTROMETER (HTS) SYSTEM | 24 |
| Hadamard Transform Spectrometry | 24 |
| Implementation of the HTS System | 25 |
| The Fast Hadamard Transform (FTS) | 30 |
| Analytical Procedure with the HTS System | 34 |
| Results and Discussion | 36 |

| Chapter | Page |
|--|------|
| V SINGLE CHANNEL SCANNING SPECTROMETER (SCSS) SYSTEM . . . | 49 |
| Preliminary Discussion | 49 |
| Description of SCSS Experimental Setup | 50 |
| Operation of the SCSS System | 56 |
| Analytical Procedure with the SCSS System | 57 |
| Results and Discussion | 59 |
| VI COMPARISON OF MULTIPLEX AND SCANNING TECHNIQUES | 77 |
| VII PROGRAMMED SLEW SPECTROMETER (PSS) SYSTEM | 82 |
| Preliminary Discussion | 82 |
| Description of Software | 83 |
| Analytical Procedure with the PSS System | 84 |
| Results and Discussion | 86 |
| VIII COMPARISON OF THE THREE SYSTEMS | 90 |
| APPENDICES | |
| I AVERAGE SIGNAL-TO-NOISE RATIOS FOR THE UV-VISIBLE SPECTRAL REGION | 93 |
| II THE COMPUTER SYSTEM | 95 |
| LITERATURE CITED | 100 |
| BIOGRAPHICAL SKETCH | 103 |

Abstract of Dissertation Presented to the Graduate Council
of the University of Florida in Partial Fulfillment of the Requirements
for the Degree of Doctor of Philosophy

HADAMARD TRANSFORM AND PROGRAMMED SCAN MULTIELEMENT
ANALYSIS - MULTIPLEX VERSUS SINGLE CHANNEL
ATOMIC FLUORESCENCE SPECTROMETRY

By

Francis William Plankey, Jr.

August, 1974

Chairman: James D. Winefordner

Major Department: Chemistry

The practice of sequential analysis for many trace elements by flame spectrometry is explained and techniques for rapid sequential and simultaneous multielement analysis are reviewed. Consideration of the three flame spectrometric techniques, atomic emission, atomic absorption and atomic fluorescence, leads one to the conclusion that the latter is most suitable for multielement work. A description of, and justification for using, a xenon arc continuum source and an argon separated air/acetylene flame for multielement analysis are discussed.

Multiplex spectrometry is explained and types of multiplex methods for simultaneously coding many spectral intervals at a detector are covered. Results of the application of multiplex methods with the advantage derived from multiplexing are presented. Of the three multiplexing techniques, Fourier transform, frequency correlation and

Hadamard transform, only the latter has been chosen for implementation in this work. Signal-to-noise relationships are investigated for the multiplex and the single channel cases, and example calculations are shown.

A description of the 255 spectral interval Hadamard transform spectrometer (HTS) covering about 25 nm in about 25 s, and the software for performing the transform is presented followed by a description of the analytical procedure and the results obtained for Ni, Co, Fe, Mn, Mg, Cu, Ag and Cr analysis. Spectra and estimates of the limits of detection are given for these elements.

The construction and operation of a computer controlled single channel scanning spectrometer (SCSS) is described, and the results for the analysis of those elements done with the HTS plus Zn, Cd, Au, Pb, Sn and Tl are presented. Next, a comparison of the results of analyses of the two methods is made, and the cause of the serious disadvantage of the multiplex method, based on proportional noise in the system, is proposed. The results indicate that in the case of atomic fluorescence flame spectrometry, the large background signal results in a factor of about 100 times poorer signal-to-noise ratio for the HTS system as compared to the SCSS when the scanning times are equivalent.

Using the same equipment as in the SCSS, it is possible to slew rapidly between intervals of interest and thereby spend more time measuring analytically useful wavelengths. The S/N increase, proportional to the measuring time, is demonstrated, and the improved limits of detection for 13 elements are compared with the SCSS limits.

CHAPTER I

INTRODUCTION TO FLAME SPECTROMETRY AND MULTIELEMENT ANALYSIS

Atomic Methods of Analysis

Flame spectrometric techniques have become the most widely used methods for the determination of trace quantities of metals in solution. Atomic emission spectrometry (AES) has been reviewed by Pickett and Koirtzohann (1), atomic absorption spectrometry (AAS) has been described by Lewis (2) and atomic fluorescence spectrometry (AFS) has been explained by Winefordner and Elser (3). The three techniques have been critically compared by Winefordner, Svoboda and Cline (4).

Each of the flame techniques measures the interaction or emission of electromagnetic radiation by ground state or excited state atoms. In AES, the excitation of ground state atoms is by thermal means in a flame. The excited atoms emit light of a characteristic (for each element) frequency, and the intensity of the light is directly proportional to the concentration of atoms in the flame. In AAS, the ground state atoms in the flame absorb radiation (from a suitable source) of a certain frequency, characteristic of the element. The amount of light absorbed is proportional to the concentration of the specified element in the flame cell. In AFS, a light source is also used but in this case, the radiation is used to excite ground state atoms in a flame. These

radiationally excited atoms emit characteristic radiation and the intensity of fluorescence is proportional to the concentration of atoms in the flame cell.

Conventionally, the three techniques differ substantially only in the mechanism of excitation of the atomic species; otherwise, they share much of the same instrumentation. Usually, a dispersive device (monochromator) is used to isolate the characteristic radiation of interest and a photomultiplier/amplifier/readout detection system is used to produce a signal proportional to the radiant flux striking the photocathode and thus proportional to the intensity of the emission, fluorescence or absorption. More detailed descriptions of flame techniques are available in books by Mavrodineanu (5) and Hermann and Alkemade (6).

Single Element Analysis

The usual procedure in the analysis of several metals in several samples is as follows. The monochromator dispersing element, usually a grating, is positioned so that a spectral line of the first element of interest is isolated at the detector. A blank solution, and a series of standard solutions containing known concentrations of the first element, are then aspirated into the flame, and the appropriate intensity readings are recorded. The concentration range should include or bracket the concentration of the unknowns. If such a concentration range cannot be determined immediately then dilution of the sample and subsequent analyses are generally necessary. Each of the unknown samples is then aspirated and the corresponding intensity readings are recorded. After the analytical curve of intensity (corrected for blank) vs. concentration is constructed, the concentration of the first element in each sample is

determined from its intensity value on this curve. The next element is selected, the monochromator is scanned to the appropriate wavelength and the next characteristic frequency spectral line is isolated. The procedure is repeated for each element.

Multielement Analysis

Recently, there has been much effort expended to develop multielement techniques with which many elements can be determined simultaneously or in rapid sequence. The longest established multielement technique has involved the use of the photographic emulsion detector. Because this method is very slow and usually requires a subsequent scanning of the plate, photographic detection has been bypassed as a viable system by most flame spectroscopists. Recently, Busch and Morrison (7) reviewed multielement systems. Types of detection systems which have been investigated include scanning monochromators (8-12), movable detector (13), non-dispersive rotating filter detector (14), sequentially pulsed source AFS (15), direct reading spectrographs (16-19) and imaging devices (20-26).

For detector-noise limited situations, as in the infrared (IR) spectral region, multiplex methods have been used to increase the signal-to-noise ratio and to decrease the analysis time. Speculation about the use of a multiplex method (7,24,27), such as Fourier transform or Hadamard transform spectrometry, in the ultraviolet (UV) region has led to the present study of the comparison of multiplex and single channel methods in multielement atomic fluorescence spectrometry.

Each of the three atomic techniques, AES, AAS and AFS, has been used by various researchers for multielement analysis. Each technique has certain advantages and certain disadvantages. The instrumental

system for AES requires no light source and is quite simple. A flame atomizer supplies sufficient energy to excite most elements whose resonant lines lie above about 350.0 nm (4). However, the spectrum of many elements is very complex in this spectral region and a good high resolution monochromator is necessary. Also, some elements do not have resonance lines which can be excited by the thermal energy present in analytical flames. Recent developments in induction coupled plasmas (28) may improve this excitation energy problem but AES is presently limited in multielement analytical flame spectrometry.

In AAS, almost every metallic element can be measured at trace quantities. The source need not be extremely intense since the measured quantity in AAS is the attenuation of the source intensity by the absorbing atoms. However, the radiation must be directed from the source through the flame and into the dispersive system. In order to avoid very complex optical arrangements, one source must then be used for multiple elements. This is a severe limitation because commercially available AAS sources are limited to about six elements.

In AFS, an intense source of radiation is required for the radiational excitation of the atoms in the flame. If such a source is available, AFS becomes the technique of choice because fluorescence spectra are relatively uncomplicated compared with those in AES and no optical geometry problems are present because fluorescence is emitted in all directions and a non-180° source-flame-monochromator optical alignment is suitable. Because AFS has these advantages, it alone was studied in this project.

CHAPTER II

MULTIPLEX SPECTROMETRY SYSTEMS

Types of Multiplex Spectrometry

Normal single channel spectrometer systems measure the intensity in one spectral interval at a time. Three "multiplexed methods" have been devised to measure the intensities of more than one spectral interval at the same time with one detector. Each of these multiplex methods uses a coding device to enable the transformation of the total intensity into the intensities at the individual spectral intervals.

In Fourier transform multiplex spectroscopy, a Michelson interferometer is used to encode the high frequency electromagnetic radiation used in spectroscopy into an audio frequency interferogram (29). In this system, all of the spectral intervals, over a wavelength region determined only by optics and detector, are multiplexed on the detector. A computer is used to perform a Fourier transform of the coded interferogram to decode the intensity versus mirror displacement signal to an intensity versus wavelength spectrum. This technique has found wide application in the infrared (IR) spectral region. Low (30-33) has written an excellent review of Fourier transform spectrometry (FTS).

A second type of multiplex method can be based on the modulation of line sources at different frequencies. If signals due to the sources

are allowed to fall on a single detector, each of the wavelengths in the sources will be frequency coded and multiplexed (34). The individual wavelength intensities can be recovered either by locking-in on their modulation frequency or, alternatively, by performing a Fourier transformation. This type of correlation spectrometry can only be used in analyses where line excitation sources are used such as AAS or AFS. No published results of this type of system are available at the present time.

In the third multiplex method, a normal grating system is used to disperse a wavelength region onto a specially constructed mask which allows some spectral interval intensities to pass onto the detector while blocking some other intensities. In this way, an equation relating the total intensity (or the flux reaching the detector) to a linear combination of the separate spectral interval intensities (fluxes reaching the detector) is formed. A series of linearly independent equations is formed for example when the mask is constructed in a manner related to mathematical Hadamard matrices, and so this method is called Hadamard transform spectrometry (HTS). HTS thus codes a specific wavelength region in a binary, on (intensity passed) or off (intensity blocked), fashion. A computer program is used to solve the set of simultaneous equations formed in the HTS process. A review of HTS principles and application in the IR spectral region can be found in articles by Ibbett, Aspinall and Grainger (35), Decker and Harwit (36) and Nelson and Fredman (37).

Previous Spectroscopic Studies with Multiplex Methods

Of these three multiplex methods discussed in the previous section, only the first and third have been previously used in

spectroscopic studies. Commercial instruments are available for FTS and HTS in the IR region. The utility of these multiplex methods in the IR is a result of the signal-to-noise (S/N) advantage. Fellgett (38) has shown that in a detector-noise limited case (such as IR spectrometry), a signal-to-noise ratio increase can be expected. The so-called Fellgett, or multiplex, advantage is the ratio of the S/N of the multiplex method to the S/N of a single channel (slit) system and is given by

$$F = \frac{(S/N)_m}{(S/N)_{sc}} = N^{\frac{1}{2}}$$

where N is the number of spectral intervals multiplexed on the detector.

$$N = \frac{\lambda_2 - \lambda_1}{\delta\lambda}$$

λ_1 and λ_2 are the extremes of the wavelength range reaching the detector and $\delta\lambda$ is the bandpass of the spectral interval. In FTS, $\delta\lambda$ depends on the displacement increment of the mirror while in HTS, $\delta\lambda$ depends on the dimensions (size of a unit slit) of the Hadamard mask. In either case, N usually ranges from a few hundred to a few thousand.

The Fellgett advantage is calculated using equal analysis time for the single channel (slit) and the multiplex system. If, on the other hand, it is desired to maintain the same signal-to-noise ratio in both systems, the increase in analysis speed is directly proportional to N for the multiplex methods. It is this factor which led to the investigation of the use of a multiplex method for atomic analysis in the ultraviolet (UV)

spectral region, in a desire to be able to rapidly scan a fairly wide wavelength region with good resolution.

FTS systems utilize an interferometer to transform radiation, e.g., frequencies of $\sim 10^{14}$ Hz, to an interferogram, e.g., frequencies of $\sim 10^2$ Hz. Interferometric methods are adaptable without tremendous problems to the IR and near IR regions, where wavelengths are of the order of fractions of a mm to a few μm . Because alignment procedures in interferometry require tolerances of a fraction of the wavelength of the light being observed, it is quite difficult to achieve stable interferometry in the 200-700 nm region of the spectrum. For this reason, FTS has not been evaluated for multielement atomic analysis.

Correlation spectroscopy has recently been discussed, but since it is limited to use with line sources and requires individual modulation for each element to be analyzed, it has not yet been studied.

The HTS method uses well-developed dispersion technology and requires only machine shop tolerances. It is capable of retrofit into existing monochromator systems, and only a Hadamard mask is needed to implement the system. The HTS system was therefore chosen for investigation of the use of a multiplexing technique to decrease analysis time in multielement atomic analysis.

Signal-to-Noise Relationships for UV-Visible HTS

The Fellgett advantage is only applicable to multiplex systems in which the major source of noise is in the detector. In other words, the advantage is only realized in systems where the noise does not increase with an increase in the signal reaching the detector. This is the case in the IR region where only noisy detectors (high noise equivalent sources) are available. In the UV-visible region, photomultiplier

detectors of very low noise are used and the major source of noise is the quantum noise or shot noise of the source. This type of noise bears a square root dependence on the total signal; it is due to the random arrival of photons at the detector. No gain in S/N can be expected from the Fellgett advantage for multiplex methods in the UV-visible region if the S/N is averaged over the entire wavelength region measured (39).

(See Appendix I for a proof of this statement.)

A single channel scanning spectrometer (SCSS) system which covers N spectral intervals in T seconds will measure each interval for T/N seconds. The signal in that time will be proportional to the number of photons incident on the photomultiplier tube, I , and the time, T , and so will be IT/N . Assuming that shot noise is the dominant noise, the noise will be the square root of the signal. (The signal-noise relationship follows a Poisson distribution, where the standard deviation of the population is equal to the square root of the mean of the population.) Now, the signal-to-noise for one spectral interval will be $(IT/N)/(IT/N)^{\frac{1}{2}} = (IT/N)^{\frac{1}{2}}$. Therefore, the S/N ratio depends only on the signal which is involved with the particular spectral interval of interest and is independent of the signals in other spectral intervals.

There are three limiting cases which are useful for comparing HTS in the UV-visible region with the SCSS:

First, the case of one line falling in one spectral interval will be considered. This single line, of flux I , will be allowed to pass to the detector for $(N+1)/2$ separate measurements and will be summed each time. With the assumption of no background, the other $(N-1)/2$ measurements will have no intensity reaching the detector. The total signal from the line, of intensity I , will be $IT(N+1)/2N$ and the signal-to-noise is thus $(IT(N+1)/2N)^{\frac{1}{2}}$ (still assuming only shot noise).

The gain in signal-to-noise at the spectral interval of interest, due to the longer observation time, is then given by

$$G = \frac{(S/N)_{HTS}}{(S/N)_{SCSS}} = \frac{[IT(N+1)/2N]^{\frac{1}{2}}}{[IT/N]^{\frac{1}{2}}} = \left[\frac{N+1}{2} \right]^{\frac{1}{2}}.$$

This advantage is essentially the same as the Fellgett advantage for HTS in the IR (37). It should be pointed out that the noise of all the N spectral intervals is exactly the same as the noise associated with the spectral interval which contains the single spectral line and, again assuming no background, this noise would now cause the baseline to fluctuate around a level of zero in the other $N-1$ spectral intervals. Therefore, the average $(S/N)_{HTS}$ is exactly equal to the average $(S/N)_{SCSS}$ and there is no average advantage. However, in the SCSS case almost all of the noise is associated with the line peak, and the baseline thus has little noise. In the HTS, the noise is distributed evenly over the entire spectrum, and therefore the peak signal has less noise in the HTS than in the SCSS, and the baseline signals have less noise in the SCSS. This is true in any case where the HTS has an advantage and the advantage is only associated with the peak signals.

The second case of interest involves the S/N relationship of a weak line in the presence of a strong line. In this case, the noise in each spectral interval will essentially be due to the noise from the strong line. Thus, the S/N of the weak line will be equal to the S/N of the strong line divided by the ratio of intensity of strong line to intensity of weak line. In the case of two lines of intensity ratio $(N+1)/2$ to 1 or greater, the S/N of the weak line would be the same or

better in the SCSS system as in the HTS system. This degradation of the S/N is called the multiplex disadvantage and results when two or more dissimilar signals are measured simultaneously with one detector. If the noise is related to the total signal at the detector, the multiplex disadvantage will degrade the S/N of very small signals in the presence of very large signals.

The third case is somewhat more realistic since a background, I^B , is now considered at all of the spectral intervals observed by HTS. At all N mask positions approximately $N/2$ slots allow the background to pass and at $(N+1)/2$ positions the line of interest with intensity I_j^S is also passed. The total signal, I_{THTS} , which will be summed will be

$$I_{THTS} = \frac{N+1}{2} I_j^S + N \sum_{i=1}^{\frac{N+1}{2}} I_i^B$$

The shot noise figure associated with this signal will be

$$N_{HTS} = \left[\frac{N+1}{2} I_j^S + N \sum_{i=1}^{\frac{N+1}{2}} I_i^B \right]^{\frac{1}{2}}$$

Since the signal of interest is still $\frac{N+1}{2} I_j^S$ the S/N ratio in the HTS system is given by

$$(S/N)_{HTS} = \frac{\frac{N+1}{2} I_j^S}{\left[\frac{N+1}{2} I_j^S + N \sum_{i=1}^B I_i^B \right]^{\frac{1}{2}}}$$

In the SCSS, the signal of interest is given by I_j^S while the total signal is

$$I_{TSCSS} = I_j^S + I_j^B$$

The noise is then $(I_j^S + I_j^B)^{\frac{1}{2}}$ and the S/N ratio is

$$(S/N)_{SCSS} = \frac{I_j^S}{(I_j^S + I_j^B)^{\frac{1}{2}}}$$

The gain in S/N at the line peak is then

$$G = \frac{(S/N)_{HTS}}{(S/N)_{SCSS}} = \frac{\frac{N+1}{2} \left[I_j^S + I_j^B \right]^{\frac{1}{2}}}{\left\{ \frac{N+1}{2} \left[I_j^S + N \bar{I}_1^B \right] \right\}^{\frac{1}{2}}}$$

where \bar{I}_1^B is the average background intensity,

$$\bar{I}_1^B = \frac{\sum_{i=1}^{(N+1)/2} I_i^B}{\frac{N+1}{2}}$$

Evaluating the limiting cases shows that if the average background is small compared to the intensity of the line of interest ($\bar{I}_1^B \ll I_j^S$) then G reduces to $[(N+1)/2]^{\frac{1}{2}}$ as in the first case considered.

Otherwise, if $I_j^S \ll \bar{I}_1^B$ then G becomes $1/\sqrt{2}$. In this circumstance the HTS system is worse by a factor of 0.7 compared with the SCSS.

In the previous exercise, only shot noise (or quantum noise) was considered and noise which is proportional to the background (flicker noise from a flame for example) or to the source (i.e., ripple noise in an AFS source) was neglected. Instrumentation has been developed to minimize the effects of these types of noises but even the best instrumental system may allow some small part of this so-called "proportional" noise. This noise is characterized by being directly proportional to the total signal which is associated with the noise. For low level signals the few percent proportional noise is usually negligible compared to the square root relationship shot noise. However, in the HTS system, with a significant background at each spectral interval the total influence of an average background of \bar{I}_1^B at each interval is $\frac{N^2 + N}{2} \bar{I}_1^B$ compared with \bar{I}_1^B contribution in the SCSS. This factor of $(N^2 + N)/2$ would almost certainly cause the majority of noise in the Hadamard system to be due to proportional noise if the background is significant.

To illustrate the concepts of this chapter it is instructive to examine a possible example in multielement AFS by the two methods. Consider the use of photon counting. Also, consider that the background consists of 1000 counts accumulated in each spectral interval for the counting period and that two lines of 100 counts and 5000 counts per measurement interval are to be determined in the same analysis time, by the HTS and SCSS system (255 spectral intervals are to be measured in 25.5 seconds).

The SCSS will measure each spectral interval for 0.1 s and will accumulate 1000 counts for each spectral interval while measuring the background alone and 1100 and 6000 counts while measuring the line peak spectral intervals. The shot noise on 1000 counts is about 32 and the shot noises at the lines plus background are about 33 and 77 respectively. If proportional noise is all due to the background and is 1.0% then proportional noise is 10 counts at each channel. Shot noise is thus dominant, and the $(S/N)_{SCSS}$ of the weak and strong lines are 3.0 and 64.5 respectively.

Now, for the HTS, the background is measured at 128 spectral intervals (on the average) and is summed for each channel 255 times. The lines are summed 128 times. The shot noise associated with each spectral interval is thus

$$((255)(128)(1000) + (128)(100) + (128)(5000))^{\frac{1}{2}}$$

or 5770. The signal for the first line is measured 128 times and so is 12800; the second line signal is 640000. From shot noise considerations, the $(S/N)_{HTS}$ of the first line is then 2.2 and the second line is 111. However, if proportional noise is 1% of the background level then for 128 spectral intervals the proportional noise is 1280 counts. This noise is independently measured 255 times, and therefore the proportional noise is

$$((255)(1280)^2)^{\frac{1}{2}} = 20440.$$

Noise values add quadratically and so the total noise in the HTS system is

$$((5770)^2 + (20440)^2)^{\frac{1}{2}} = 21239$$

Now the $(S/N)_{HTS}$ for the two lines is reduced to 0.6 and 30, a factor of 5, and 2.2 times worse for the two lines by HTS as compared with the SCSS.

It can be seen that in a real system, the scanning technique might be shot noise limited while the multiplex technique may suffer tremendous losses in S/N because of proportional noise.

CHAPTER III

ATOMIC FLUORESCENCE COMPONENTS COMMON TO THE SYSTEMS STUDIED

The Atomic Fluorescence Excitation Source

In recent years, most AFS workers have been using intense line sources of excitation. Metal vapor discharge lamps (MVL's) (40,41), hollow cathode lamps (HCL's) (42,43), electrodeless discharge lamps (EDL's) (44,45) and, more recently, tunable dye lasers (TDL's) (46) have been shown to be excellent single element AFS sources. In most cases, these sources have to be tuned, adjusted or thermostated for optimum performance for one specific element. The results obtained thereby are quite good for most elements - limits of detection range from a few hundred ng/ml down to fractions of a ng/ml for more than 30 elements (3).

Some attempts have been made to use multielement HCL's (47) and especially multielement EDL's (48) as AFS sources. Combination problems and optimization trade-offs have severely limited use of multielement sources in multielement AFS (49). If single element sources are used in multielement AFS each must be individually powered and adjusted for optimum conditions. Furthermore, the spatial arrangement of such a situation becomes difficult if more than 4 to 6 sources are to be used.

Continuum sources have been used in the past (50-53) with some success. Workers note two difficulties with continuum sources: the spectral

radiance of xenon arcs falls off rapidly below about 250 nm (where many useful resonance lines occur), and scattering by the incompletely vaporized particles in the flame leads to high backgrounds and thus to poorer detection limits when compared to intense line sources. Despite these shortcomings, the xenon arc lamp appears to be the source of choice in multielement AFS at the present time for three reasons: first, although the lamp's output drops off below 250 nm, some fraction of the output is still available down to about 200 nm (see Figure 1) allowing excitation of just about every element of interest; secondly, only one source is necessary, which simplifies the front-end geometrical arrangement, e.g., even if six-element combination sources (as EDL's) could be made, still five source/power supplies, lens/chopper systems would be needed to allow excitation of 30 elements, compared with one continuum source with one power supply; finally, the continuum source is convenient to operate, requires only minimal adjustment and is stable after a few minutes warm up time, as shown in Figure 2. The particular continuum lamp used in this study is a high pressure, short arc xenon lamp with an internal aluminum parabolic reflector. The manufacturer claims that this lamp collimates 85% of the total arc output and uses a sapphire window for output down to at least 200 nm.

The Atomization Cell

Flames are the most common atomizers for present-day atomic spectroscopy. A sample is aspirated into a flame, usually with a premixed, laminar flow burner, where the solvent is evaporated, and the solute vaporized and atomized by the thermal action of the flame. Much of the previous work in AFS has made use of the low quenching combustible gases such as oxyhydrogen or hydrogen-air diffusion flames; molecular

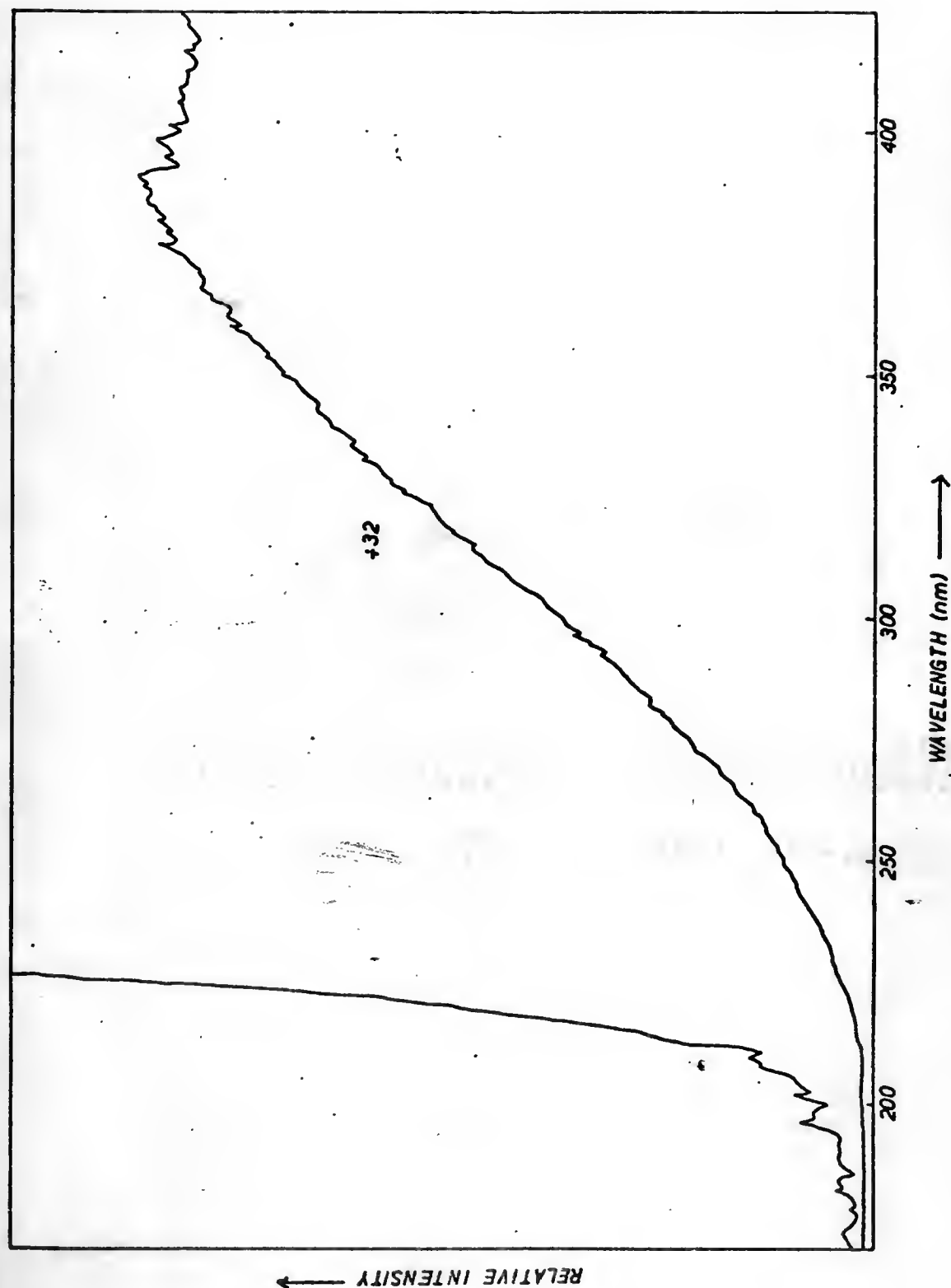


Figure 1.-- Spectral output of the xenon arc continuum lamp used in this study. The lower curve has been scaled down by a factor of 32.

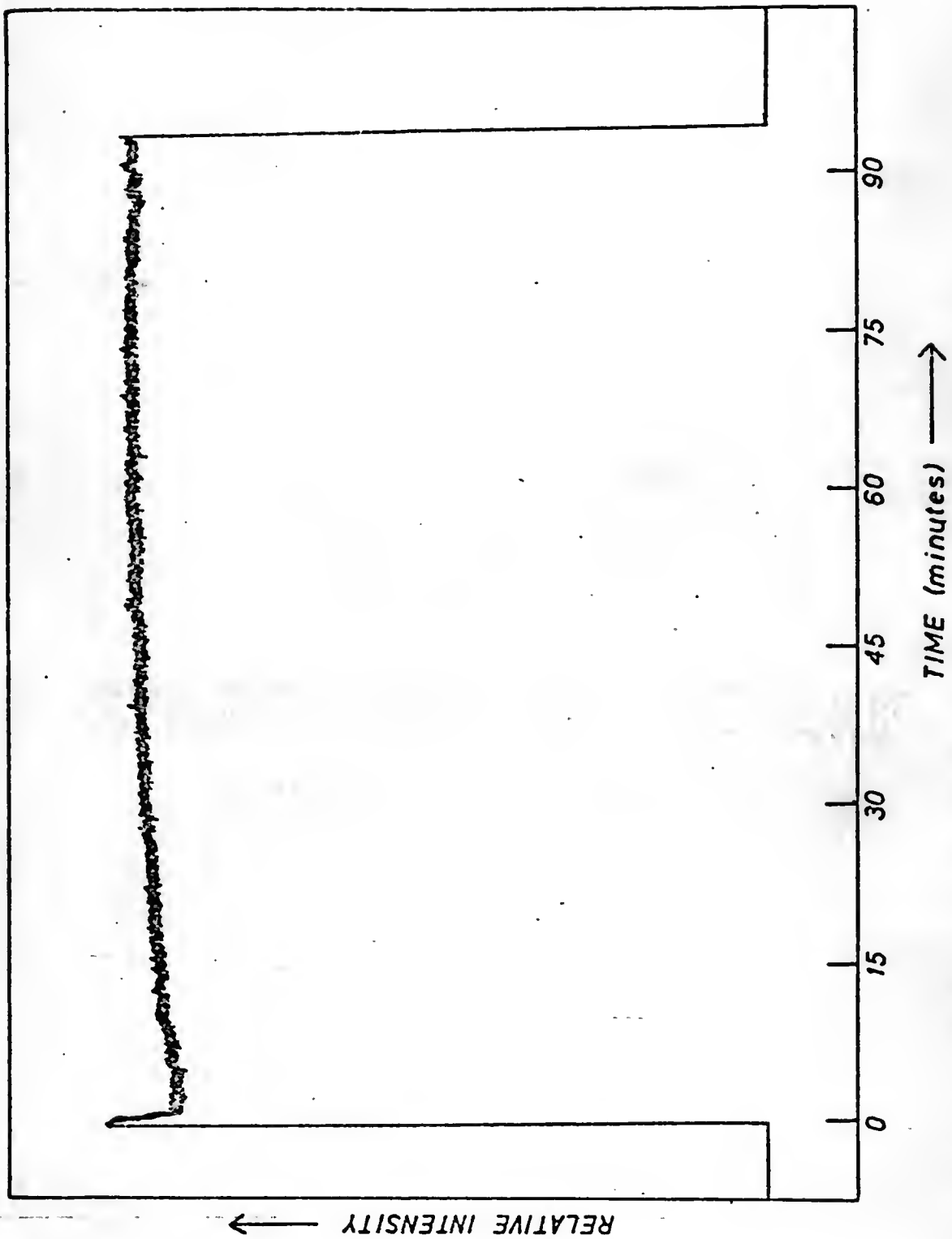


Figure 2.-- Time-stability of the Xenon Arc Continuum Lamp used in this study.

species such as CO and CO₂ enhance the non-radiational deactivation (quenching) of excited atoms in the flame. The hydrogen flames are also much cooler than hydrocarbon flames and have higher burning velocities and therefore the desolvation, vaporization and atomization processes, which are very necessary to avoid scattering of the continuum source radiation, are not as efficient. The use of the cooler hydrogen flame and real samples necessitates a scatter correction even when used with line sources (54).

In order that the multielement systems investigated would have maximum versatility, the higher temperature air/acetylene flame was used for all of the AFS work in this study. Although the quenching species in this flame, together with a higher background, could mean a factor of 5 to 100 lower (poorer) fluorescence quantum yields, the flame proved to be an excellent atomization source and no noticeable scatter was observed even when aspirating solutions with more than 500 µg/ml of solids.

The flame was produced by a premixed nebulizer/burner assembly together with a capillary type burner head (55). The flame was separated by an argon sheath. The fuel/air flow rates were established so that the flame was slightly fuel-rich; the cones above the capillaries were somewhat "fuzzy" and had some noticeable yellow color. This fuel/air ratio led to the lowest background and allowed good atomization of all of the elements studied. Some improvement might be possible if the flame were changed to maximize the S/N for each individual element, but this would have been too complicated for the present study and so was not attempted. The flow rate for acetylene was 1.5 l min⁻¹, for air 9.7 l min⁻¹ and for argon 15.5 l min⁻¹ as measured with a wet test meter.

The Optical System

The front-end optics and source/atomizer were the same in all of the work described later in this study. The source was focused through a chopper operated at about 50 Hz. The chopped radiation was collected by a lens and focused into the flame. On the other side of the flame a 140 mm diameter, UV enhanced mirror with a 62 mm focal length focused the source radiation back into the flame. At right angles to the source light path, a lens collected the fluorescence and formed a 1:1 image of the flame at the entrance slit of the monochromator. All of the lenses used were of fused quartz. Figure 3 shows a block diagram of the front-end arrangement used throughout this study, and Table 1 lists the components used and their sources.

Few problems were encountered with the present set-up. However, it should be stressed that the mirror behind the flame and in line with the source should not focus the exciting beam directly back into the continuum lamp because of the danger of overheating the source and destroying the lamp. A procedure involving slight defocusing of the mirror-source optics was adopted after the explosive destruction of a lamp. This procedure reduced the fluorescence signal by only 10-20%.

The major emphasis in this study was to develop and evaluate systems for multielement analysis. While doing this, it was also possible to compare multiplex and single channel methods in the UV-visible spectral region. Much of the equipment used throughout this study was exactly the same for both the Hadamard and programmed scan systems; however, in the multiplex system an analog detection system was used and in the single channel set-up a digital detection (photon counting) system was employed. This led to problems in a direct comparison of the Hadamard and scanning methods. The primary advantage of the digital

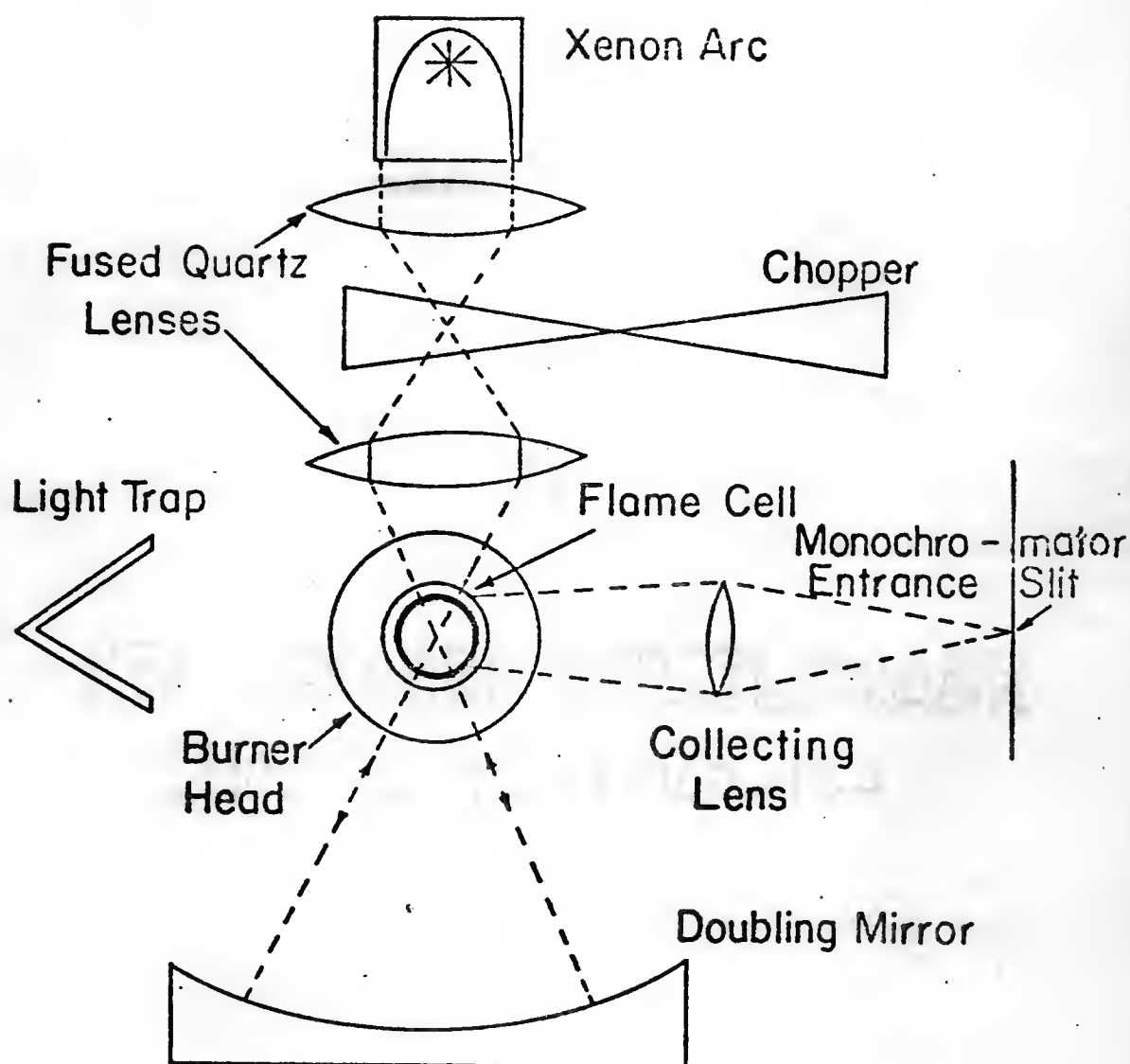


Figure 3.-- Atomic Fluorescence Source and Flame Cell Arrangement used throughout this study.

TABLE 1
COMPONENTS OF THE ATOMIC FLUORESCENCE
SOURCE AND FLAME CELL.

| <u>ITEM</u> | <u>DESCRIPTION (MODEL NUMBER)</u> | <u>SOURCE</u> |
|---|--|---|
| Xenon Arc Continuum and Power Supply | VIX-150-7UV | Eimac/Varian, San Carlos, CA 94070 |
| Nebulizer/Burner | 303-0110 | Perkin-Elmer, Norwalk, CT 06852 |
| Lenses | 2" diameter, 2 $\frac{1}{2}$ " focal length | ESCO Products, Oak Ridge, NJ 07438 |
| Doubling Mirror | 140 mm diameter, 62 mm focal length | Optical Industries, Inc., Costa Mesa, CA 92626 |
| Chopper | 46 Hz, 50% duty cycle | Laboratory fabricated. |

detection system was one of dynamic range. The analog system, coupled to a computer, allowed a dynamic range of only 1024 discrete levels. The photon counter has a dynamic range of about 10^7 . However, in this study a range of only 10^5 was normally used. The second advantage of the digital system is one of convenience, i.e., the photon counter needs no adjustment between ranges while the analog system had to be switched through different ranges.

So, although a comparison was sought, it was felt that the best system available should be developed with the equipment on hand. When the results are discussed (see Chapters IV and V) possible advantages due to the analog/digital detection systems will be noted.

CHAPTER IV

THE HADAMARD TRANSFORM SPECTROMETER (HTS) SYSTEM

Hadamard Transform Spectrometry

The multiplex method of Hadamard transform spectrometry (HTS) makes use of conventional grating spectrometer technology. In place of a single exit slit, which is used to isolate a narrow bandpass (spectral interval) region of the electromagnetic spectrum, a multi-slit mask is used to allow portions of a much wider spectral region to reach the detector. The mask is specially constructed to block some spectral intervals and allow others to pass. Therefore, the signal reaching the detector for a given mask position, i , is given by

$$Y_i = \sum_{j=1}^{j=N} a_{ij} X_j$$

where the a_{ij} 's ($j=1$ to N) are either 0 (if the light is blocked at spectral interval X_j) or 1 (if the light is allowed to pass at spectral interval X_j). When a set of N orthogonal equations is formulated with various combinations of a_{ij} 's, then the individual X_j 's can be determined by solving the set of simultaneous equations given by N intensity readings with N different mask configurations. Hadamard matrices give

the relationships necessary to form independent equations with a set of N different masks or, alternatively, a cyclic mask, constructed so that an orthogonal set of coefficients (a_{ij} 's) can be created by moving the mask one slot width N times at N positions to form the set of N equations.

Implementation of the HTS System

A cyclic mask can be designed for any N ($N = 2^n - 1$; n any integer) according to the method of primitive polynomials given by Nelson and Fredman (37).

For this work, $N = 2^8 - 1 = 255$ spectral intervals are covered at the exit focal plane. A cyclic mask would then have $2N - 1 = 509$ transparent (open) and opaque (closed) slots. The order of 1's (open slots) and 0's (closed slots) is determined once the first n (8 in this case) coefficients are given. The first 8 coefficients used for this mask were 10001110. The ninth coefficient can be found from the first eight coefficients by modulo 2 addition. (In mod 2 addition $0 + 0 = 0$, $1 + 0 = 1$, $0 + 1 = 1$ and $1 + 1 = 0$ with carry = 1.) Now, if the first, third, fourth and fifth coefficients are added, mod 2, the result is the ninth coefficient. Thus the ninth coefficient is $1 + 0 + 0 + 1 = 0$. Each subsequent coefficient can be determined from the previous eight coefficients in this same manner. The 509 coefficients, implemented into the mask, are shown in Table 2. The coefficients at the first mask position are determined from the portion of the mask consisting of the first 255 coefficients 10001...to 00000 (see underlined section of Table 2). The coefficients of the second mask position are formed by shifting, one place to the right, and so are 00011...to 00001, and so forth until the last (255th) mask position has coefficients 01000...to 00000.

TABLE 2

255 SLOT CYCLIC MASK CODE: "1" DENOTES TRANSPARENT SLOT AND "0" DENOTES OPAQUE SLOT. NOTE THAT THE 255 SLOT CYCLIC MASK IMPLIES 509 TOTAL MASK SLOTS. THE UNDERLINED PORTION REPRESENTS THE SLOTS ILLUMINATED AT THE FIRST MASK POSITION

| | | | | | | | | | |
|--------------|--------------|--------------|--------------|--------------|--------------|--------------|--------------|--------------|--------------|
| <u>10001</u> | <u>11000</u> | <u>10010</u> | <u>11100</u> | <u>00001</u> | <u>10010</u> | <u>01001</u> | <u>10111</u> | <u>00100</u> | <u>00010</u> |
| <u>10110</u> | <u>11010</u> | <u>11001</u> | <u>01100</u> | <u>00111</u> | <u>11011</u> | <u>01111</u> | <u>01011</u> | <u>10100</u> | <u>01000</u> |
| <u>01101</u> | <u>10001</u> | <u>11100</u> | <u>11100</u> | <u>11000</u> | <u>10110</u> | <u>10010</u> | <u>00101</u> | <u>00101</u> | <u>01001</u> |
| <u>11011</u> | <u>10110</u> | <u>01111</u> | <u>01111</u> | <u>11010</u> | <u>01100</u> | <u>11010</u> | <u>10001</u> | <u>10000</u> | <u>01110</u> |
| <u>10101</u> | <u>01111</u> | <u>10010</u> | <u>10000</u> | <u>10011</u> | <u>11111</u> | <u>10000</u> | <u>10111</u> | <u>10001</u> | <u>10100</u> |
| <u>00000</u> | 10001 | 11000 | 10010 | 11100 | 00001 | 10010 | 01001 | 10111 | 00100 |
| 00010 | 10110 | 11010 | 11001 | 01100 | 00111 | 11011 | 01111 | 01011 | 10100 |
| 01000 | 01101 | 10001 | 11100 | 11100 | 11000 | 10110 | 10010 | 00101 | 00101 |
| 01001 | 11011 | 10110 | 01111 | 01111 | 11010 | 01100 | 11010 | 10001 | 10000 |
| 01110 | 10101 | 01111 | 10010 | 10000 | 10011 | 11111 | 10000 | 10111 | 10001 |
| 10100 | 0000 | | | | | | | | |

The Hadamard spectrometer was constructed from a Czerny-Turner scanning monochromator, a single pass, 0.35 m focal length, f/6.8 mount with a 48 mm x 48 mm, 1180 lines per mm grating blazed for 250 nm. The reciprocal linear dispersion with this configuration was approximately 2.0 nm/mm. The slits are straight-edged and bilaterally adjustable in width from 5 to 2000 μm and in height with values of 12, 5, 3, 1 or 0.5 mm. The folding mirror at the exit slit was removed, and a laboratory-fabricated translation stage was mounted at the front panel with the front edge of the slide assembly (as shown in Figure 4) mounted at the exit focal plane. A field stop, 0.510 in x 0.5 in, was aligned to allow approximately 12.5 nm on either side of the exit focal point to fall on the mask which was connected to the slide assembly. The mask consisted of a copper-nickel bimetallic strip 1" x 3" x 0.010". The 255 slot cyclic mask (509 total slots) was inscribed on the bimetallic strip with each slot having a width of 0.002 in (50 μm) and a height of 0.387 in; the total mask code length was 1.018 in. The slide assembly was spring loaded in the translation stage and was driven by a 40 turns-per-in micrometer which in turn could be stepped in increments of 1/19200 in by a 480 steps-per-revolution stepping motor.

The detector was a 30 mm diameter end-on photomultiplier tube with S-13 spectral response, and it was operated at 750-1000 V. The photoanode current was amplified by a current-to-voltage converter and measured by a lock-in amplifier, which was tuned to the phase and frequency of the chopper described in Chapter III. The output of the lock-in amplifier was directed to the analog input of the PDP-11 computer (see Appendix II for a description of the computer system). A block diagram of the complete HTS system is shown in Figure 4. The components used in the system are listed in Table 3.

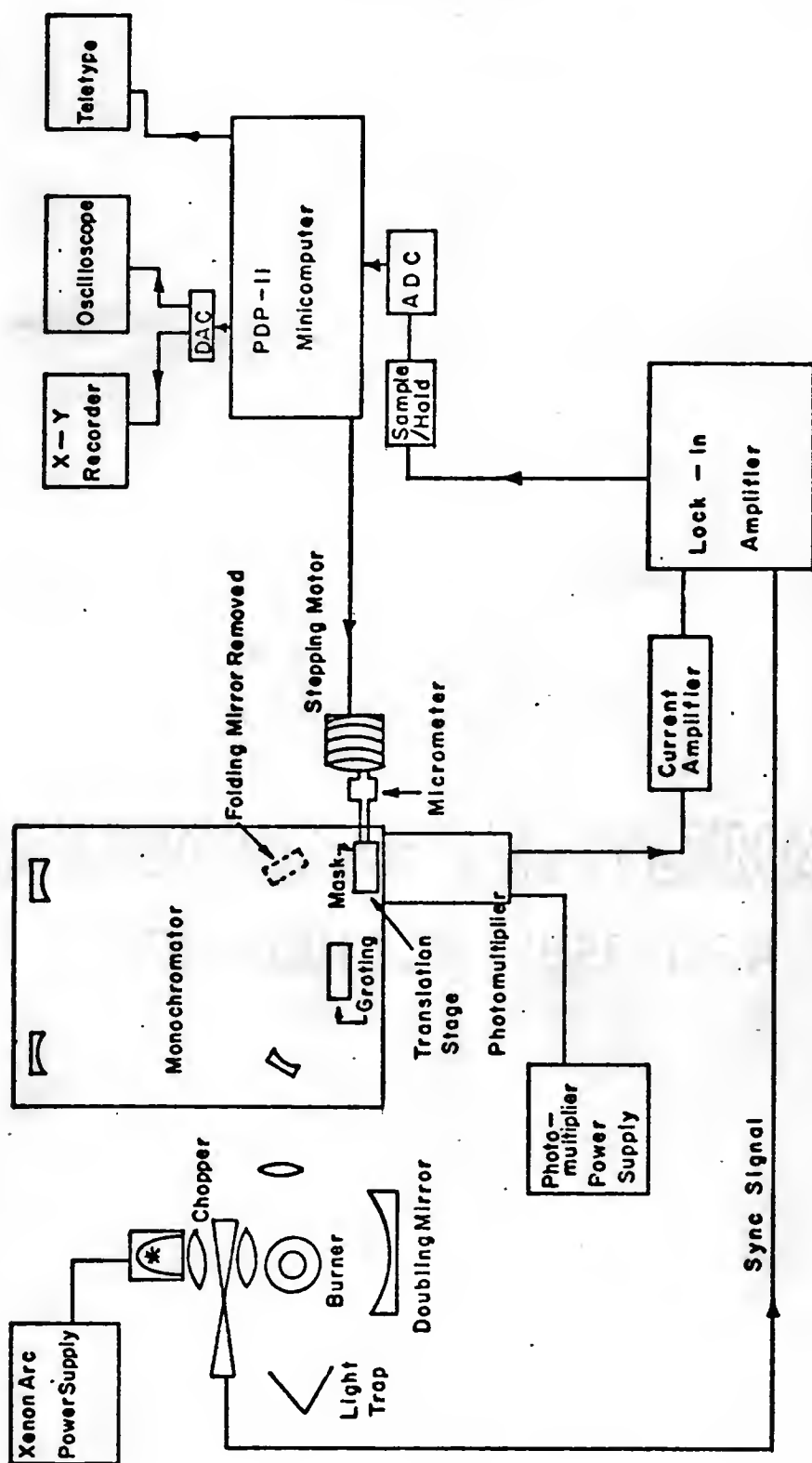


Figure 4.-- Block diagram of the Hadamard transform spectrometer used in this study.

TABLE 3
COMPONENTS OF THE HADAMARD TRANSFORM SPECTROMETER^a

| <u>ITEM</u> | <u>DESCRIPTION (MODEL NUMBER)</u> | <u>SOURCE</u> |
|---------------------------------|---------------------------------------|---|
| Mask | 509 Total Slot 255 Cyclic Code | Dynamic Research Corp., Wilmington, MA 01887 Under license from Spectral Imaging, Concord, MA |
| Monochromator | EU-700 | Heath Co., Benton Harbor, MI 49022 |
| Photomultiplier | EMI 9526B | Gencom Div., Plainview, NY 11803 |
| Stepping Motor | HDM-12-480-4 | USM Corp., Wakefield, MA 01880 |
| Photomultiplier Power Supply | EU-42A | Heath Co., Benton Harbor, MI 49022 |
| Lock-in Amplifier | 804 | Keithley Instruments, Cleveland, OH 44139 |

^a Note: Other components (excitation source, flame, computer system) are listed in Tables 1 and 12.

The Fast Hadamard Transform (FHT)

The process of accumulating data in an orthogonal fashion in order to form a set of linearly independent simultaneous equations is begun when the atomic fluorescence system, including the light source and flame cell described in Chapter III, and the spectrometer and electronics described in the last section, is aligned and adjusted. The monochromator is set so that the center of the desired 25 nm span is displayed on the wavelength counter. The computer program is loaded and started with the command "G". The computer steps the mask to the first position and takes a series of 255 readings from the lock-in amplifier by means of the analog-to-digital converter (ADC). These readings are averaged, and the average is added to or subtracted from a double precision (two 16 bit words) 255 point data buffer storage array according the following scheme. The first eight coefficients, corresponding to the first eight slots of the mask as it is currently positioned, are determined in the same manner as the coefficients for the mask were calculated in the previous section. For example, for the first mask position, the first eight coefficients are 10001110. These binary digits are designated b_0 to b_7 . The double precision accumulators are numbered 1 to 255 and are determined as eight bit binary numbers a_0 to a_7 (00000001 for the first accumulator number). Corresponding bits are added, mod 2, according to $(a_0 + b_0) + (a_1 + b_1) + \dots + (a_7 + b_7)$; the sum determined will be 1 if the number of matching set (1) bits in these two eight bit words is odd, and the average signal at this slot position is then added to the respective accumulator. If, on the other hand, the number of matching set bits is even (0), then the average signal is subtracted from the particular accumulator. It can be seen that for the first code word (10001110), there are no matching 1's for

the first storage location (00000001), and so the signal is subtracted from the first accumulator.

The accumulator is then incremented by one and the new set of bits, representing the new accumulator number, is matched with the code word; the average signal is then added to or subtracted from the next accumulator (10001110 has 1 matching set bit with 00000010 so the first signal is added to the second accumulator). The code word remains the same (until the mask is stepped to the next location), the accumulator number is increased by one and the add/subtract process is repeated until the average signal at this mask position has been added to or subtracted from each of the 255 accumulators.

At this point, the code word describing the first eight slots of the next mask position is determined in the same manner as used to determine the coefficients in the last section. Briefly, the bits $b_0 + b_2 + b_3 + b_4$ are added, modulo 2, and the result is used as b_8 . A shift, one to the right results in the eight bit word b_1 to b_8 . These bits are used as the new code word. The mask is then stepped one slot width to the new mask position, and the data gathering and addition/subtraction process is repeated.

After 255 mask steps, the spectral signal values are stored as double precision, octal (base 8) integers with any noise portion of the signal resulting in a baseline fluctuation about zero. To eliminate problems caused by negative numbers being routed to a unipolar digital-to-analog converter (DAC), each signal value is digitally offset until no negative numbers remain in the data buffer.

A final permutation is needed to obtain the actual signal versus wavelength spectrum. The real channel in a monotonically increasing spectrum (denoted by X_i ; $i = 1$ to 255) is related to the stored

channel (S_k) by an eight bit binary number which can be found according to the following procedure.

The intensities of the first eight spectral elements (X_i ; $i = 1$ to 8) are contained in the storage channels (accumulators) S_k as follows:

$$X_i = S_k$$

where; $k = 2^{i-1}$ and $i = 1$ to 8.

Thus

$$X_1 = S_1;$$

$$X_2 = S_2;$$

$$X_3 = S_4;$$

$$X_4 = S_8;$$

⋮

$$X_8 = S_{128}.$$

Subsequent spectral intensities (X_i ; $9 \leq i \leq 255$) may then be found in storage locations calculated from the binary representations of the previous eight storage locations. Spectral intensity X_i ($9 \leq i \leq 255$), with binary representation ($x_{i,1} x_{i,2} x_{i,3} x_{i,4} x_{i,5} x_{i,6} x_{i,7} x_{i,8}$) will be found in accumulator S_k where the binary representation of k is ($s_1 s_2 s_3 s_4 s_5 s_6 s_7 s_8$) and where,

$$s_j = x_{i+j-9,1} + x_{i+j-9,3} + x_{i+j-9,4} + x_{i+j-9,5} \pmod{2},$$

where s_j is the value of the first binary bit of the S_k accumulator and $x_{i+j-9,1}$ is the value of the first binary bit of the $(i+j-9)^{\text{th}}$ spectral interval and the other x -terms are correspondingly defined. For example, for X_9 (the ninth spectral) interval, the eight pervious accumulators

in binary notation are

$$\begin{aligned}
 X_1 &= 00000001, \text{ i.e. } X_1 = x_{1,1} x_{1,2} x_{1,3} x_{1,4} x_{1,5} x_{1,6} x_{1,7} x_{1,8}, \\
 X_2 &= 00000010, \\
 X_3 &= 00000100, \\
 X_4 &= 00001000, \\
 X_5 &= 00010000, \\
 X_6 &= 00100000, \\
 X_7 &= 01000000, \\
 X_8 &= 10000000, \text{ i.e. } X_8 = x_{8,1} x_{8,2} x_{8,3} x_{8,4} x_{8,5} x_{8,6} x_{8,7} x_{8,8}.
 \end{aligned}$$

Thus for $i = 9$

$$\begin{aligned}
 s_1 &= x_{9+1-9,1} + x_{9+1-9,3} + x_{9+1-9,4} + x_{9+1-9,5} = x_{1,1} + x_{1,3} + x_{1,4} + x_{1,5}, \\
 s_1 &= 0 + 0 + 0 + 0 = 0 \\
 s_2 &= x_{2,1} + x_{2,3} + x_{2,4} + x_{2,5} = 0 + 0 + 0 + 0 = 0, \\
 s_3 &= x_{3,1} + x_{3,3} + x_{3,4} + x_{3,5} = 0 + 0 + 0 + 0 = 0, \\
 s_4 &= x_{4,1} + x_{4,3} + x_{4,4} + x_{4,5} = 0 + 0 + 0 + 1 = 1, \\
 s_5 &= x_{5,1} + x_{5,3} + x_{5,4} + x_{5,5} = 0 + 0 + 1 + 0 = 1, \\
 s_6 &= x_{6,1} + x_{6,3} + x_{6,4} + x_{6,5} = 0 + 1 + 0 + 0 = 1, \\
 s_7 &= x_{7,1} + x_{7,3} + x_{7,4} + x_{7,5} = 0 + 0 + 0 + 0 = 0, \\
 s_8 &= x_{8,1} + x_{8,3} + x_{8,4} + x_{8,5} = 1 + 0 + 0 + 0 = 1.
 \end{aligned}$$

Therefore, $k = (00011101) = 35_8 = 29_{10}$ so $X_9 = S_{29}$ and so the ninth spectral element is found in the 29th sequential storage location. Each subsequent location can therefore be determined from the eight binary words describing the eight previous storage locations.

The storage locations are determined, and each stored value is divided by $(N+1)/2$ or 128 in the present case ($N = 255$). These final values are stored in a sequential (increasing with wavelength) data buffer area of the computer. At this time, the transform is complete, and the digital data are available for processing.

It can be seen that the FHT can be accomplished in this way with $N \times N$ additions (or subtractions), and N simple divisions. For this reason, the FHT can be programmed on any computer without the need for a hardware multiply/divide or a slow, software multiply/divide package. This one-step arithmetic process is the basis for the order of magnitude increase in speed of the FHT (56) compared with the fast Fourier transform (FFT) which requires $N \log_2 N$ multiplications (or divisions) (57).

Because the spectral intensity values are stored, they are available for digital manipulation. The data can be read out on an oscilloscope or an x-y plotter. Alternatively, the entire set of signals can be punched on paper tape for storage. Also, the data can be smoothed, and the baseline averaged. Peaks can be located and integrated, and comparisons with calibration standards or previous spectra can be made. Multiple scans can be generated and added or subtracted.

Analytical Procedure with the HTS System

Stock aqueous solutions of $1000 \mu\text{g ml}^{-1}$ of the metals listed in Table 4 were prepared from reagent grade chemicals. Appropriate serial dilutions of the combinations of elements were made in the concentrations shown. The spectrometer was manually scanned to the center wavelength shown in Table 4 for the wavelength range desired.

The system was then energized. The illuminator was started and allowed to stabilize, the flame was ignited and adjusted, and the

TABLE 4
ELEMENTS INVESTIGATED WITH THE
HADAMARD TRANSFORM SPECTROMETER SYSTEM

| <u>ELEMENTS</u> | <u>CENTER WAVELENGTH^a</u> | <u>CONCENTRATIONS</u> |
|-----------------|--------------------------------------|--|
| Ni, Co, Fe | 240 nm | 30 $\mu\text{g ml}^{-1}$ - 500 $\mu\text{g ml}^{-1}$ |
| Mn, Mg | 285 nm | 5 $\mu\text{g ml}^{-1}$ - 200 $\mu\text{g ml}^{-1}$ |
| Cu, Ag | 330 nm | 10 $\mu\text{g ml}^{-1}$ - 200 $\mu\text{g ml}^{-1}$ |
| Cr | 359 nm | 10 $\mu\text{g ml}^{-1}$ - 200 $\mu\text{g ml}^{-1}$ |

^a Wavelength setting of grating spectrometer.

computer program was loaded and readied. Solutions, including a blank and the standards, were aspirated each in turn and the data gathering process was initiated by means of software (the keyboard). The current amplifier and lock-in were set to give 10^7 volts per amp and 30 mV full scale, respectively. Thus, the current measured and amplified by the lock-in was about 3 nA. The settings were adjusted if necessary on a subsequent run if the readings during a run exceeded full scale out from the lock-in or if no reading during a run exceeded 10% full scale out. The maximum S/N in the output resulted when there was a maximum difference in the reading obtained as the mask was stepped across the exit plane. All of the adjustments to the electronics were performed to maximize this difference in readings. The photomultiplier tube dc voltage was initially set at 800 V but was also adjusted in the range 750 V to 850 V to maximize the difference in readings. The results from the FHT were available about 30 s after the start of a scan via the oscilloscope display. The results were typed out as intensity vs. channel number and also were plotted via the x-y recorder.

Results and Discussion

It was intended that analytical curves (log intensity vs. log analyte concentration) be obtained by gathering digital data from the printout of the intensity of the channels as a function of the concentration of analyte introduced into the flame. After an exhaustive study of this possibility it was determined that this was not feasible for two reasons; (i) the concentrations which allowed signal-to-noise ratios of greater than about 10 were found to be on the non-linear portions of an analytical curve; lower concentrations of analyte, which would fall

in the linear portion of the working curve would not give S/N ratios greater than about 2 or 3; (ii) all variations in electronic parameters, in order to increase differences in the readings as the mask was stepped, resulted in vastly different background noise levels. For these reasons, the x-y plots of the spectra were used to estimate the limits of detection for the elements of interest.

One problem became evident during the preliminary operation of the system. With the electronic sensitivity used in these studies, i.e., about 3 nA current and 100 ms time constant with the lock-in, a blank solution resulted in considerable noise in the baseline as depicted in Figure 5. The background, which is reproducible in peak-to-peak noise intensity but not in spectral distribution, was probably due to slight fluctuations in scattered radiation in the flame. Since about one-half of the mask slots are transparent, a total spectral region of approximately 12.5 nm of the background is passed at each mask position. Any noise (due to the source) on the background is passed to the detector. This effect, which is a direct consequence of the multiplexing effort, was a major cause of the poor performance of the HTS.

The resolution capability of the HTS system is demonstrated by the multielement AFS spectra shown in Figure 6. $200 \mu\text{g ml}^{-1}$ each of Mn and Mg were aspirated. Entrance slit widths of 200 μm and 50 μm resulted in the spectra shown. In each case, a digital filtering technique was used to average the noise on the baseline in order to better demonstrate the resolution possible. The Mn triplet at 279.5, 279.8 and 280.1 shows baseline resolution with 50 μm entrance slit width, and the spectral bandpass is less than 0.3 nm per channel with this slit width.

In Figures 7 to 10 results are given of Hadamard scans of wavelength centered as listed in Table 4. In Figure 7 the AFS spectrum

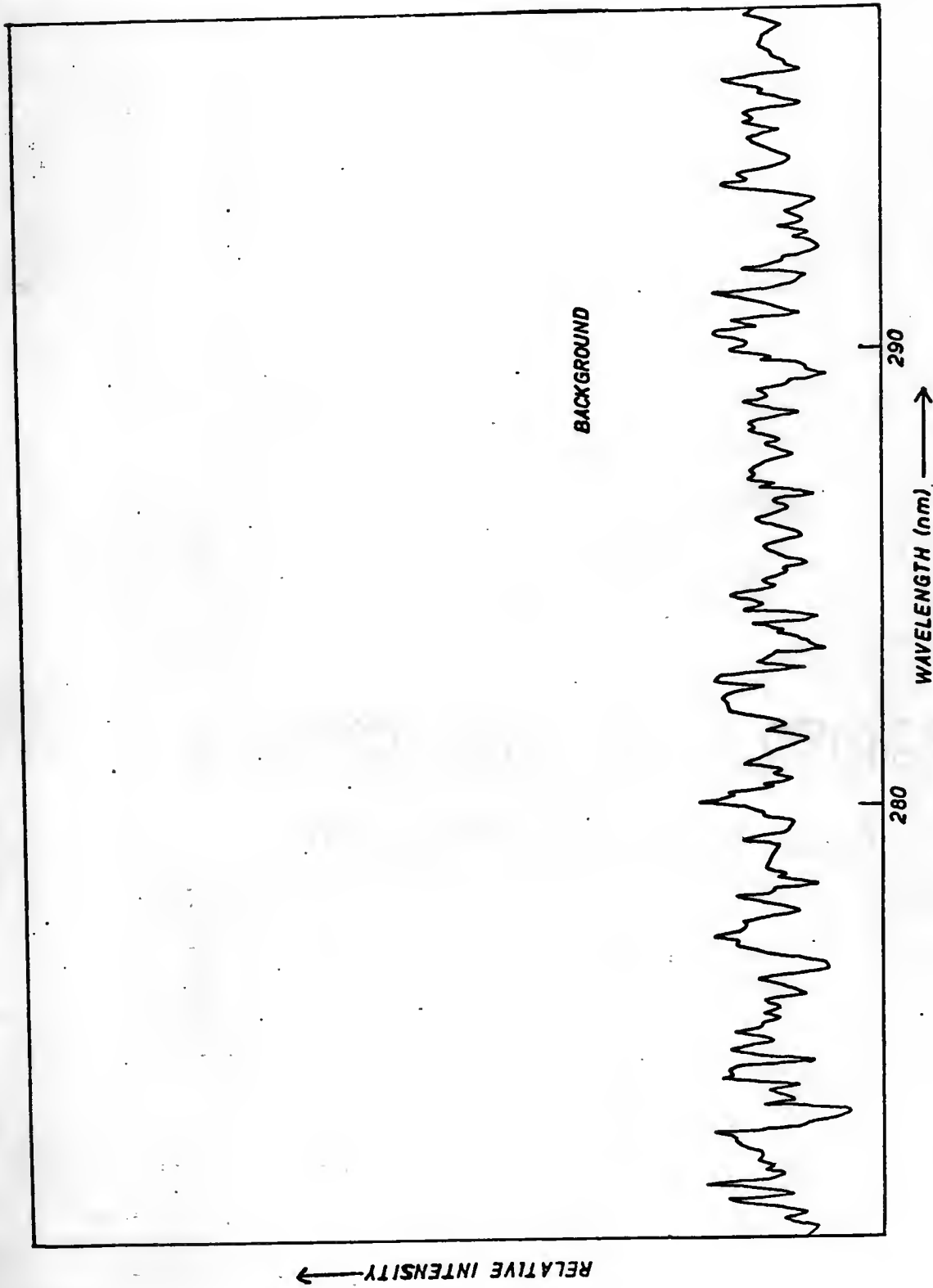


Figure 5.-- Atomic fluorescence background with the Hadamard transform spectrometer.

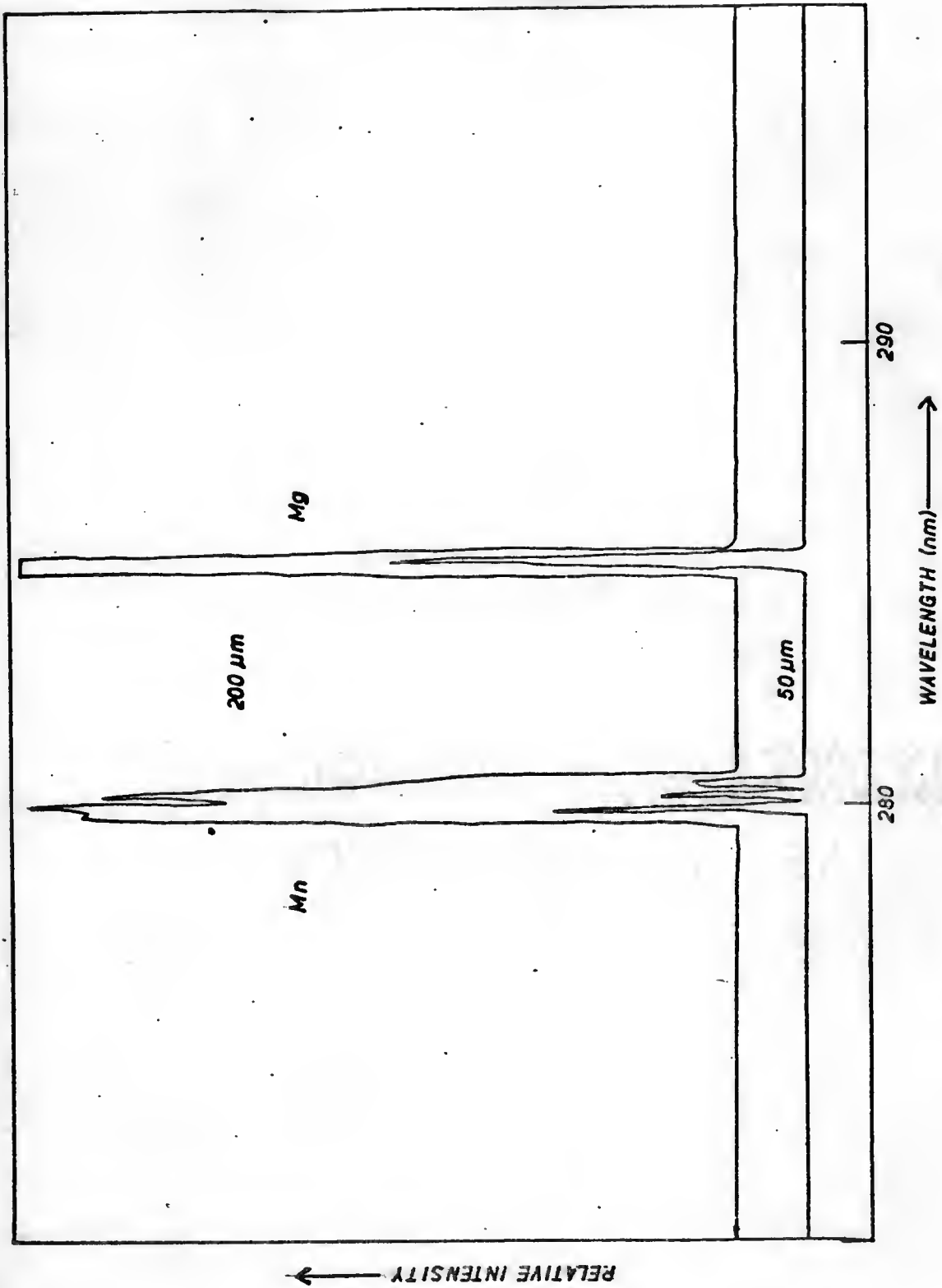


Figure 6.-- Resolution capabilities of the Hadamard transform spectrometer while aspirating $200 \mu\text{g ml}^{-1}$ each of Mn and Mg.

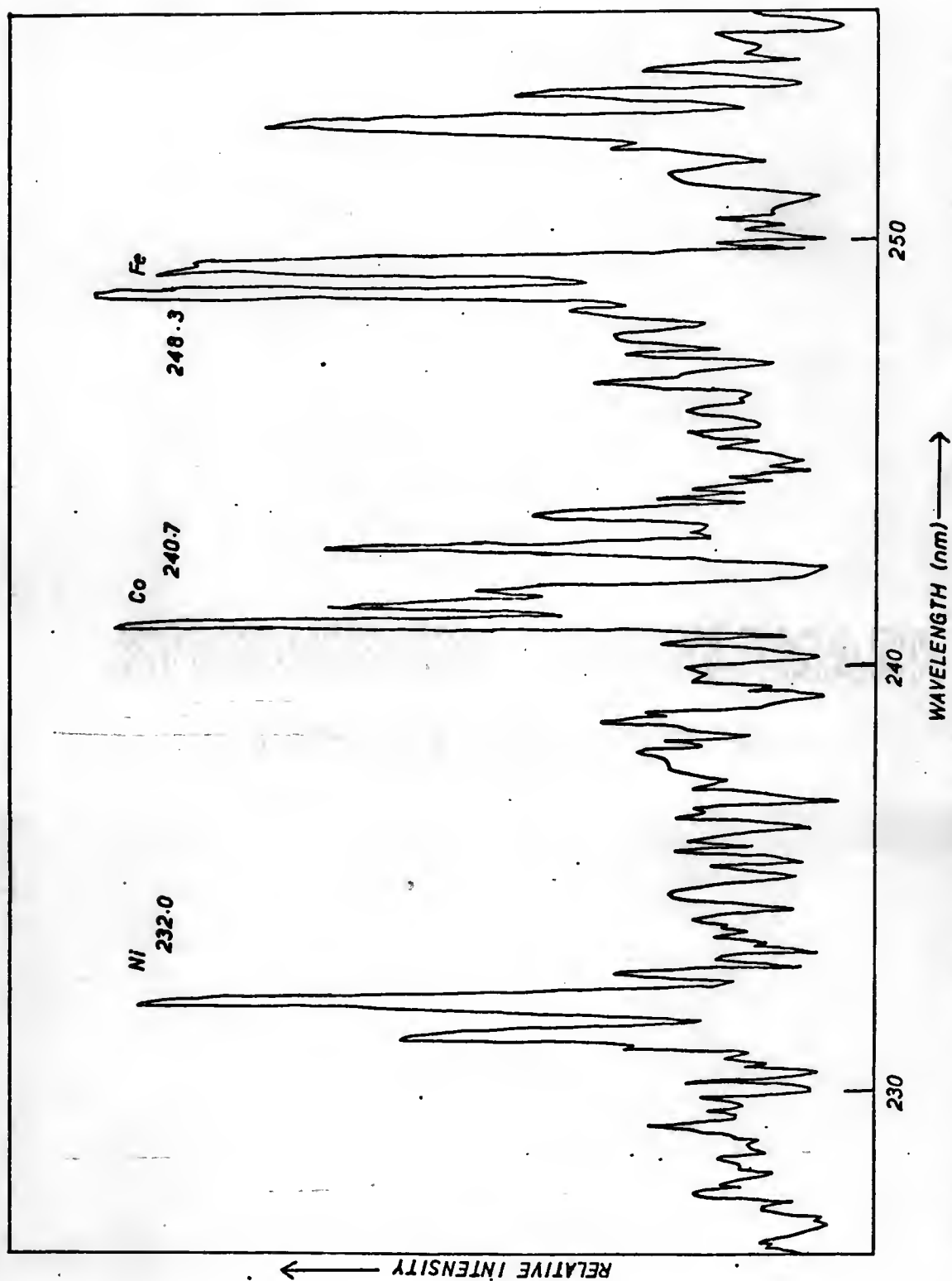


Figure 7.-- Multielement atomic fluorescence of $300 \mu\text{g ml}^{-1}$ Ni and $200 \mu\text{g ml}^{-1}$ each of Co and Fe with the Hadamard transform spectrometer.

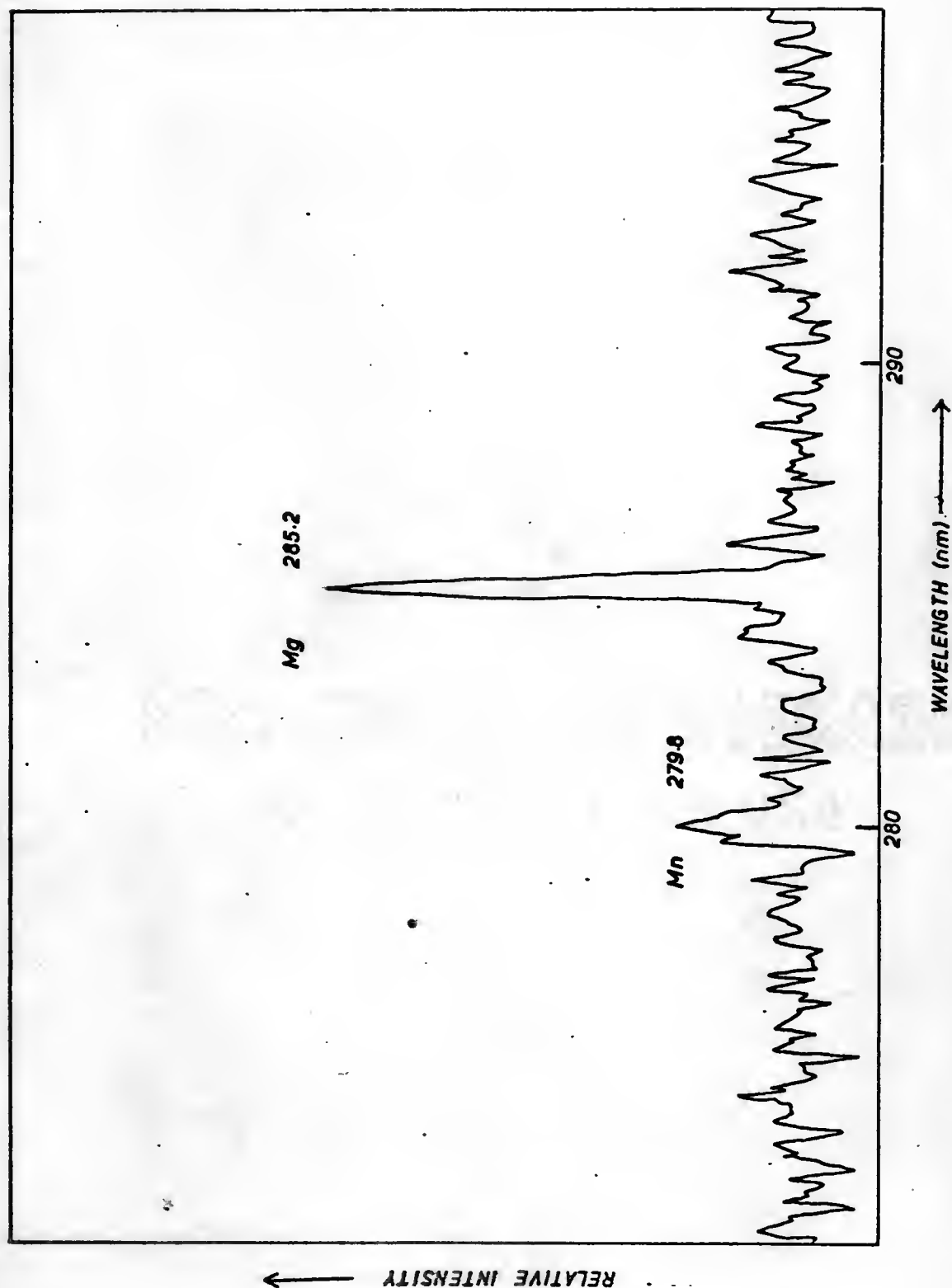


Figure 8.-- Atomic fluorescence of $10 \mu\text{g ml}^{-1}$ each of Mn and Mg with the Hadamard transform spectrometer.

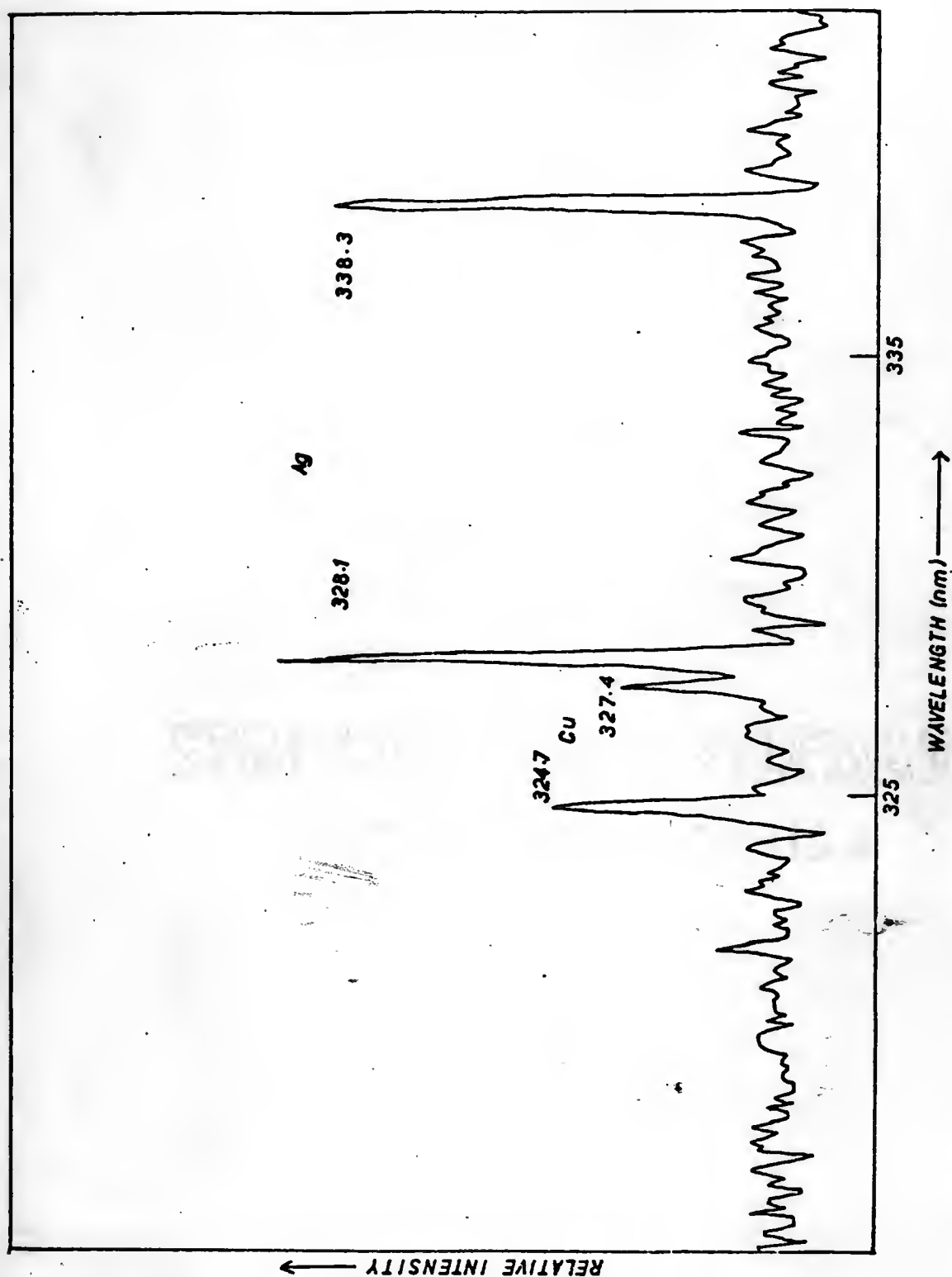


Figure 9.-- Atomic fluorescence of 100 $\mu\text{g ml}^{-1}$ each of Cu and Ag with the Hadamard transform spectrometer.

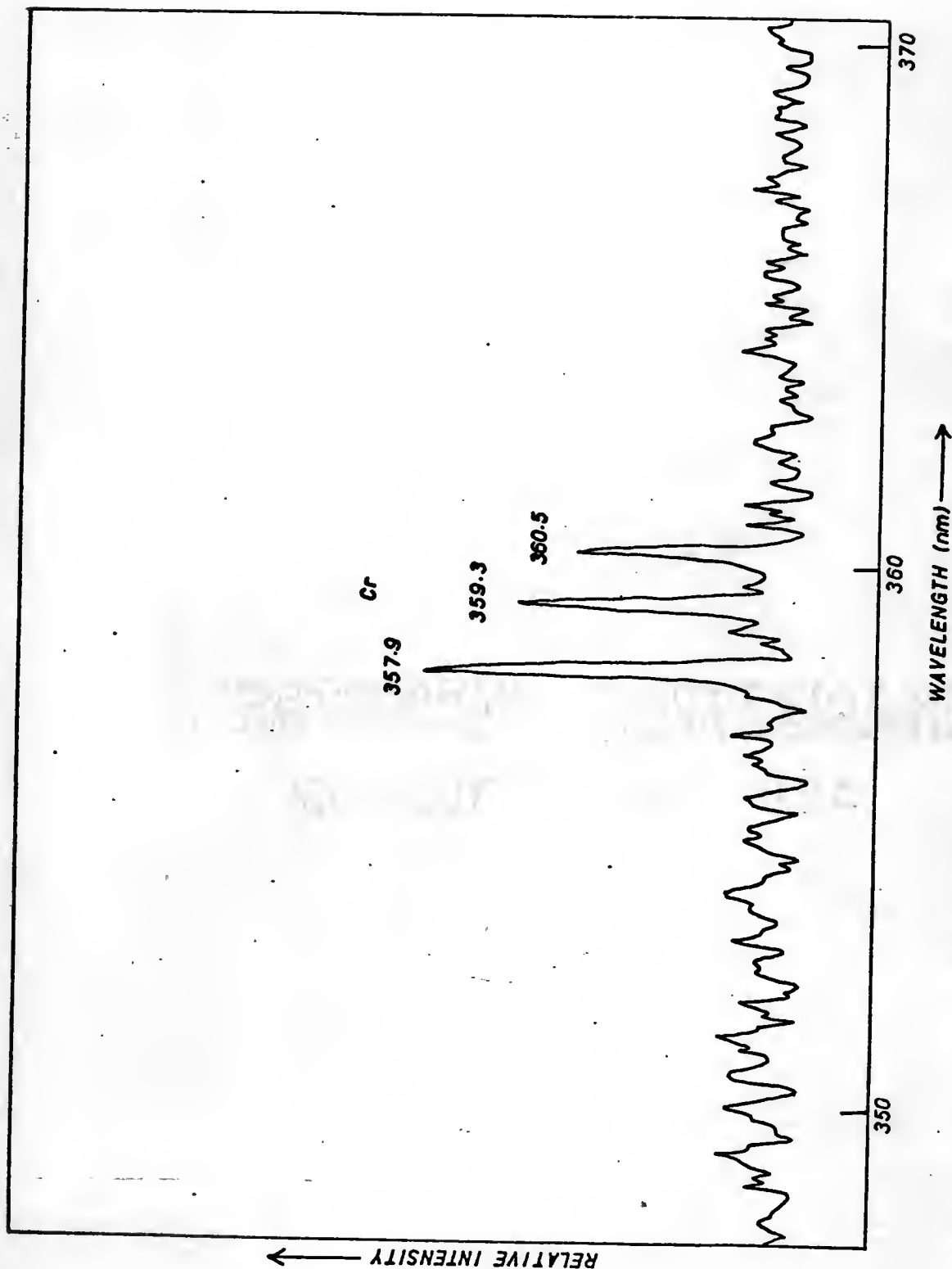


Figure 10.-- Atomic fluorescence of $100 \mu\text{g ml}^{-1}$ Cr with the Hadamard transform spectrometer.

is given for $300 \mu\text{g ml}^{-1}$ Ni, $200 \mu\text{g ml}^{-1}$ Co and $200 \mu\text{g ml}^{-1}$ Fe; in Figure 8 the AFS spectrum is for $10 \mu\text{g ml}^{-1}$ each of Mn and Mg; in Figure 9 the AFS spectrum is for $100 \mu\text{g ml}^{-1}$ each of Cu and Ag; in Figure 10 the AFS spectrum is for the Cr triplet from $100 \mu\text{g ml}^{-1}$ Cr. Each of the spectra was scanned in 28 s with an entrance slit of $100 \mu\text{m}$. From results such as these, estimates of limits of detection for these eight elements were made and are given in Table 5. Also listed there are the detection limits found for those elements using a single channel system in a stationary mode, and the same type of 150 W xenon continuum source (53).

A comparison of these results show that the HTS system results in detection limits some orders of magnitude less than for a stationary, single channel system. It can be estimated that the loss in S/N due to the extremely wide spectral region for the background scatter is at least one order of magnitude. This result was estimated from the background noise levels in a single channel scanning system with similar time constant and sensitivity. The root-mean-square (rms) noise ratio is about 10 for the HTS/single channel system.

All of the detection limits listed in Table 5 are for similar signal levels from all fluorescent lines in the wavelength region under investigation. This situation would not normally occur in real samples where vastly differing concentrations of elements could lead to large differences in signal levels. To investigate potential problems in multiplex systems for the analysis of mixtures of different concentrations, the Mg-Mn mixture shown in Figure 11, i.e., a mixture of $50 \mu\text{g ml}^{-1}$ Mg and $25 \mu\text{g ml}^{-1}$ Mn, was measured. The Mn signal is clearly evident. When the ratio is increased from 2:1 to 3:1 ($60 \mu\text{g ml}^{-1}$ Mg and

TABLE 5

LIMITS OF DETECTION (LOD)^a FOR THE ELEMENTS
ANALYZED BY THE HADAMARD TRANSFORM SPECTROMETER SYSTEM

| <u>ELEMENT</u> | <u>WAVELENGTH</u> | <u>LOD(this work)</u> <u>μg ml⁻¹</u> | <u>LOD(reference 53)</u> <u>μg ml⁻¹</u> |
|----------------|-------------------|--|---|
| Ni | 232.0 | 40 | 10 |
| Co | 240.7 | 25 | 10 |
| Fe | 248.3 | 25 | 5.0 |
| Mn | 279.8 | 5 | 0.3 |
| Mg | 285.2 | 1 | 0.04 |
| Cu | 324.7 | 5 | 1 |
| Ag | 328.1 | 2 | 0.1 |
| Cr | 357.9 | 5 | - |

^a Note: The limit of detection is defined as the concentration of analyte which gives a signal twice the rms noise observed when a blank is measured.

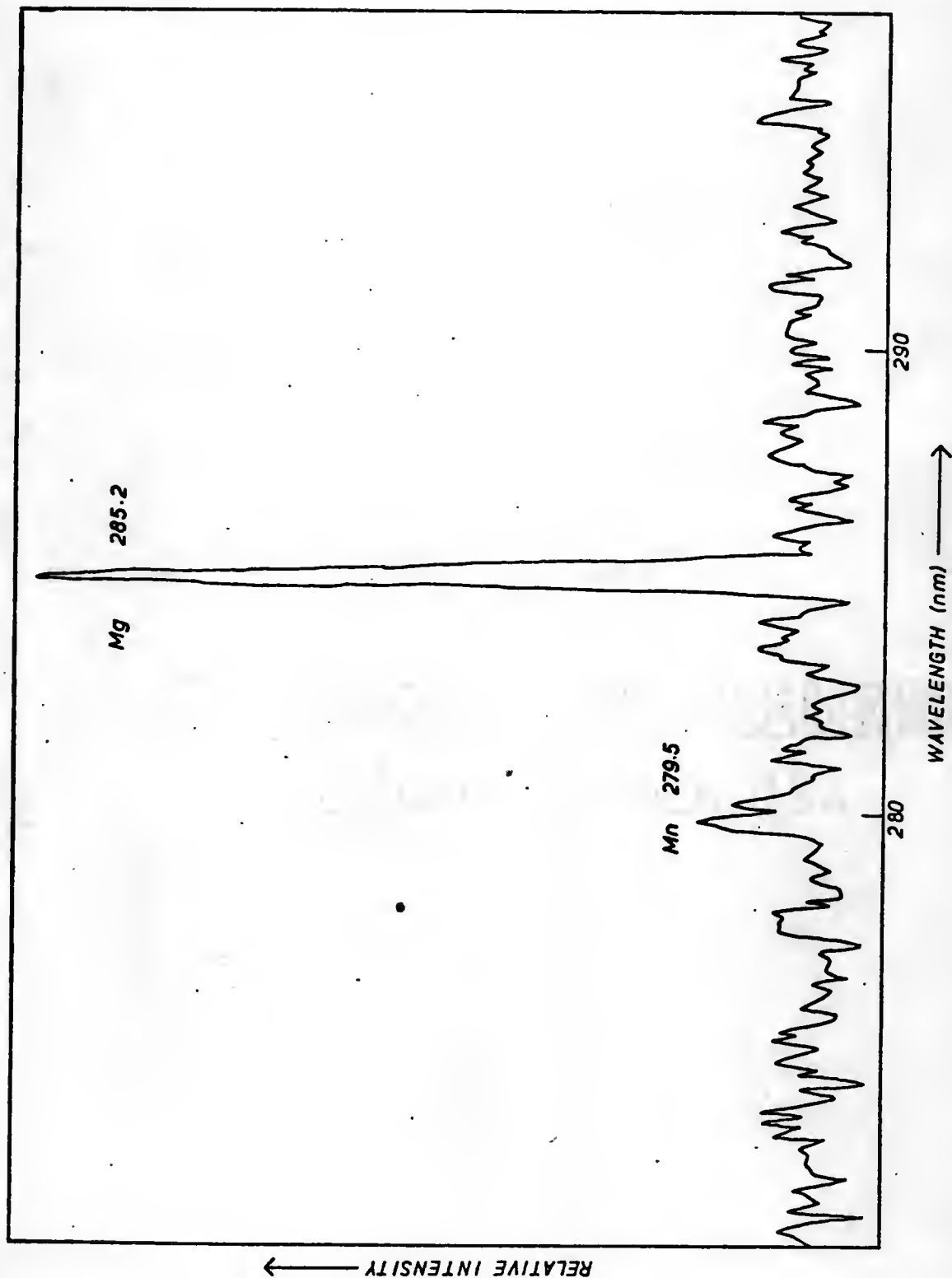


Figure 11.-- Atomic fluorescence spectrum of $50 \mu\text{g ml}^{-1}$ Mg and $25 \mu\text{g ml}^{-1}$ Mn with the Hadamard transform spectrometer.

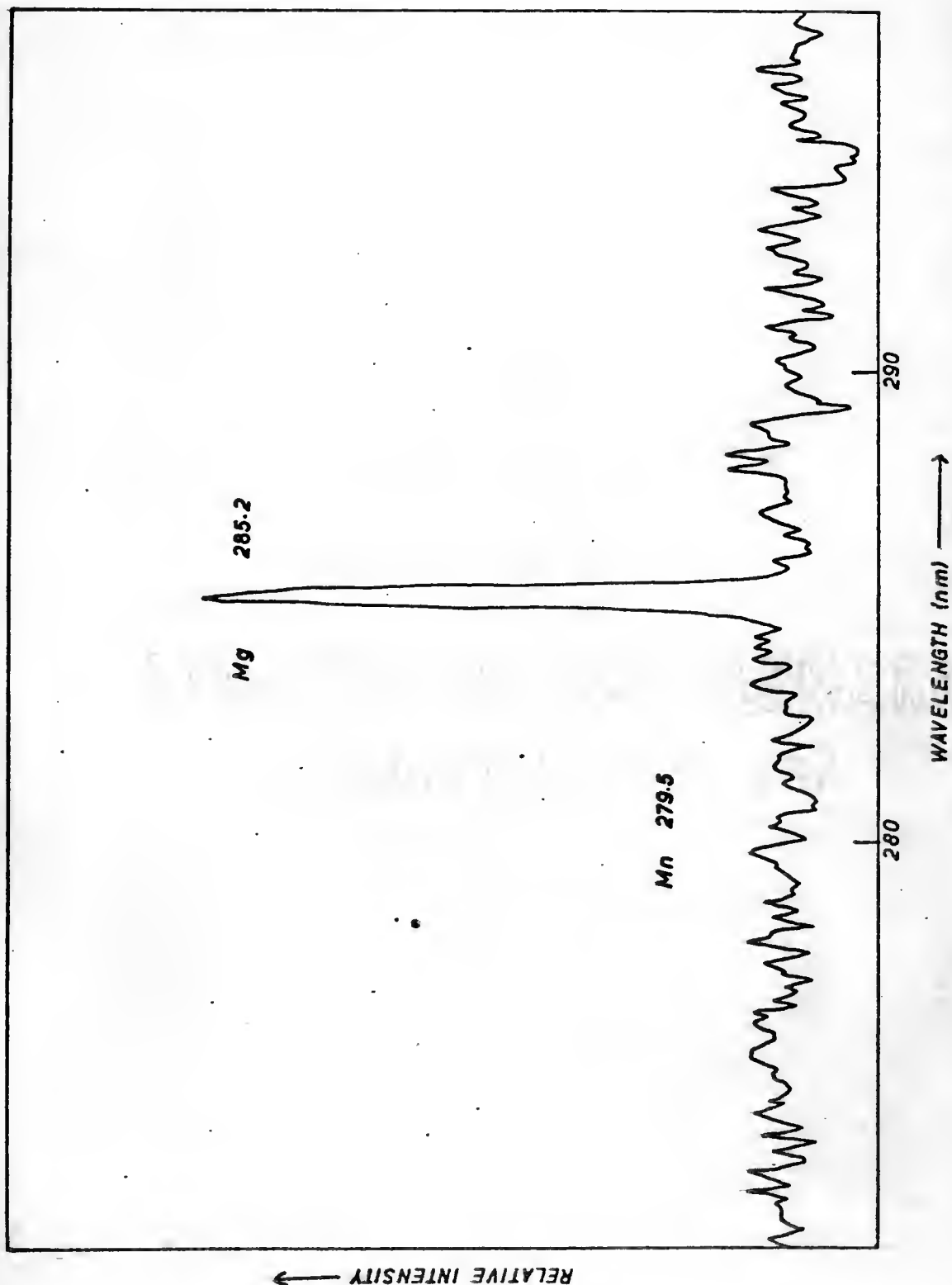


Figure 12.--- Atomic fluorescence spectrum of $60 \mu\text{g ml}^{-1}$ Mg and $20 \mu\text{g ml}^{-1}$ Mn demonstrating the multiplex disadvantage with the Hadamard transform spectrometer.

20 $\mu\text{g ml}^{-1}$ Mn), the noise level increased, and the signal from the Mn was no longer clearly visible (Figure 12). This effect of the multiplex disadvantage is certainly a major limitation of this type of spectrometric system.

CHAPTER V

SINGLE CHANNEL SCANNING SPECTROMETER (SCSS) SYSTEM

Preliminary Discussion

Most conventional spectrometric systems are able to scan the wavelength which is presented to the detector. In order to be able to scan at speeds greater than about 0.2 nm/s all that is needed is a means of rapid data handling and some method to determine the wavelength accurately and reproducibly during the scan. These functions are easily performed by means of a computer, and so, with a computer available, the scanning technique is easily implemented.

Because only one spectral interval is measured at a time, only conventional problems of spectral interference are encountered. The spectral bandpass of the instrument must be chosen so that possible spectral interferences will be of low probability. At the same time, the dispersion of the instrument should be chosen such that the time necessary for scanning the grating is as short as possible.

An obvious advantage to a single slit scanning system is that the range of wavelength which can be covered during a scan is only limited by the data handling capability of the system. However, in order to compare this system with the HTS only 25 nm wavelength scans are appropriate.

Description of SCSS Experimental Setup

The AFS excitation source and atomization flame cell described in Chapter III were used in the SCSS experimental setup as well as in the HTS setup. Only the dispersion device and detection system are changed from the HTS system.

A 0.3 m, f/5.3 modified Czerny-Turner mount monochromator with a 50 mm x 50 mm, 600 grooves/mm grating was used as a dispersion device. This monochromator has individual bilaterally adjustable straight slits variable in width from 5 μm to 2000 μm and in height from 0 to 20 mm. The reciprocal linear dispersion with the specified grating was 5.41 nm/mm and the resolution with 10 μm wide 4 mm high slits was 0.12 nm. Throughout this work, the slits were set at 75 μm wide and 10 mm high to correspond closely to the HTS system bandpass. With these conditions the bandpass was approximately 0.3 nm.

The normal scanning motor/gear system for this monochromator was disengaged, and a stepping motor was coupled directly to the shaft of the precision screw which rotates the grating. The stepping motor, which makes 480 steps per revolution (0.75° per step) can be driven at speeds to about 1200 steps second⁻¹. Because one revolution of the precision screw scans the monochromator 10.0 nm, the resolution capability of the monochromator/stepping motor system was 480 steps/10 nm = 4.8 steps/0.1 nm or about 0.02 nm per step. Maximum stepping speed used in this application was about 1000 steps s⁻¹ so that the maximum slewing rate was about 20 nm s⁻¹.

A high gain, low dark current photomultiplier tube with S (Q) spectral response (EMI 6256S) was used in a photon counting mode within a magnetically and electrostatically shielded housing at the exit slit. The tube was operated at -1450 V from the photon counting ratemeter/power

supply described later. The dark count with this system was 70-100 counts per second (cps).

The photon counting system consisted of a fast amplifier/discriminator, ratemeter/power supply, and a digital synchronous computer. The amplifier/discriminator was powered by the ratemeter/power supply low voltage power out. Output from the discriminator was sent through the ratemeter to the digital synchronous computer. The ratemeter was used as an intermediate analog output device and power supply for the photomultiplier tube and the amplifier/discriminator. These components were operated according to the manufacturers instructions.

The digital synchronous computer (DSC) is essentially a photon counter with two high speed 8 digit scalers, an arithmetic processing unit and timing and control signals and functions. In a mode called CHOP, it is able to function as a "lock-in photon counter" by use of the two scalers in conjunction with a mechanical chopper. When a synchronizing signal indicates that the data signal to be measured is present at the photomultiplier tube, the DSC uses a scaler designated as "DATA". Switches and a clock are available for setting the observation time, in microseconds, for which the DATA scaler is to be used. After that observation time, the scaler is shut down and the DATA is stored. The synchronizing signal next indicates that the background signal is present and the counts from the background are routed to a scaler designated "BACKGROUND". This scaler accumulates counts for the same observation time as the DATA scaler. The DSC has thumb-wheel switches on which the operator can set a "preset number" of chopper cycles. After each DATA-BACKGROUND cycle, the preset N counter is checked to see if the number of chopper cycles set there has been

finished. If not, further cycles are started and the total of DATA and BACKGROUND are stored in the appropriate scaler. If the preset N counter has been accomplished then the results are displayed on light emitting diodes on the control panel of the instrument in floating point notation (3 significant digits and an exponent). The information displayed can be either the DATA, the BACKGROUND, or the sum or difference of these two counts. At the same time, a "ready" light is lighted, and if the instrument is in the automatic cycle mode, the process is started again (see Figure 13 for a timing diagram of this process). The components of the SCSS are listed in Table 6 and a block diagram of the system is shown in Figure 14.

The DSC is ideally suited to computer control because two connectors at the rear of the instrument allow all of the functions of the DSC to be controlled by TTL level signals from a computer interface. Also, the data is available as TTL levels in binary coded decimal (BCD) notation. Synchronization signal lines are provided to allow communication between the DSC and a laboratory computer. For a more detailed description of the DSC/computer interface, see Appendix II.

The software for the SCSS is designed for simple control/data acquisition. Briefly, the computer steps the grating 0.1 nm and then counts for 4 chopper cycles. The fluorescence information (difference between the DATA and BACKGROUND scalers) is picked up after each cycle, and, at the end of 4 cycles, the sum is stored in a data buffer. The computer steps the grating 0.1 nm again and the data gathering is repeated until a wavelength scan of 25.6 nm is complete. The data can be displayed or printed or normalized to values between 0 and 1023 for plotting by means of an x-y recorder. The routines are quite easily

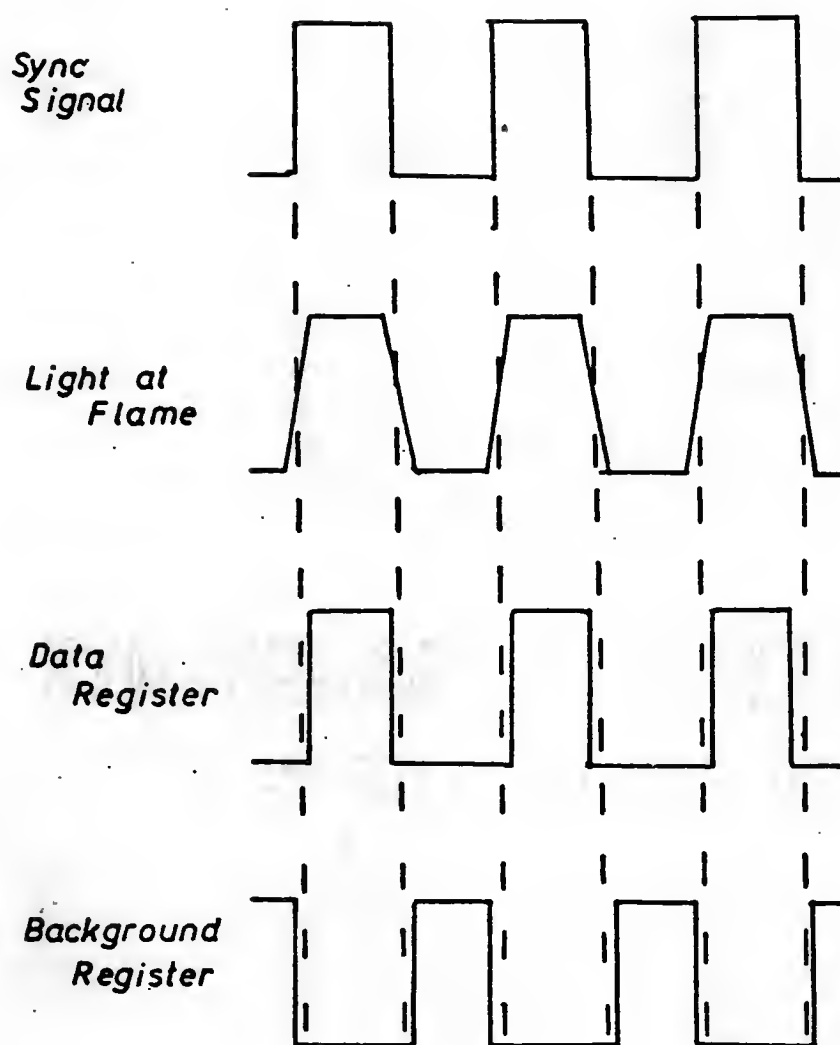


Figure 13.-- Timing diagram showing when the DATA and BACKGROUND registers of the Digital Synchronous Computer are open with respect to the source modulation.

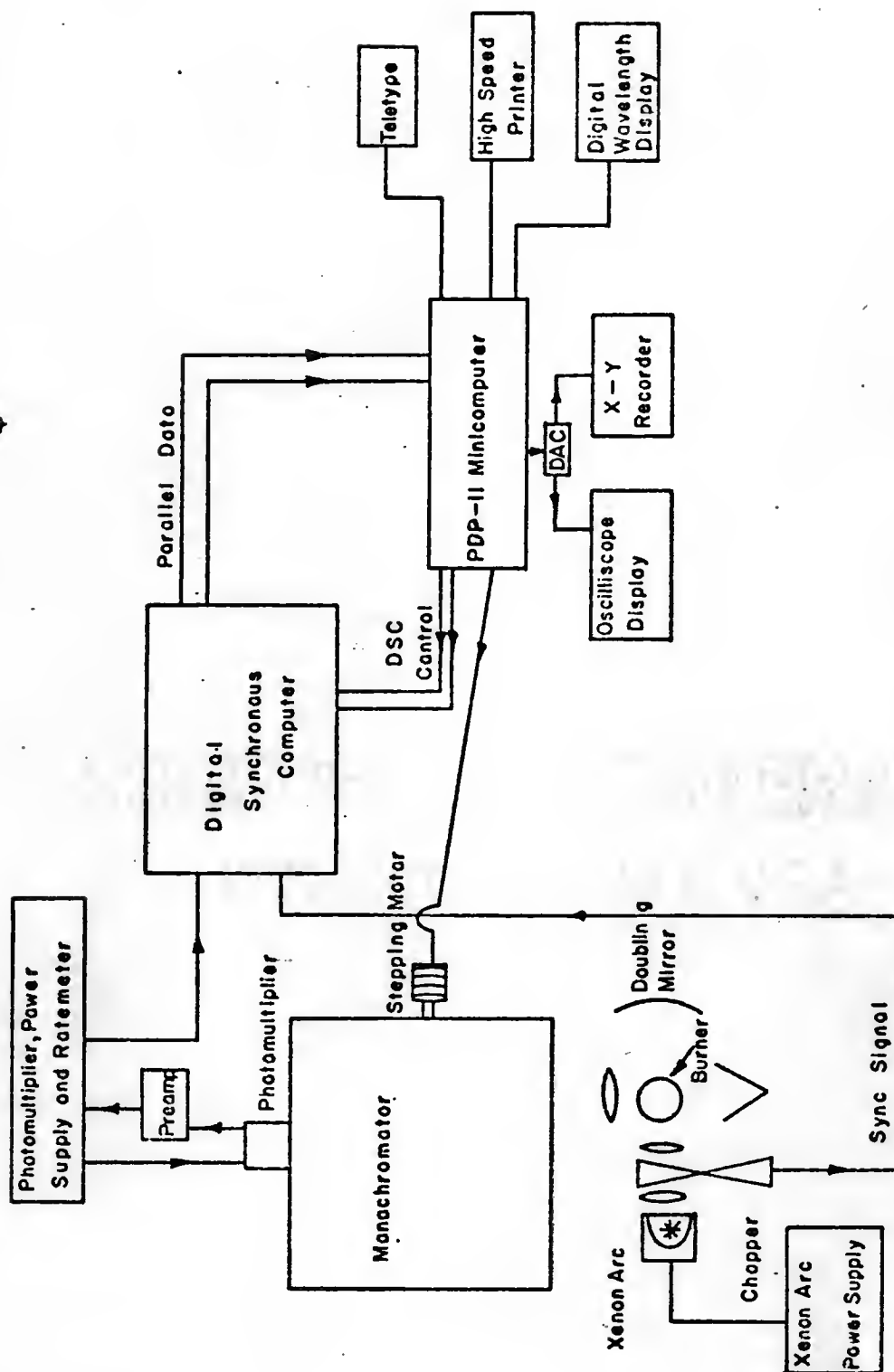


Figure 14.-- Block diagram of the single channel scanning spectrometer used in this study.

TABLE 6
COMPONENTS OF THE SINGLE CHANNEL SCANNING SPECTROMETER^a

| <u>ITEM</u> | <u>DESCRIPTION (MODEL NUMBER)</u> | <u>SOURCE</u> |
|------------------------------|---------------------------------------|---|
| Monochromator | 218 | GCA/McPherson Instr. Co., Acton, MA 01720 |
| Photomultiplier | EMI 6256S | Gencom Div., Plainview, NY 11803 |
| Photomultiplier Housing | 1151 | SSR Instrument Co., Santa Monica, CA 90404 |
| Amplifier/Discriminator | 1120 | |
| Digital Synchronous Computer | 1110 | |
| Power Supply/Ratemeter | 1105 | |
| Stepping Motor | HDM-12-480-12 | USM Corp., Wakefield, MA 01880 |

^aNote: Other components (excitation source, flame, computer system) are listed in Tables 1 and 12.

written and, since no transformation is necessary, almost all the computer time is used in data acquisition.

Operation of the SCSS System

When the system is in operation (flame and optics aligned and adjusted, chopper and electronics energized and computer program loaded), the monochromator is initially positioned at 190.0 nm. The wavelength region to be scanned can be approached by slewing. The keyboard command "F" will accept an octal (base 8) number at 0.1 nm steps to be slewed forward from 190.0 nm. The digital display will show the wavelength at all times during all operations. When the starting wavelength is reached, a "G" keyboard command will initiate the scan. The scan time is 31 s for a 25.6 nm scan. Upon completion of the scan the TTY will type "READY", and the fluorescence intensity vs. wavelength will be displayed on the oscilloscope. This may be plotted on the x-y recorder by typing "P", or the set of intensities may be printed with the command "W". Plot time on the x-y recorder is 65 s and printing time on the high speed printer is 28 s. Also, the data may be normalized so that the intensities are between 0 and 1023 for the 10-bit digital-to-analog converter. This routine, on an "A" command, will divide or multiply the entire data buffer by 2 as many times as necessary until the data points all have a magnitude of 1023 or less. The normalized data are stored in a separate data buffer (number 1) and a further buffer (number 2) can be used to save ("S" command) whichever data buffer is currently displayed. The buffer on the display can be changed by the commands 0, 1 or 2 corresponding to the data buffer of interest. The plot and print commands operate on the buffer which is currently displayed.

When the operation is finished with the data from the current scan, a scan from the present location can be achieved with commands "C" (continue) followed by "G". The next 25.6 nm wavelength region will then be scanned. Alternatively, the operation can begin the same scan over again with "B" to rewind and "G". The rewind time is 1.3 s. A "control R" command at any time will slew the monochromator to the original starting wavelength (190.0 nm).

Because of the limited dynamic range of the DAC-display system, the most useful results are obtained from printing the original results (data buffer 0). If the display is normalized, then the ratio between lines in the wavelength region is maintained, and this ratio can readily be observed. The printed data may be corrected for off-wavelength background and plotted in an intensity vs. concentration analytical curve.

Analytical Procedure with the SCSS System

Stock aqueous solutions of $1000 \mu\text{g ml}^{-1}$ of the metals listed in Table 7 were prepared from reagent grade chemicals. Appropriate serial dilutions of the combination of elements shown in Table 7 were made in the range $0.1 \mu\text{g ml}^{-1}$ to $100 \mu\text{g ml}^{-1}$.

When the system was energized, the command was given to slew rapidly to the starting wavelength for the particular element combination as given in Table 7. A blank solution (deionized water) was aspirated, and the scan was initiated with the "G" command. After the scan was complete, both a plot of fluorescence intensity vs. wavelength, and a digital printout was requested. After this was accomplished, the monochromator was slewed back to the starting position, and a standard solution was aspirated; the intensity values were plotted and printed each in turn. Three replicate analyses of each standard solution were

TABLE 7

ELEMENTS ANALYZED BY THE SINGLE CHANNEL SCANNING
SPECTROMETER BY GROUPS WITH WAVELENGTH RANGE AND
CONCENTRATION RANGE

| <u>ELEMENT</u> | <u>WAVELENGTH RANGE (nm)</u> | <u>CONCENTRATION RANGE ($\mu\text{g ml}^{-1}$)</u> |
|--------------------|------------------------------|---|
| Zn, Cd | 210.0 - 235.5 | 0.1 - 100 |
| Ni, Co, Fe | 230.0 - 255.5 | 1.0 - 100 |
| Au, Mn, Pb, Sn, Mg | 265.0 - 290.5 | 0.03 - 100 |
| Cu, Ag | 320.0 - 345.5 | 0.1 - 100 |
| Cr, Ti | 355.0 - 380.5 | 0.1 - 100 |

performed. The printed results were used in the preparation of analytical curves. The average, off-wavelength background was subtracted from the peak intensity, and the average of the three replicates was plotted vs. the concentration of the analyte.

Results and Discussion

Some of the results from the SCSS system are shown in Figures 15 to 20. In Figure 15 the background (obtained in 31 s) is given for the wavelength range from 265.0 nm to 290.5 nm while aspirating deionized water into the flame. In Figure 16, the spectrum is given for $1 \mu\text{g ml}^{-1}$ each of Zn and Cd. This figure shows the effect of normalization on small peaks (of less than one-half full scale) as each of the readings is multiplied until at least one spectral interval is more than one-half full scale. In Figure 17, the AF spectrum for $10 \mu\text{g ml}^{-1}$ each of Ni, Co and Fe is given. Five elements can be measured in the wavelength range 265.0 nm to 290.5 nm as shown in Figure 18; $30 \mu\text{g ml}^{-1}$ each of Au, Mn, Pb, Sn and Mg give discernable signals with the SCSS. The signals from Mn and Mg are extremely large at $30 \mu\text{g ml}^{-1}$ and they cannot be plotted on the same scale with Au, Pb and Sn at this same concentration. Also, $1 \mu\text{g ml}^{-1}$ each of Cu and Ag gives large S/N ratios as seen in Figure 19. The resolution of this system is demonstrated in the slight separation of the 327.4 nm line of Cu and the 328.1 nm strong line of Ag. The signal at approximately 336 nm appears in the spectra in this region and has tentatively been assigned to the molecular fluorescence of NH in the flame (58). Finally, the Cr triplet and the resonance line of Tl are shown at a concentration of $1 \mu\text{g ml}^{-1}$ in Figure 20. This figure has also been scale expanded by a factor of 2 for clarity.

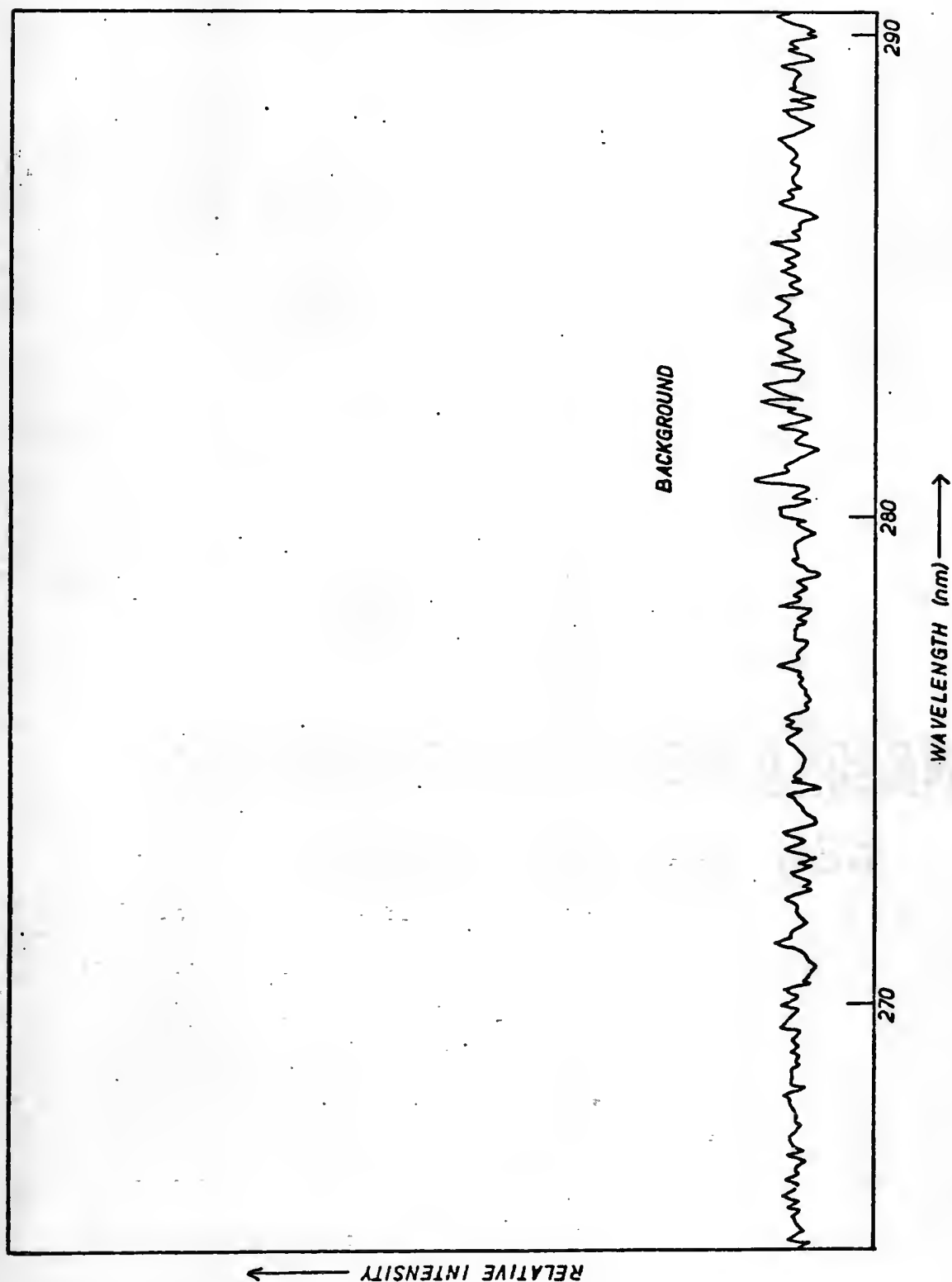


Figure 15.-- Atomic fluorescence background with the single channel scanning spectrometer.

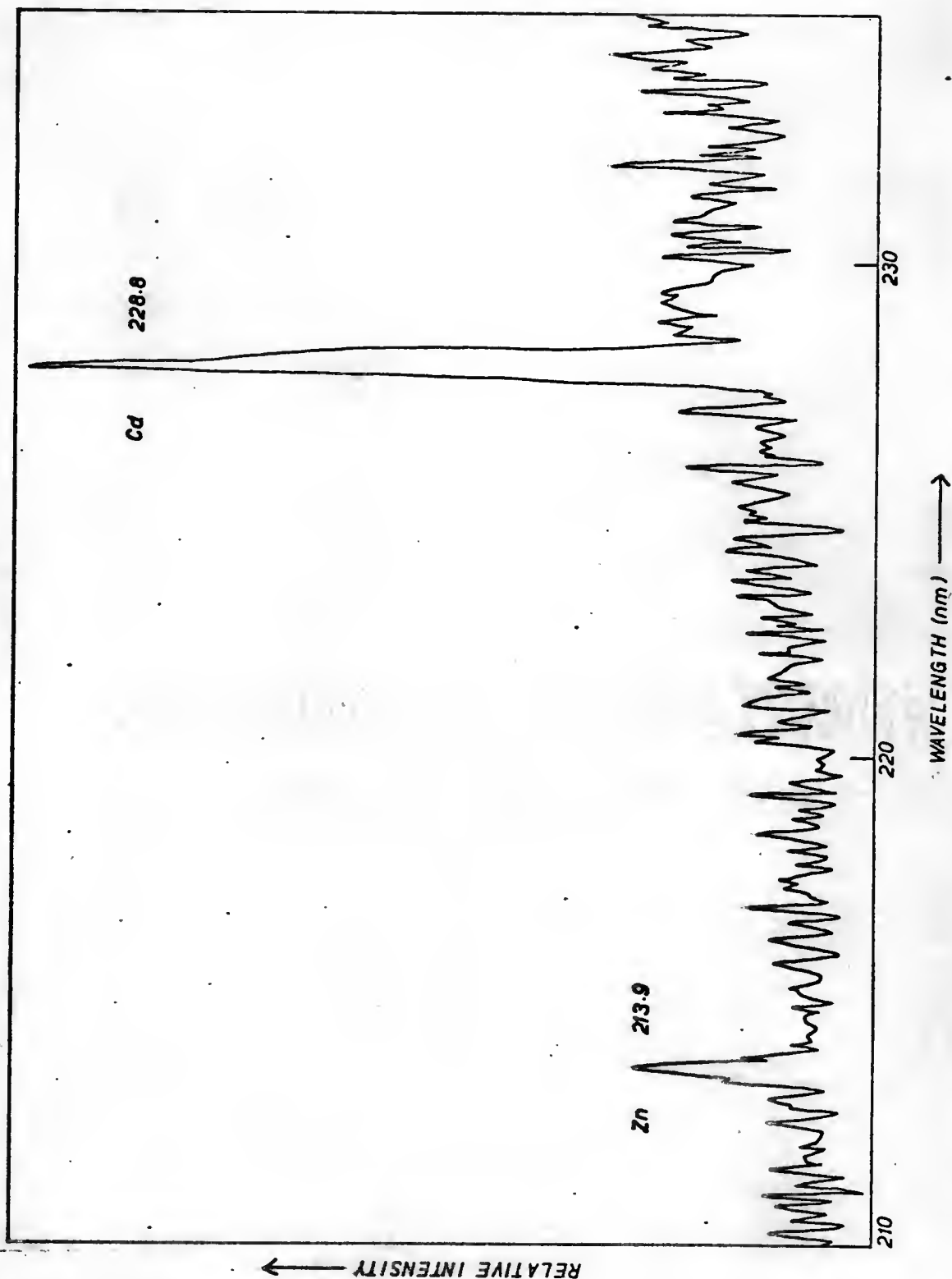


Figure 16.-- Atomic fluorescence of $1 \mu\text{g ml}^{-1}$ each Zn and Cd with the single channel scanning spectrometer.

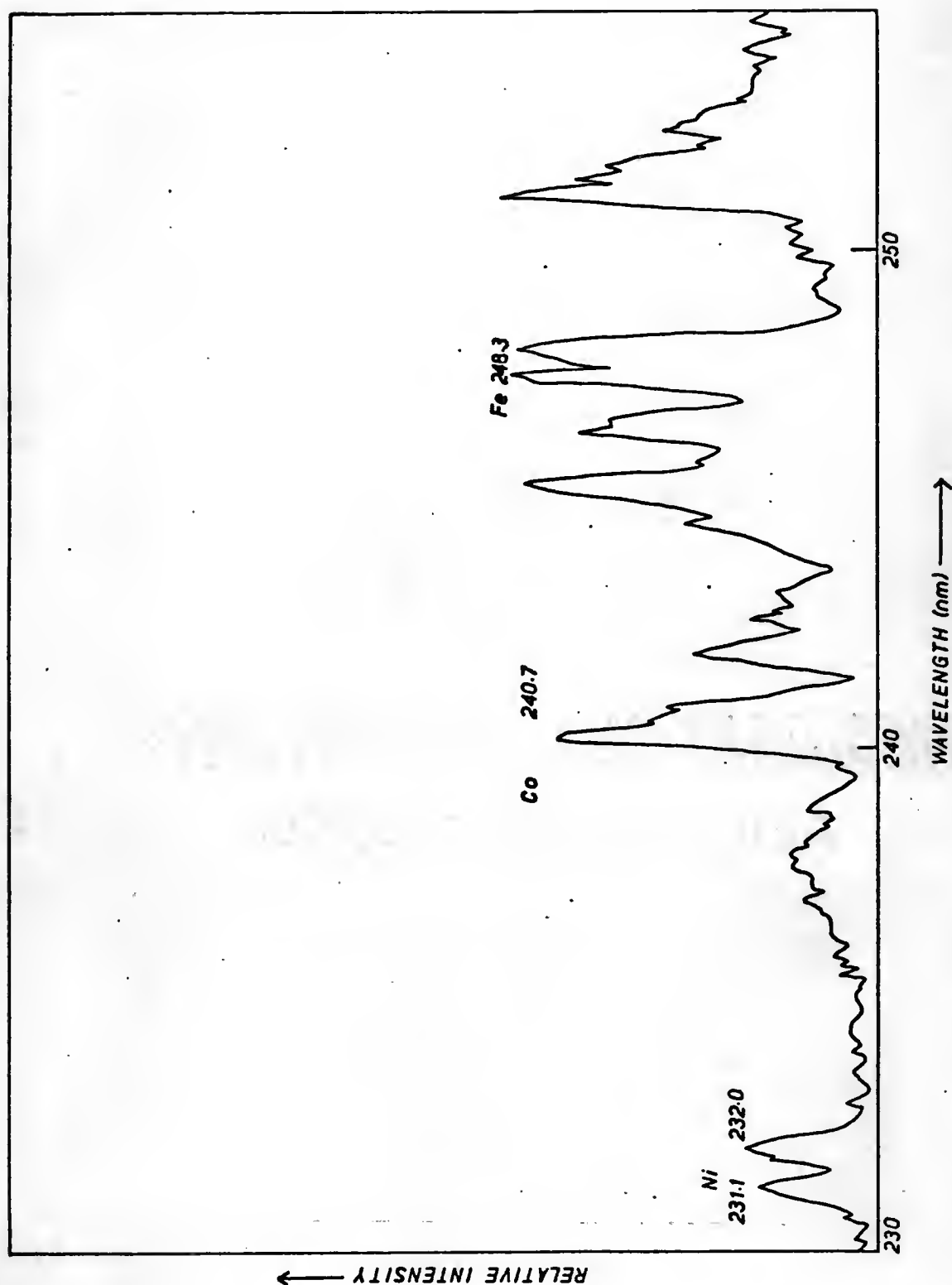


Figure 17.-- Multielement atomic fluorescence of $10 \mu\text{g ml}^{-1}$ each Ni, Co and Fe with the single channel scanning spectrometer.

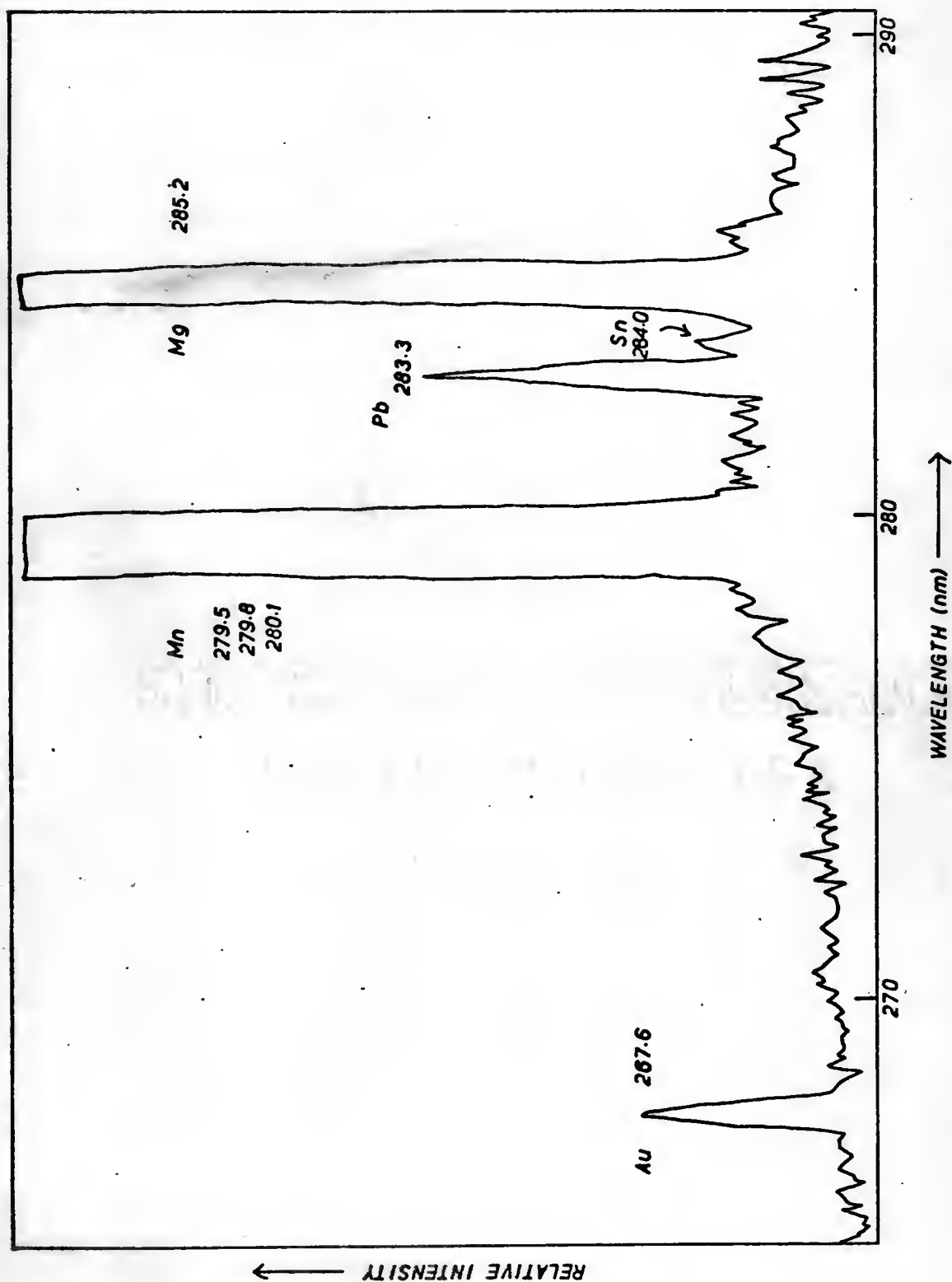


Figure 18.-- Multielement atomic fluorescence of $30 \mu\text{g ml}^{-1}$ each Au, Mn, Pb, Sn and Mg with the single channel scanning spectrometer.

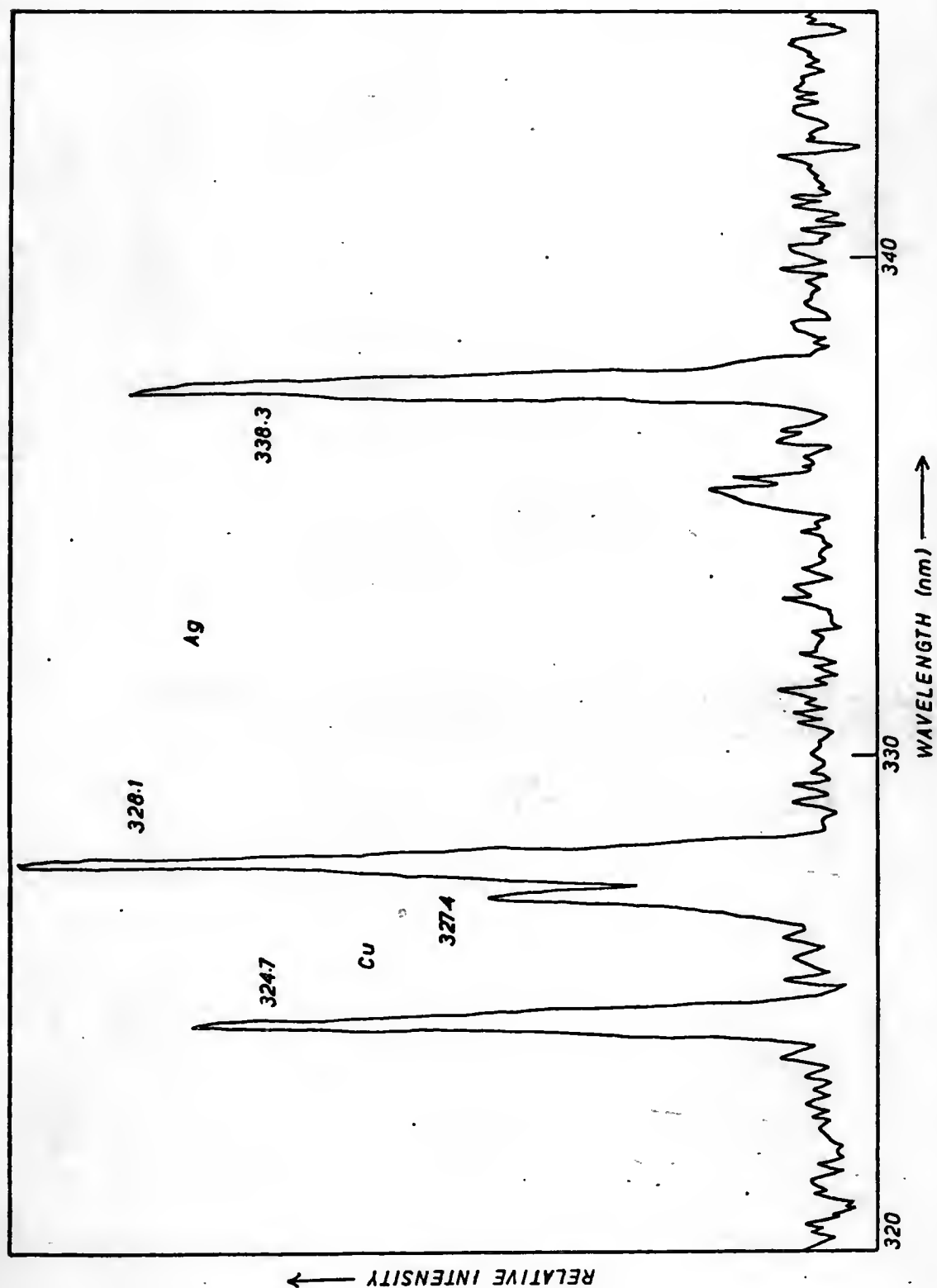


Figure 19.-- Atomic fluorescence of $1 \mu\text{g ml}^{-1}$ each Cu and Ag with the single channel scanning spectrometer.

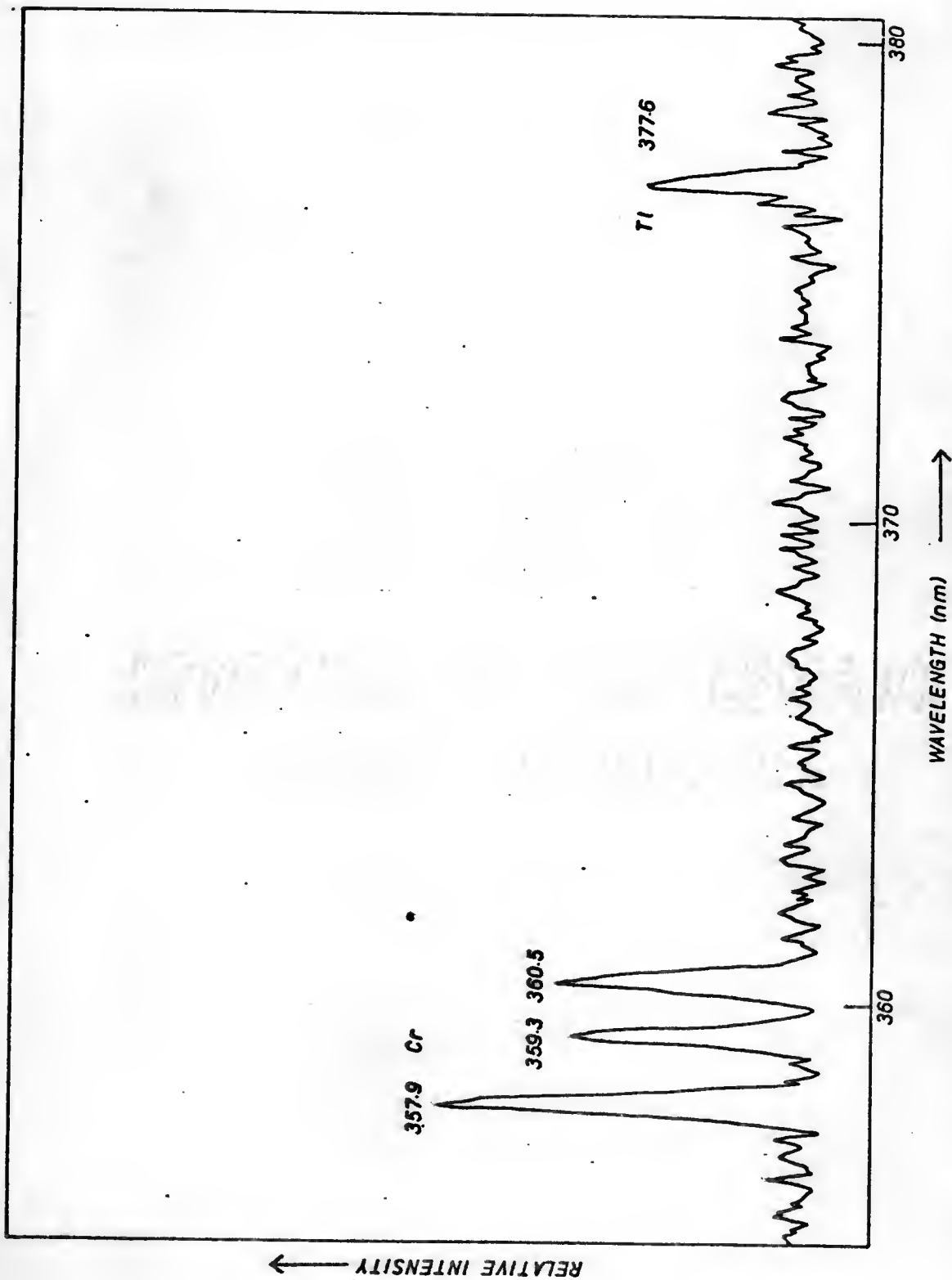


Figure 20.-- Atomic fluorescence of $1 \mu\text{g ml}^{-1}$ each Cr and Tl with the single channel scanning spectrometer.

The analytical working curves for the 14 elements studied with the SCSS system are shown in Figure 21 and Figure 22. The shapes of the curves are expected for AFS with a continuum source (59). The curves for Pb (measured at 283.3 nm) and Sn (measured at 284.0 nm) do not have the characteristic slope of 1, probably because of the strong influence of the Mg fluorescence (measured at 285.2 nm). The limits of detection, defined as the concentration of analyte which would result in a signal two times the rms noise on the background, for the 14 elements are listed in Table 8.

The background in the 230.0 nm to 255.6 nm wavelength region was seen to contain significant flame fluorescence background (see Figure 23). The effect of the background on elemental analysis in this region is shown clearly in Figure 24, which gives the spectrum of $30 \mu\text{g ml}^{-1}$ each of Ni, Co and Fe. The molecular species involved in this background is believed to be CO (58).

The S/N of any spectral interval of the SCSS should, according to Chapter II, be independent, as far as the resolution and stray light capability of the optical system allows, of the signal in any other spectral interval. To check this premise, and as a comparison with the HTS system, dissimilar concentrations of elements within a wavelength scan were aspirated, and plots made of the intensity vs. wavelength. In Figure 25, the lack of any interelement effects of a mixture of $10 \mu\text{g ml}^{-1}$ Zn plus $1 \mu\text{g ml}^{-1}$ Cd and a further mixture of $10 \mu\text{g ml}^{-1}$ Zn and $0.3 \mu\text{g ml}^{-1}$ Cd is shown. The results for Cd are unchanged and are also the same as if equal concentrations of Zn and Cd were used. If $700 \mu\text{g ml}^{-1}$ Co is combined with $10 \mu\text{g ml}^{-1}$ each Fe and Ni, the Co fluorescence lines are extremely intense (Figure 26) but, except for a rise in the baseline, the Ni and Fe signals remain the same as when

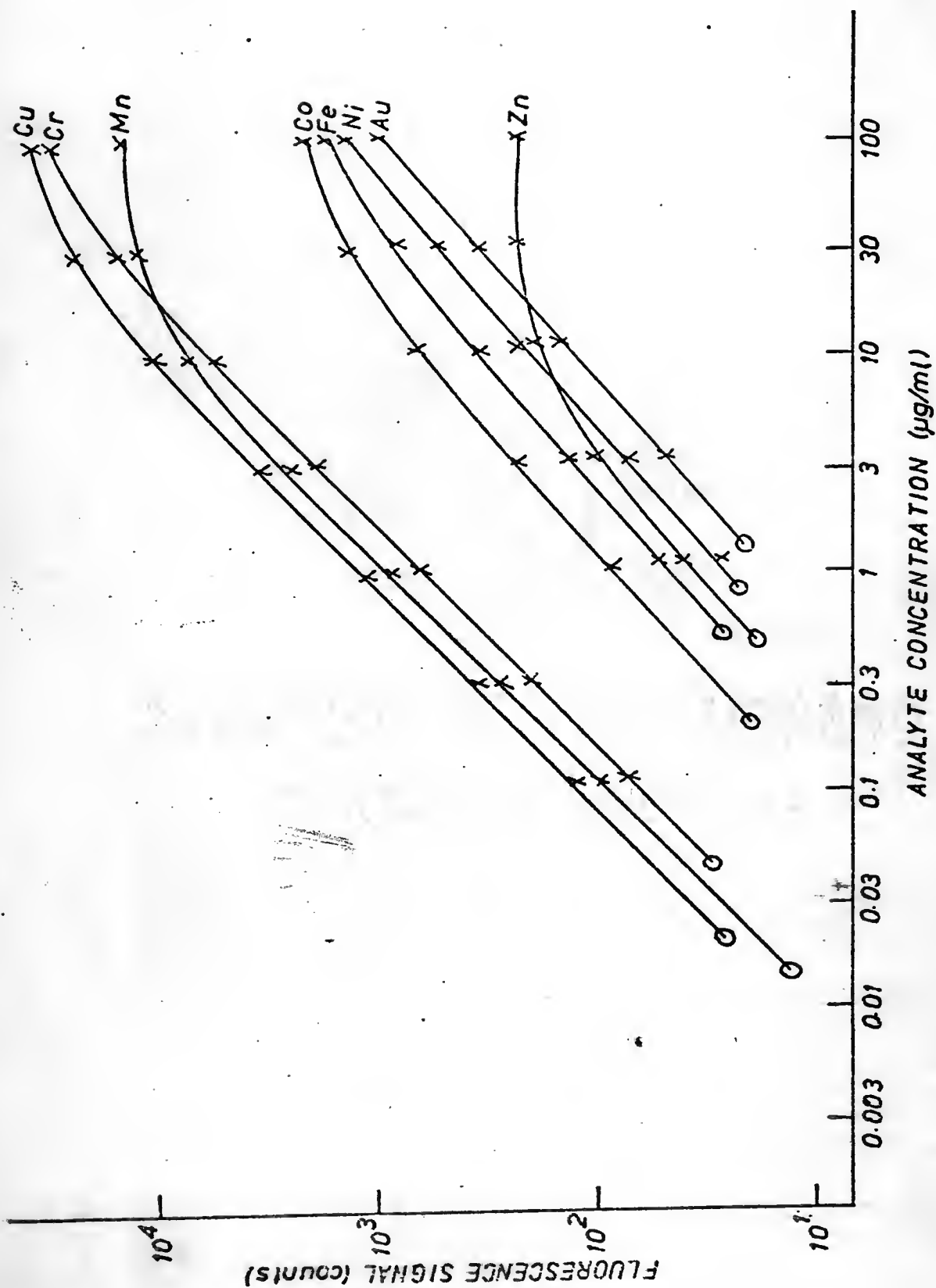


Figure 21.-- Analytical curves obtained for Au, Co, Cr, Cu, Fe, Mn, Ni and Zn with the single channel scanning spectrometer.

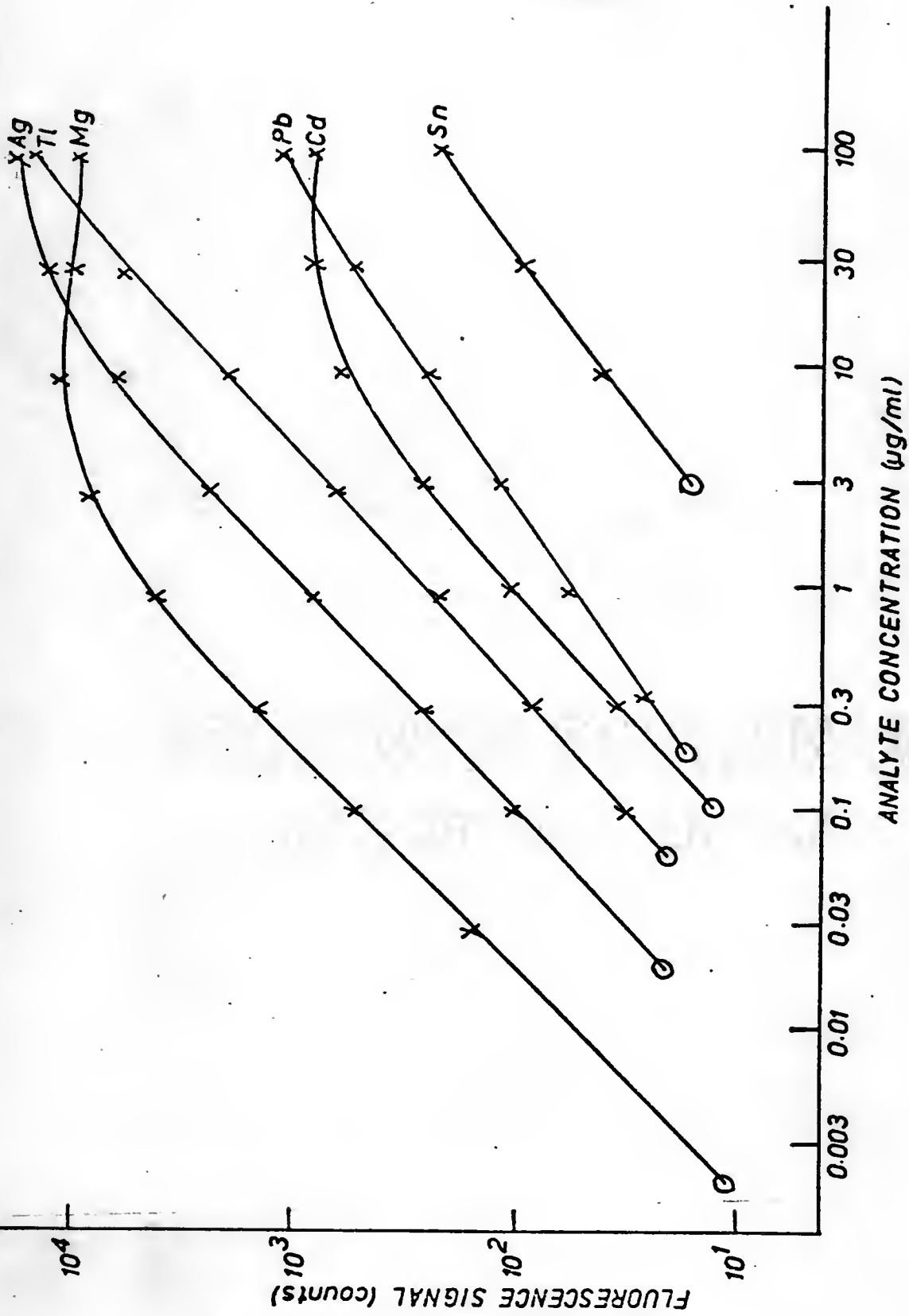


Figure 22.-- Analytical curves obtained for Ag, Cd, Mg, Pb, Tl and Sn with the single channel scanning spectrometer.

TABLE 8
LIMITS OF DETECTION (LOD'S) FOR THE ELEMENTS
ANALYZED BY THE SCSS SYSTEM

| <u>ELEMENT</u> | <u>WAVELENGTH</u> | <u>LOD(this work)</u> <u>$\mu\text{g ml}^{-1}$</u> | <u>LOD(reference 53)</u> <u>$\mu\text{g ml}^{-1}$</u> |
|----------------|-------------------|--|---|
| Zn | 213.7 | 0.3 | 7 |
| Cd | 228.8 | 0.1 | 0.08 |
| Ni | 232.0 | 0.6 | 10 |
| Co | 240.7 | 0.2 | 1 |
| Fe | 248.3 | 0.4 | 5 |
| Au | 267.6 | 1 | - |
| Mn | 279.5 | 0.01 | 0.2 |
| Pb | 283.3 | 0.2 | 20 |
| Sn | 284.0 | 3 | 5 |
| Mg | 285.2 | 0.002 | 0.04 |
| Cu | 324.7 | 0.02 | 0.2 |
| Ag | 328.1 | 0.02 | 0.05 |
| Cr | 357.9 | 0.04 | - |
| Tl | 377.6 | 0.06 | 1 |

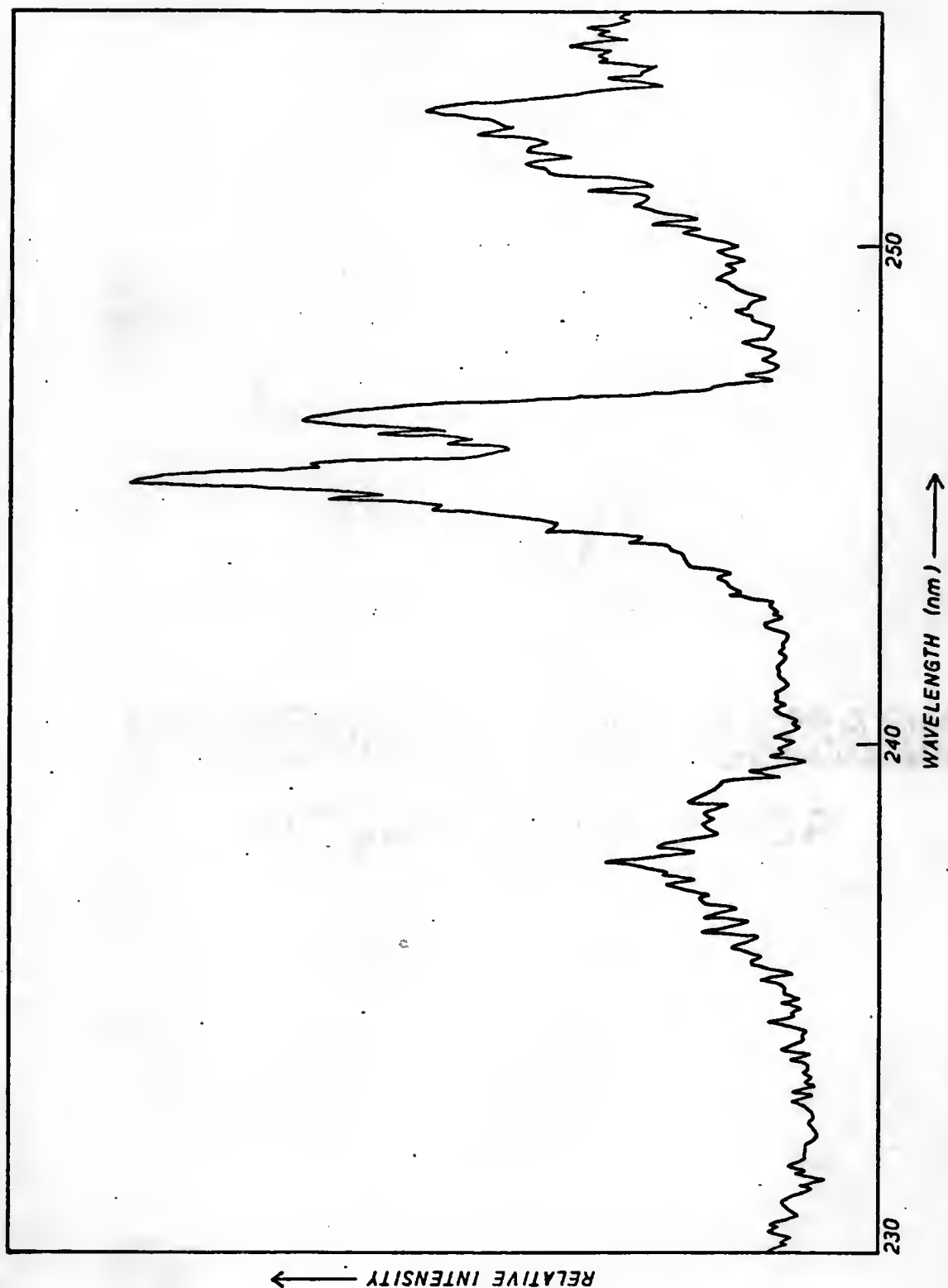


Figure 23.-- Flame fluorescence in the 230 nm - 255 nm region.

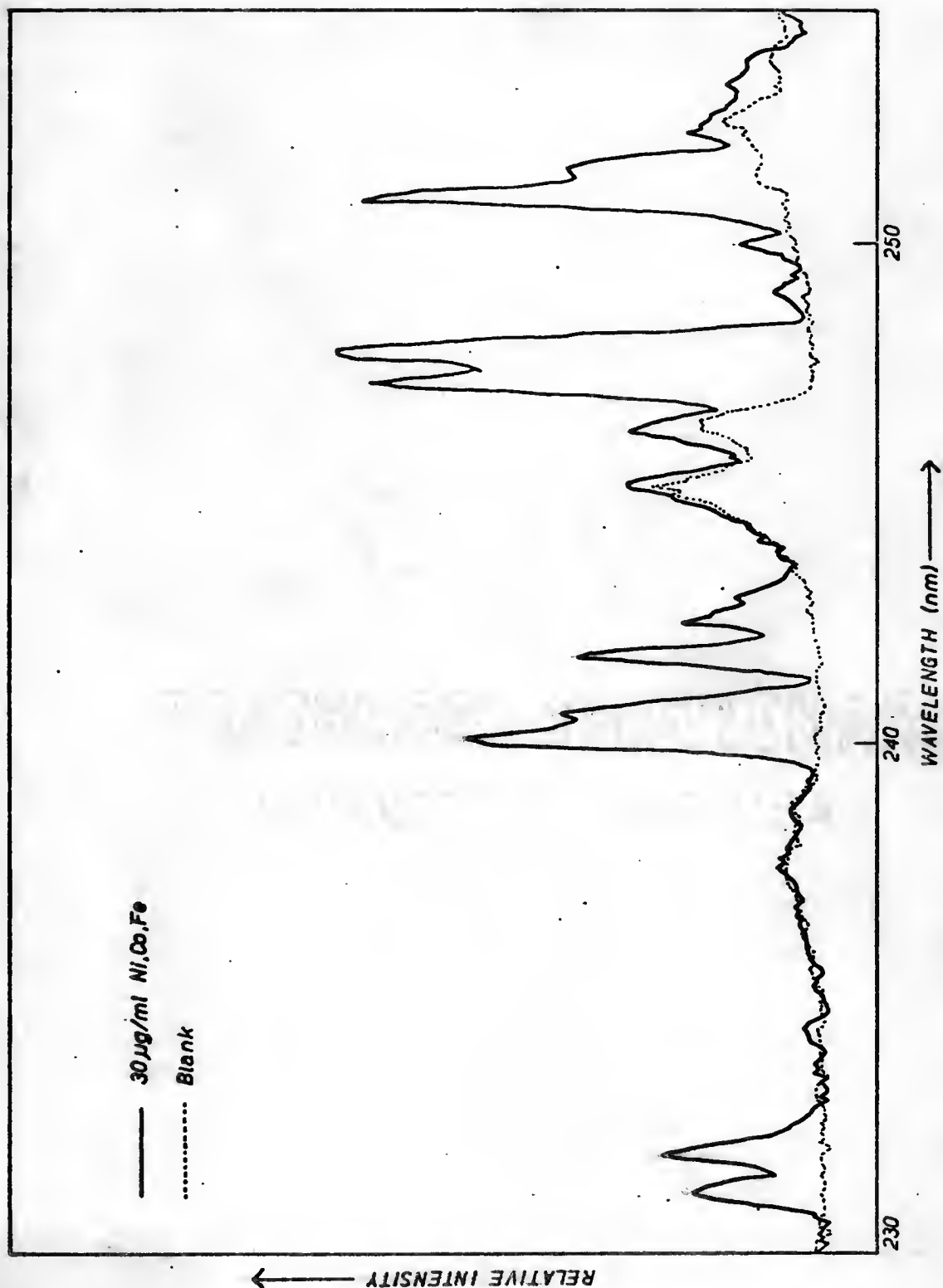


Figure 24.-- The effect of flame fluorescence on atomic fluorescence in the 230 nm to 255 nm region with the single channel scanning spectrometer.

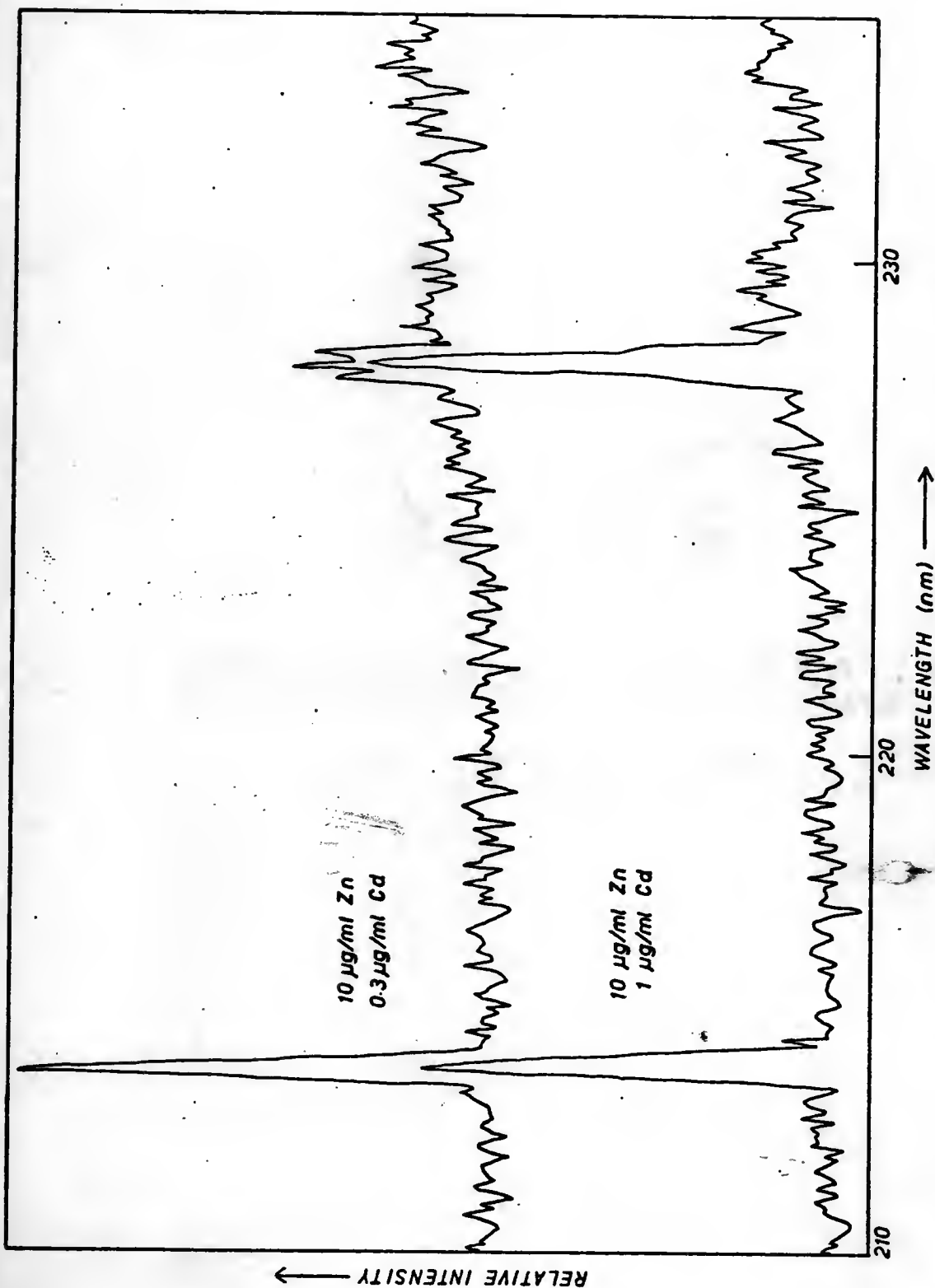


Figure 25.-- Two spectra showing no interference with Cd atomic fluorescence in the presence of 10 µg ml⁻¹ Zn with the single channel scanning spectrometer.

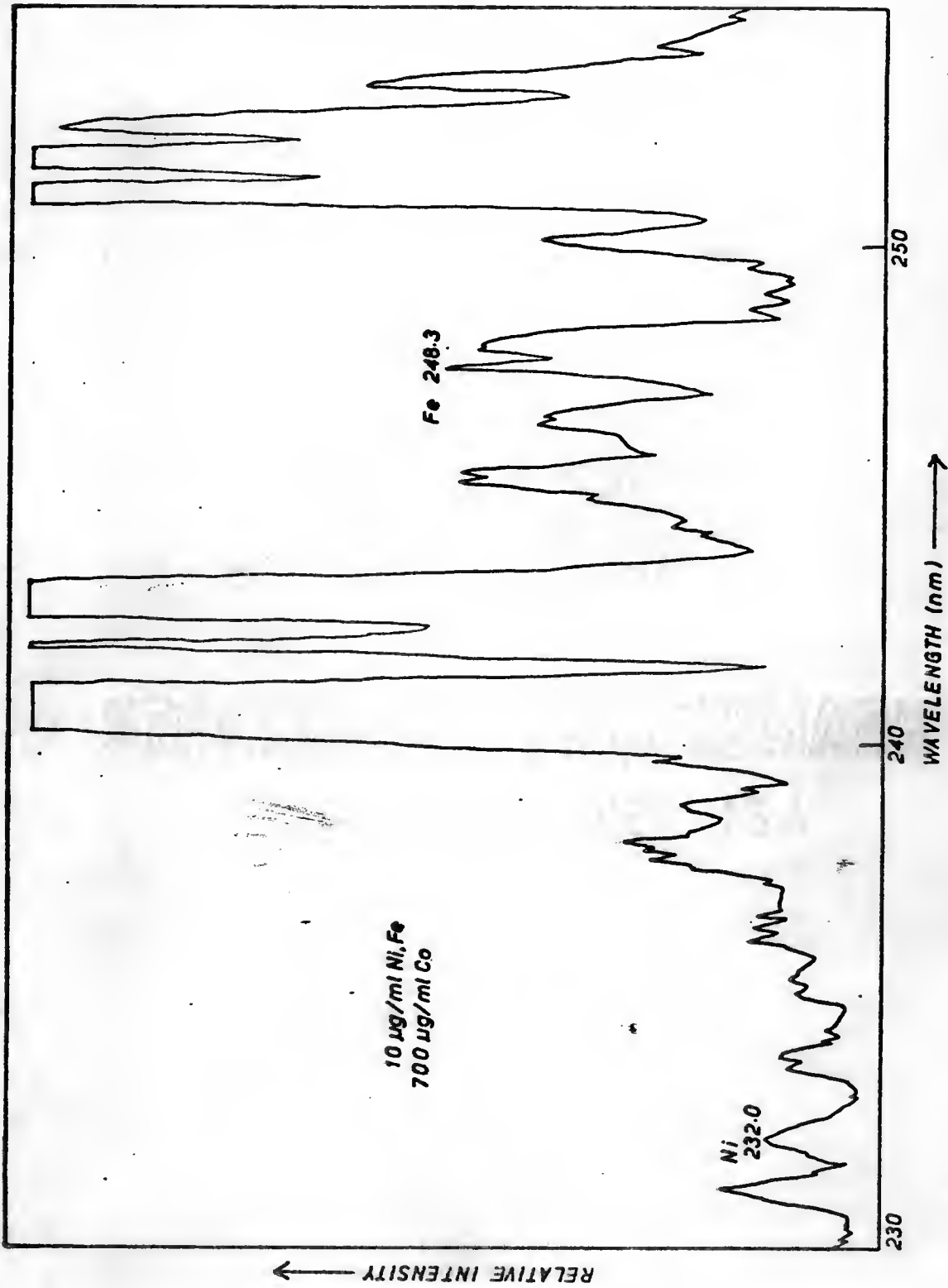


Figure 26.-- Atomic fluorescence of Ni and Fe in the presence of a high concentration of Co with the single channel scanning spectrometer.

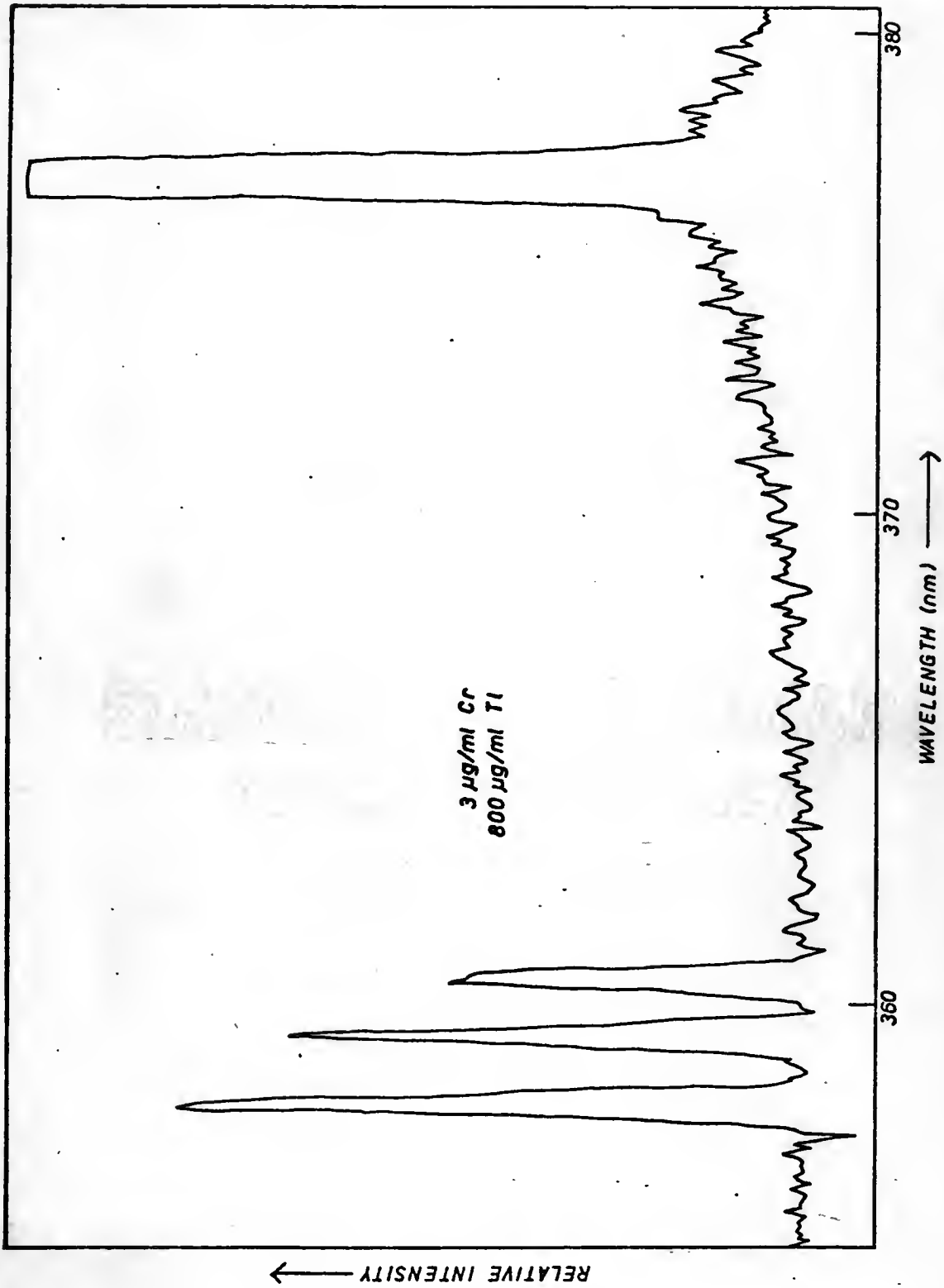


Figure 27,-- Atomic fluorescence of Cr in the presence of a high concentration of Tl with the single channel scanning spectrometer.

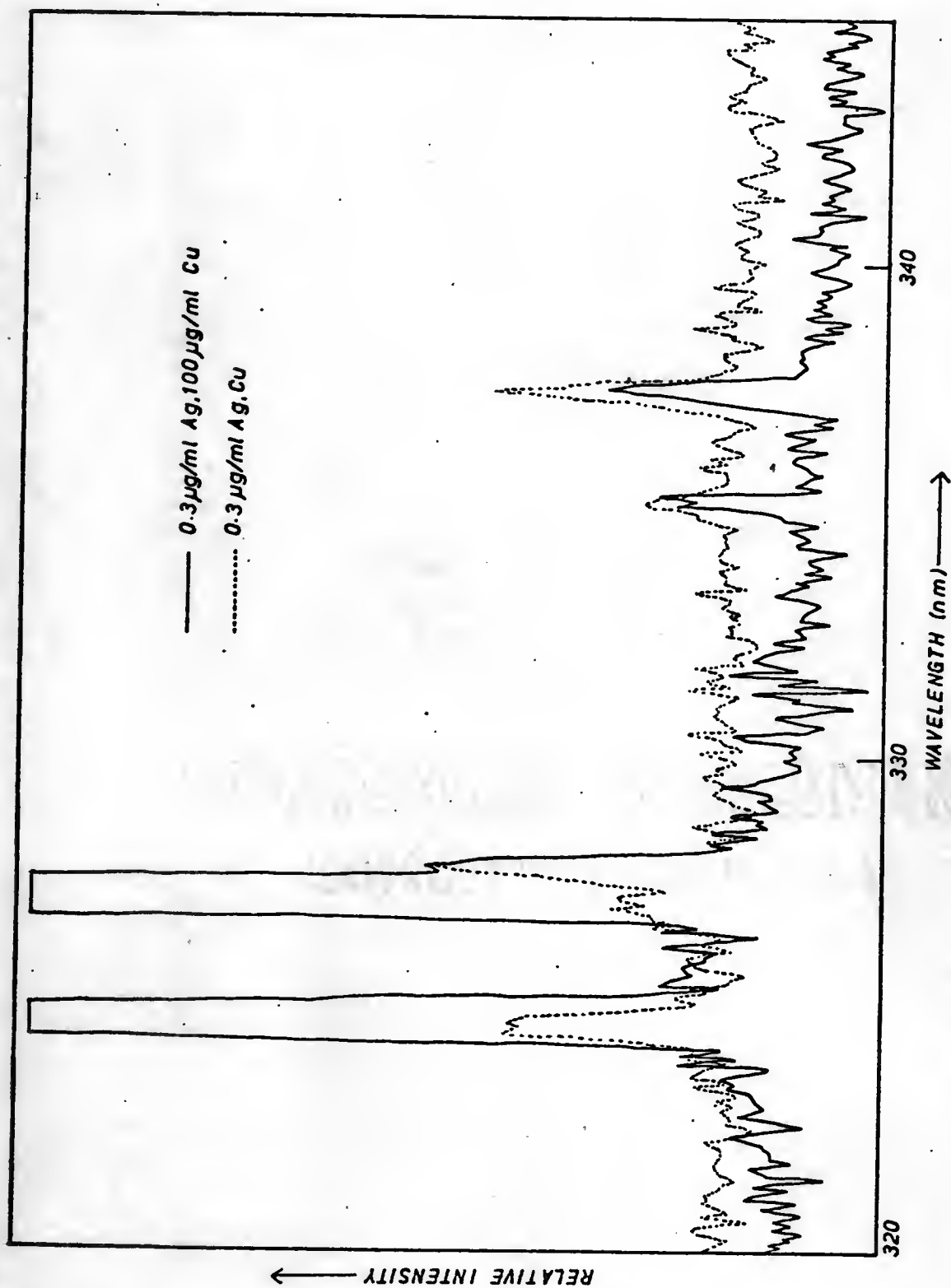


Figure 28.--- Two spectra showing no interference with Ag atomic fluorescence in the presence of a high concentration of Cu with the single channel scanning spectrometer.

the concentrations of all three were the same. In Figure 27, $800 \mu\text{g ml}^{-1}$ Tl has essentially no effect on the signal from $3 \mu\text{g ml}^{-1}$ Cr. However, $100 \mu\text{g ml}^{-1}$ Cu raised the background substantially in the vicinity of the 327.4 nm Cu line and the 328.1 nm Ag line. Even here, as shown in Figure 28, no effect on even the 328.1 nm Ag line is noticed if the increase in background is taken into account. It is apparent that, within the limits of the dispersive system, no adverse effects of spectral interference are noticed with the SCSS system.

CHAPTER VI

COMPARISON OF MULTIPLEX AND SCANNING TECHNIQUES

The Hadamard transform spectrometer (HTS) and the single channel scanning spectrometer (SCSS) share almost every hardware feature and the design and construction of these two instruments is similar with respect to time and costs. The HTS system does require a relatively expensive, precision mask for coding the spectral interval intensities. Furthermore, the multiplex method requires some mask alignment precautions to assure that the mask is in the correct optical position. Otherwise, the complete systems are similar in operating characteristics. Because the HTS system used a shorter dynamic range analog lock-in amplifier, it was necessary to change scales to obtain the optimum S/N benefit from the system. However, a photon counting system could eliminate the problem in the HTS system as it did in the SCSS.

Software considerations show that the HTS system software is somewhat more complex than the SCSS software. Because some logical functions and comparisons must be performed to determine the addition/subtraction process and further decisions are necessary to complete the final permutation of the stored values, so that a monotonically increasing spectrum results (see Chapter IV), the HTS software requires both moderate assembly programming effort and some time during the scan.

The SCSS, on the other hand, is essentially straightforward data accumulation and stepping functions. In each case, the final data are stored in digital form within the computer, and are available for various filtering, integration or comparison purposes.

The wavelength range of the HTS is determined by the dimensions of the mask and the dispersion of the grating. Likewise, the resolution is limited to one point for each channel determined and in this study. The wavelength range was about 25.0 nm with maximum resolution of about 0.1 nm per channel. If more than one wavelength region is to be studied, the grating must be manually slewed from one region to the next. Indeed, this function could be incorporated under computer control, but this would involve more hardware and software considerations.

The SCSS is essentially limited only by computer memory storage locations and in the present case more than 4000 data points could be stored. The total number of points accumulated in a scan is software controlled. Also, the resolution capabilities of the SCSS are limited to 48 points per nm, a factor of about 4.8 more than with the HTS. The number of points per nm is also under software control, and so, in the SCSS, both the wavelength range and the resolution can be controlled by the software.

From these considerations, it can be noted that the HTS system is essentially a SCSS with a few more problems and complexities added on and a little less versatility. The use of the multiplex HTS system in the area of multielement atomic fluorescence analysis can only be justified if this method can improve on the sensitivity of rapid AFS analysis.

A comparison of the results of the two methods shown in Chapters IV and V is probably best seen in the limits of detection (LOD's)

obtained for similar elements by the two methods. Because the analysis time was almost the same for the two techniques, the ratios of LOD's are good estimates of the S/N ratios of the analytical lines determined in a multiplex compared to a single channel mode. The HTS resulted in LOD's worse by a factor of 50 to 500 in the eight elements common to the two systems as seen in Table 9. The other 6 elements, studied with the SCSS, could not be determined with the HTS (except for Tl which was not attempted with the multiplex method) because the noise in the multiplex method severely limited the sensitivity of that system.

Because the systems were designed to maintain as many similarities as possible as far as excitation source, flame cell, optics and monochromator speed are concerned, it may be assumed that instrumental influence can account only for a factor of 2 to 5 in the S/N ratios of the two systems. The S/N considerations, described in Chapter II, expect at most a degradation of S/N by a factor of 0.7 in the HTS system if the background is large, and only shot noise is considered. The last part of Chapter II considers the effect of proportional noise (fluctuation or scintillation noise (52)) in multiplex systems. It can be determined that if the noise due to scatter from the flame or molecular fluorescence from the flame is the major source of noise in the HTS system used in this study, then the S/N ratio of the HTS system may be degraded by as much as 16 (the square root of the increase of the number of spectral intervals measured) when compared with the SCSS. This, combined with other small factors, may account for the ratios in the LOD's found in the two systems.

The increase in the intensities measured with a multiplex method is fundamental in the expected increase in S/N. When this increase in signal is enough to allow noise, proportional to a high

TABLE 9

COMPARISON OF LIMITS OF DETECTION (LOD'S)
WITH THE HTS AND SCSS SYSTEMS.

| <u>ELEMENT</u> | <u>HTS LOD</u> <u>ug ml⁻¹</u> | <u>SCSS LOD</u> <u>ug ml⁻¹</u> | <u>RATIO</u> <u>HTS</u> <u>SCSS</u> |
|----------------|---|--|--|
| Ni | 40 | 0.6 | 67 |
| Co | 25 | 0.2 | 125 |
| Fe | 25 | 0.4 | 63 |
| Mn | 5 | 0.01 | 500 |
| Mg | 1 | 0.002 | 500 |
| Cu | 5 | 0.02 | 250 |
| Ag | 2 | 0.02 | 100 |
| Cr | 5 | 0.04 | 125 |

background level, to prevail over the random, photon noise of lower signal levels, then the multiplex method has serious disadvantages compared with a single channel system. This seems to be the case with multielement atomic fluorescence flame spectrometry.

It is appropriate to consider the premise that a wavelength scan is actually necessary in multielement analysis. Measuring the intensity at wavelengths where no analytical line can appear is certainly a waste of analysis time (unless an off-wavelength intensity is desired) which could be put to better use by increasing the measurement time (and thereby the S/N ratio) at spectral intervals of interest. Overcoming the analyst's preference for an intensity vs. wavelength spectrum is of primary importance to rapid multielement analysis.

CHAPTER VII

PROGRAMMED SLEW SPECTROMETER (PSS) SYSTEM

Preliminary Discussion

The conclusion of Chapter VI leads naturally to the suggestion that analysis time can be reduced substantially if intensities are measured only at the wavelengths of interest in multielement atomic fluorescence. Such a programmable slewing system would rapidly and accurately slew to specific wavelengths, make measurements for some time and then slew to another wavelength. In this way, little time would be wasted between spectral intervals of interest. The signal-to-noise relationships for the single channel scanning spectrometer would still hold for the individual spectral intervals. If the time spent slewing to the wavelength is considerably shorter than the measurement time, then S/N ratios can be increased by spending more time with useful measurements. For the shot noise limited case, the S/N is proportional to the square root of the measurement time. Now, if there are five spectral intervals of interest in a 25.0 nm wavelength region and the slewing rate is 20 nm s^{-1} , the intensities at the five wavelengths can be measured for 5 s each, and the total analysis time would be about 26 s. The S/N of each of the spectral intervals would increase by a factor of $(5/0.1)^{\frac{1}{2}}$, or about 7, as compared to the scanning system where the spectral intervals are measured for 0.1 s each.

The equipment for such a programmable monochromator is completely contained in the single channel scanning spectrometer. The computer is able to slew the grating at 20 nm s^{-1} by use of the stepper motor. All that is necessary is additional software for the computer.

Description of Software

An assembly language program was developed to accept a list of elements from the teletype and convert these atomic symbols to stepper motor steps necessary to slew from 190.0 nm to the analytical wavelength. The element symbols can be typed in any order - the computer sorts them according to increasing wavelength. After the elements are specified, the computer asks if a background scan should be performed and if desired the computer will store the background intensities at each analytical wavelength while a blank solution is being aspirated. This background will be subtracted during subsequent cycles. At each spectral interval, the computer gathers the DATA, BACKGROUND, SUM and DIFFERENCE for each chopper cycle (see Chapter V) and sums them individually for 255 chopper cycles (about 5 s). At that time, each of these readings is printed out, with the atomic symbol of the element at that wavelength, by a high speed printer. If a background had been stored, it is subtracted before printing, and if no background subtraction is made, a symbol is printed denoting that the reading is uncorrected. The monochromator is slewed to the next spectral interval, and the process is continued. Alternatively, a command will allow the computer to wait at the wavelength and take more readings, continuing only on command from the keyboard.

A separate routine is used in conjunction with a mercury penlight for alignment of the monochromator/stepper/computer system. The penlight

is placed in the monochromator optical path and the slits are closed to 5 μm . On command, the computer slews the wavelength to within 5 nm of the 253.7 nm line of mercury. It then scans rapidly until the intensity reading reaches a peak and starts to fall off. The computer then considers this point to be one step beyond the mercury line and proceeds backwards until it has set the monochromator at exactly 190.0 nm. This procedure takes only a few minutes and allows excellent alignment of the system.

Analytical Procedure with the PSS System

A solution of 50 $\mu\text{g ml}^{-1}$ each (and listed in Table 10) of the elements analyzed by the SCSS was prepared from 1000 $\mu\text{g ml}^{-1}$ stock solutions. Silver was not included because AgCl precipitate was formed by the reaction of Ag^+ with the chloride from HCl used in preparing stock solutions of some elements. Serial dilutions were prepared from the mixture until the least concentrated solution contained 0.01 $\mu\text{g ml}^{-1}$ of each element.

The programmed slew spectrometer (PSS) was initialized, the source started and allowed to warm-up, the electronics energized and the computer program was loaded and started. Before the analysis, an alignment procedure, described in the previous section, was performed with a mercury penlight. Then, the 13 elements were entered on the keyboard and the analysis was begun.

A background run was stored while aspirating deionized water. Then each of the standard solutions was aspirated, and the system slewed the spectrometer, measured the intensities and printed the results for each element of interest. Ten complete replicates of the above procedure were done for the entire range of standards. The analysis

TABLE 10
LIMITS OF DETECTION (LOD'S) WITH THE PSS

| <u>ELEMENT</u> | <u>WAVELENGTH</u> | <u>LOD(this work)^a</u> | <u>LOD(ref. 53)^a</u> |
|----------------|-------------------|-----------------------------------|---------------------------------|
| Zn | 213.7 | 0.05 | 7 |
| Cd | 228.8 | 0.01 | 0.08 |
| Ni | 232.0 | 0.2 | 10 |
| Co | 240.7 | 0.06 | 1 |
| Fe | 248.3 | 0.08 | 5 |
| Au | 267.6 | 2 | - |
| Mn | 279.8 | 0.003 | 0.2 |
| Pb | 283.3 | 0.06 | 20 |
| Sn | 284.0 | 0.1 | 5 |
| Mg | 285.2 | 0.0005 | 0.04 |
| Cu | 324.7 | 0.002 | 0.2 |
| Cr | 357.9 | 0.006 | - |
| Tl | 377.6 | 0.01 | 1 |

^aLimits of detection are measured in $\mu\text{g ml}^{-1}$.

time for each of the solutions was 86 s. The wavelengths used for each of the elements of interest are listed in Table 10.

Results and Discussion

The printed results were analyzed and growth curves from the averages of results are depicted in Figures 29 and 30. As expected, the results are very similar to the results obtained for the SCSS with some additional extension towards lower limits. The limits of detection for the 13 elements are listed in Table 10.

The analysis time of 86 s represents a factor of 2 better than if the SCSS were used to cover the wavelength range covered in the PSS. (213.7 nm to 377.6 nm could be covered in 164 s at 1 nm s^{-1} with the SCSS.) When the increase of sensitivity of about 7 is also considered, it can be seen that the PSS is more than an order of magnitude better as far as speed-sensitivity is concerned. If an intensity vs. wavelength spectrum is not necessary then the PSS is the system of choice for multielement AFS.

Normal precautions must be made with regard to spectral overlap and precise background corrections. For example, the large signal from Mg fluorescence at 285.2 nm affects the intensity observed for Sn at 284.0 nm and Pb at 283.3 nm. This is the probable cause of the non-unity slope of the analytical curve observed in Figure 29 for Pb and in Figure 30 for Sn. Alternative spectral lines should be considered if this condition is evident in the real analytical situation. Also, it may be more appropriate to sample an off-wavelength spectral interval intensity rather than store a blank for the background correction. These functions can be implemented with suitable software but have not been considered in this study. The results for Au at 267.6 nm are

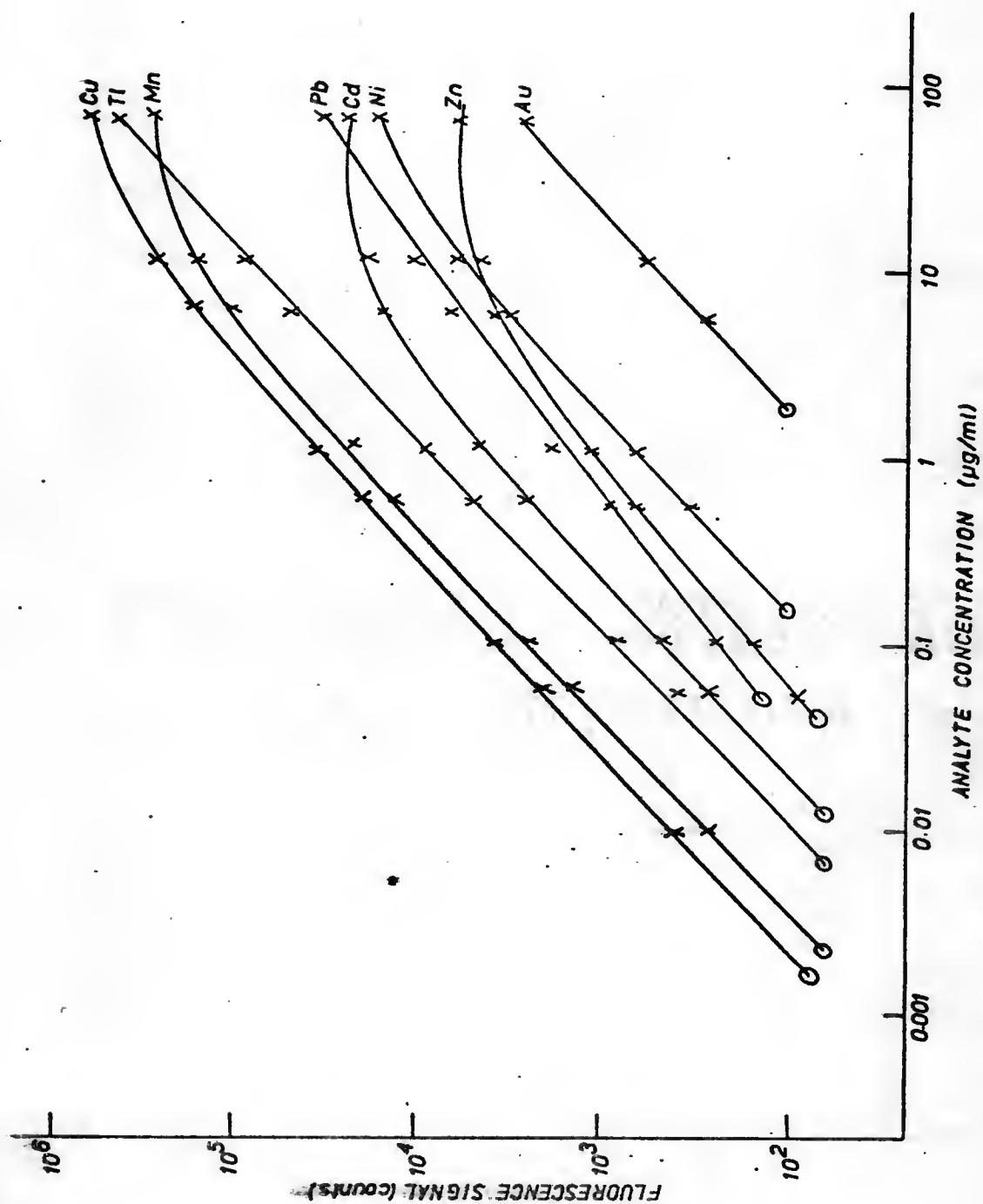


Figure 29.-- Analytical curves obtained for Au, Cd, Cu, Mn, Ni, Pb, Tl and Zn with the programmed slow spectrometer.

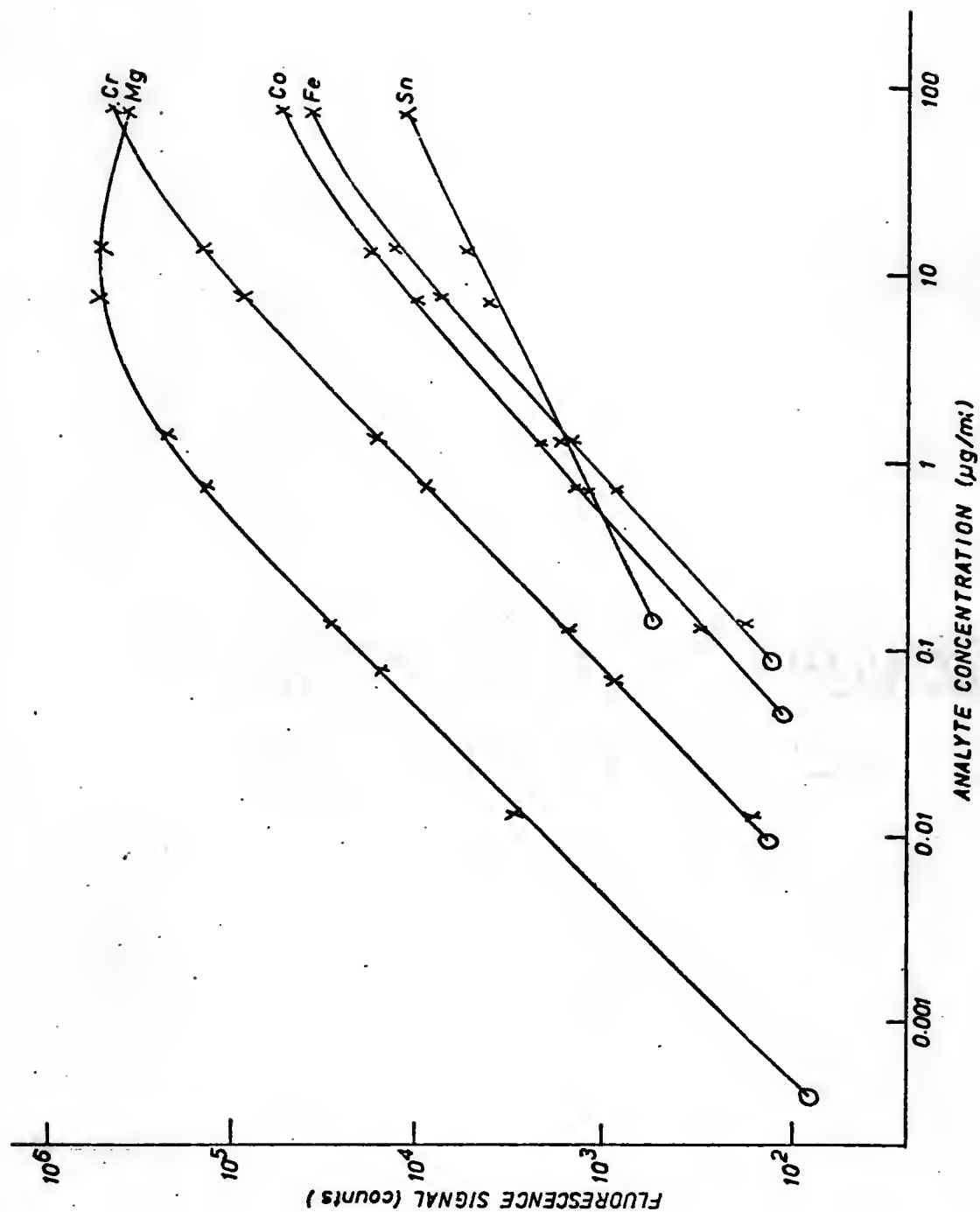


Figure 30.-- Analytical curves obtained for Co, Cr, Fe, Mg and Sn with the programmed slew spectrometer.

somewhat poorer than the results obtained with the SCSS (2 ug ml^{-1} vs. 1 ug ml^{-1} respectively). The mixture of elements, prepared for the PSS, had some finely, divided metallic precipitate after standing for a period and analysis of this precipitate showed it to be Au. This type of interference must be carefully avoided and a dedicated study of multielement standard solution preparation is certainly needed.

The tabulated results, printed in digital form, are free from operator bias and require no judgment as to baseline or peak values. With further software refinements, it would be possible to have the computer determine the analytical curves for each element of interest and then calculate the concentrations of the elements in unknown samples and present the results as a finished report. The assembly language programming of this level of software sophistication is a matter best left to computer programmers.

CHAPTER VIII

COMPARISON OF THE THREE SYSTEMS

Three spectrometric systems have been constructed and evaluated for the purpose of achieving rapid analysis of multielement samples. In each case, the best equipment available was used for the construction. This procedure resulted in the best possible devices, but unfortunately, disallowed an accurate comparison of the techniques on their own merits. Nevertheless, the experimental results lead to several conclusions. First, Hadamard transform spectrometry in the UV-visible region is very sensitive to the high backgrounds found in flame spectrometry and to the time-varying fluctuations in the background. The single channel scanning spectrometer and programmed slew spectrometer systems are not as sensitive to this type of signal fluctuation, because only one channel and one instant in time is used in the latter systems. Second, if HTS systems are to function with the theoretical advantage in the UV-visible region, then every effort should be made to keep the background as low as possible, and also the dynamic range and response of the detector should be as large and as fast as is possible. The photon counting system used in the SCSS would probably make an ideal detector for a future HTS system. Finally, and most important, is the consideration of the necessity of a wavelength scan. If a scan is not necessary, then a

system of slewing, stopping and measuring is more appropriate and versatile than the SCSS for multielement atomic analysis. This approach is only an extension of the original procedure of sequential analysis; but with the same type of equipment as used in the scanning methods, it is possible to devise a system which will determine elemental concentrations at any desired wavelength and in less time than would be spent scanning over informationless spectral regions. The limits of detection found for the three systems studied in this work are tabulated in Table 11. It is readily apparent that the PSS is faster and more sensitive than either the HTS or the SCSS. The S/N relationships can even be programmed so that the measurement phase of the cycle is a time-dependent function of the counting rate. This would allow for more time to be spent measuring low level signals while less time could be spent where the signal level is high. Because of the versatility in wavelength selection and S/N relationships, this slewing system is undoubtedly the most useful multielement measurement system available at the present time.

TABLE 11
LIMITS OF DETECTION^a (LOD'S) COMPARED
FOR THE THREE SYSTEMS STUDIED IN THIS WORK

| <u>ELEMENT</u> | <u>LOD-HTS</u> <u>$\mu\text{g ml}^{-1}$</u> | <u>LOD-SCSS</u> <u>$\mu\text{g ml}^{-1}$</u> | <u>LOD-PSS^b</u> <u>$\mu\text{g ml}^{-1}$</u> |
|----------------|---|--|---|
| Zn | - | 0.3 | 0.05 |
| Cd | - | 0.1 | 0.01 |
| Ni | 40 | 0.6 | 0.2 |
| Co | 25 | 0.2 | 0.06 |
| Fe | 25 | 0.4 | 0.08 |
| Au | - | 1 | 2 |
| Mn | 5 | 0.01 | 0.003 |
| Pb | - | 0.2 | 0.06 |
| Sn | - | 3 | 0.1 |
| Mg | 1 | 0.002 | 0.0005 |
| Cu | 5 | 0.02 | 0.002 |
| Ag | 2 | 0.02 | - |
| Cr | 5 | 0.04 | 0.006 |
| Tl | - | - | 0.06 |

^a Note: The limit of detection is defined as the concentration of analyte which gives a signal twice the rms noise observed when a blank is measured.

^b The PSS is two times faster than the HTS or the SCSS.

APPENDIX I

AVERAGE SIGNAL-TO-NOISE RATIOS FOR THE UV-VISIBLE SPECTRAL REGION (39).

The Fellgett advantage (F is the gain in signal-to-noise (S/N) ratio for equal analysis time) applies over the entire spectral region of interest when a multiplex method is compared with a single channel (SC) method in the IR spectral region. Consider the specific case of Hadamard transform spectrometry (HTS) measuring N spectral intervals in T s analysis time. Each of the spectral interval intensities is measured for one-half the total analysis time, e.g., $T/2$ s. A scanning system measures each spectral interval for T/N s. Therefore, the increase in measurement time for the HTS case is $(T/2)/(T/N) = N/2$. For a signal with only random errors (as compared with systematic errors) an increase in measuring time is the same as an increase in the number of independent measuring samples. The accuracy of such independent measurements is increased by the square root of the ratio of the measurement times for the HTS and SC systems e.g., $(N/2)^{\frac{1}{2}}$.

In the IR region, the increase in precision is due to the fact that the major source of noise is in the detector and is completely independent of the signal level. At each spectral interval, there is an average gain in S/N of $(N/2)^{\frac{1}{2}}$ in the HTS compared to the SC. In the UV-visible region, low noise photomultipliers are used, and the major

source of noise is shot noise (photon noise or quantum noise) associated with the random arrival of photons at the detector. This noise is proportional to the square root of the signal level (because the arrival statistics follow a Poisson distribution). Since the HTS allows the intensity at about $N/2$ spectral intervals to pass to the detector, the average signal at the detector is $N/2$ times the signal at the detector with a single channel system. The average noise with the HTS is $(N/2)^{\frac{1}{2}}$ times the average noise of the single channel system if only shot noise is considered.

The average gain in precision of the signal, which was shown for the IR, also holds in the UV-visible (still assuming random sources of error) and is $(N/2)^{\frac{1}{2}}$. However, the increase in the average noise level of $(N/2)^{\frac{1}{2}}$ exactly cancels the average accuracy gain, and so no average advantage is found for the HTS in the UV-visible region.

APPENDIX II

THE COMPUTER SYSTEM

Each of the three systems studied in this work made use of a laboratory minicomputer for instrument control, data acquisition, and data presentation. The versatility of software control of various parameters (scan speed, integration time, output format, for example) is a major feature of each of the analytical systems. Further software developments could lead to commercial development of a high speed multi-element trace metal analytical instrument based on atomic fluorescence, which would produce a finished report listing the concentrations of many elements in many samples in a short time with good sensitivity and precision.

The components and sources comprising the computer system are listed in Table 12. The system is based on a Digital Equipment Corporation (DEC) PDP-11/20 minicomputer with 8K (8192 words) of 1.2 μ s access-time core memory. The structure of the PDP-11 is centered around a high speed, bidirectional bus called a "Unibus". This 56-line bus connects the central processing unit (CPU) with the memory and all of the peripherals and provides a common path between any two units on the bus. In this way, any peripheral device can be associated with an unique address and therefore everything connected to the Unibus can be

TABLE 12
COMPONENTS OF THE COMPUTER SYSTEM

| <u>ITEM</u> | <u>DESCRIPTION (MODEL NUMBER)</u> | <u>SOURCE</u> |
|---------------------------------|-----------------------------------|---|
| CPU | PDP-11/20 (8K core memory) | Digital Equipment Corp., |
| ADC | A811 | Maynard, MA 01754 |
| S/H | A404 | |
| DAC(2) | A618 | |
| Digital I/O system | Deckit 11-H | |
| Magnetic Tape Storage system | 2020 | Canberra Industries, Meridan, CT 06450 |
| High Speed Paper Tape Reader | RR 304 | Remex Electronics, Hawthorne, CA 90250 |
| High Speed Printer | 120 | Scope Data Inc., Orlando, FL 32808 |
| Digital Display | DPD-105 | Durgin & Browne Inc., So. Burlington, VT 05401 |
| x-y Recorder | 715M | MFE Corp., Salem, NH 03709 |
| Oscilloscope | 1735D | ITT Corp., Van Nuys, CA 91409 |
| Stepping Motor | HDM-12-480-4 | USM Corp., Wakefield, MA 01880 |

accessed just as core memory locations. This facilitates interfacing and software since no special input/output (I/O) channels or instructions are necessary to input data from a peripheral.

The peripherals implemented on the Unibus are shown in Figure 31. A Teletype is used as the console terminal with a I/O speed of 10 characters per s (cps). A high speed paper tape reader operates at 300 cps, and a high speed printer outputs at 100 cps. The cassette magnetic tape storage system is used for bulk external storage, and a cassette operating software system is used for program development and monitoring functions. With further software refinements, it would be possible to store data on magnetic tape also, and libraries of data files could be stored for later retrieval and manipulation.

The laboratory instrumentation control and data acquisition system is composed of the devices at the top of Figure 31. Analog signals can be digitized with a sample and hold (S/H) amplifier and a 10-bit analog-to-digital converter (ADC). The conversion time with this setup is about 10 μ s, and voltages can be sampled from 0 to +10 volts. The throughput rate with software control is limited to approximately 50 kHz. Two digital-to-analog converters (DAC's) are available to convert 10 bit binary numbers from the computer to 0 to +10 volt levels. With suitable software, one DAC is used for the x axis of an x-y recorder or oscilloscope and the other DAC drives the y axis. Maximum output rates for the (x,y) pair is about 50 kHz, suitable for oscilloscope display, and this rate is slowed by software to allow x-y plotting at about 4-5 Hz.

The stepping motor is interfaced to the computer by means of a laboratory-fabricated logic circuit. The motor may be driven, in either direction, at rates up to 1000 steps s^{-1} under software control.

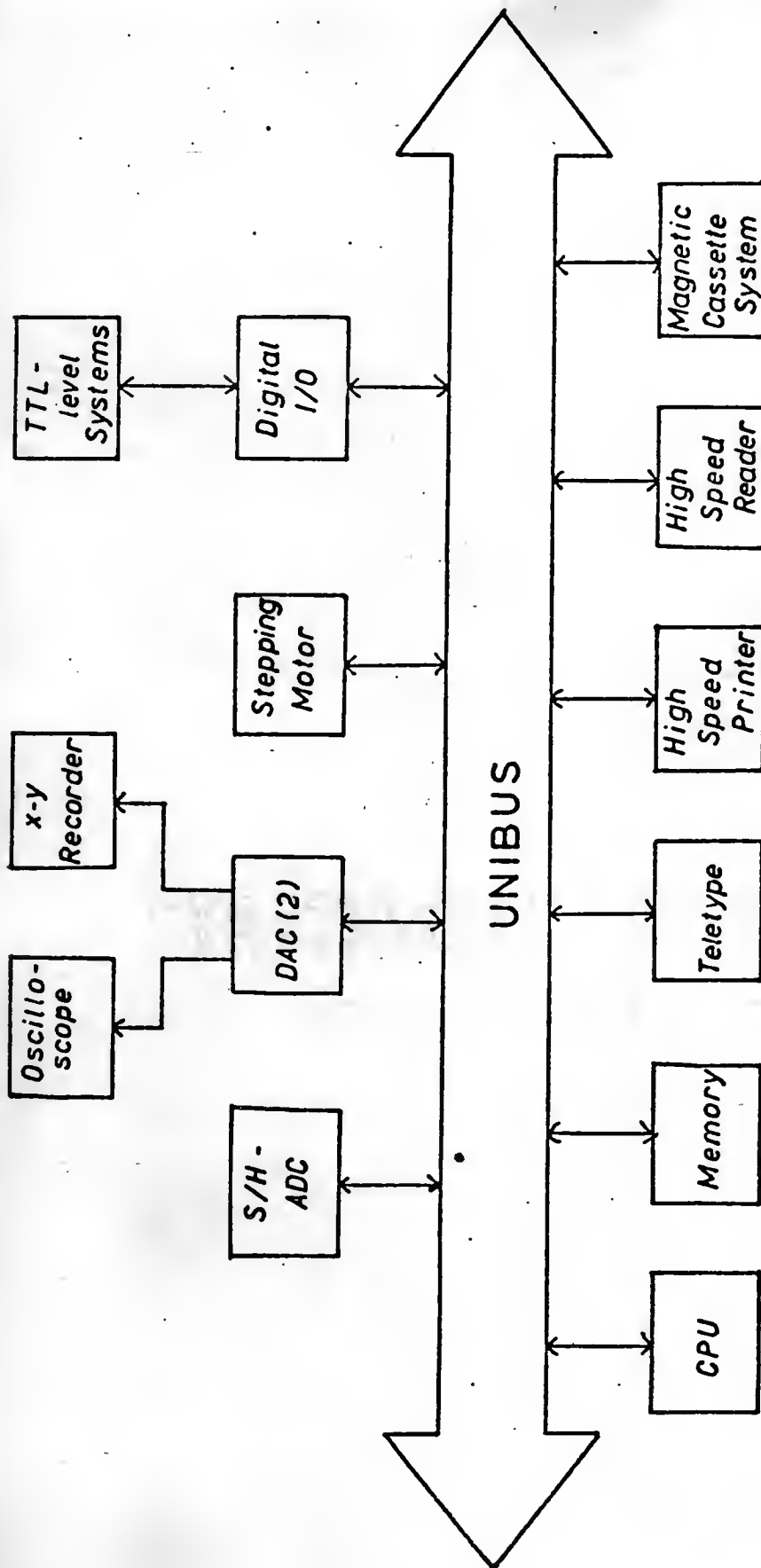


Figure 31.-- Block diagram of the computer system used in this study.

The digital I/O section is composed of a prewired kit supplied by DEC, which allowed 64 bits of data to be input to the computer and 64 bits of control functions or digital data to be output from the computer. Four addresses are available for 16 bit words of data input and four more can be used to control TTL level control functions in instrumentation designed for this type of control. 16 bits of output are used to drive a 4 digit panel meter under software control.

Each of these peripherals can be programmed under interrupt control, whereby the computer continues with the program while waiting for the device to signal that it is ready for some I/O action. Otherwise, the software can specify a 'hand-shaking' control where the computer loops in a wait cycle until the external device signals. The former is a more efficient type of control but is also more difficult to program. In actual use, a mixture of these two types of control is usually used.

The computer system described here has proved to be a versatile, rapid and conveniently programmed instrumentation device. Analog and digital input and output coupled with control and display functions allow control of and data acquisition from a variety of analytical laboratory instruments.

LITERATURE CITED

1. E.E. Pickett and S.R. Koirtyohann, Anal. Chem., 41, (14), 28A (1969).
2. L.L. Lewis, Anal. Chem., 40, (12), 28A (1968).
3. J.D. Winefordner and R.C. Elser, Anal. Chem., 23, (4), 24A (1971).
4. J.D. Winefordner, V. Svoboda and L.J. Cline, CRC Crit. Rev. Anal. Chem., 1, 233 (1970).
5. R. Mavrodineanu, "Analytical Flame Spectroscopy," Macmillan and Co. Ltd., London, 1970.
6. R. Hermann and C.T.J. Alkemade, "Chemistry Analysis by Flame Photometry," P.T. Gilbert, translator, John Wiley and Sons, Inc., New York, 1963.
7. K.W. Busch and G.H. Morrison, Anal. Chem., 45, 712A (1973).
8. J.D. Norris and T.S. West, Anal. Chem., 45, 226 (1973).
9. D.O. Cooke, R.M. Dagnall, H.N. Johnson, G.F. Kirkbright and T.S. West, Lab. Pract., 21, 171 (1972).
10. J.B. Dawson, J.D. Ellis and R. Milner, Spectrochim. Acta, 23B, 695 (1968).
11. J.L. Dye and L.H. Feldman, Rev. Sci. Instrum., 37, 154 (1966).
12. R.K. Brehm and V.A. Fassel, J. Opt. Soc. Amer., 43, 886 (1953).
13. L.R.P. Butler and A. Strasheim, Spectrochim. Acta, 21, 1207 (1965).
14. D.G. Mitchell and A. Johansson, Spectrochim. Acta, 25B, 175 (1970).
15. A. Walsh, Pure Appl. Chem., 23, 1 (1970).
16. V. Haish, K. Laqua and W.D. Hagenah, Spectrochim. Acta, 26B, 651 (1971).
17. W. Snelleman, T.C. Rains, K.W. Yee, H.D. Cook and O. Menis, Anal. Chem., 42, 394 (1970).

18. D.W. Golightly, R.N. Kniseley and V.A. Fassel, Spectrochim. Acta, 25B, 451 (1970).
19. I. Balslev, Phys. Rev., 143, 636 (1966).
20. M. Margoshes, Spectrochim. Acta, 25B, 113 (1970).
21. M. Margoshes, Paper at the Pittsburgh Conference on Analytical Chemistry and Applied Spectroscopy, 1970.
22. P.W.J.M. Boumans and G. Brouwer, Spectrochim. Acta, 27B, 247, (1972).
23. P.W.J.M. Boumans, R.F. Rumphorst, L. Willemsen and F.J. De Boer, Spectrochim. Acta, 28B, 227 (1973).
24. G. Horlick and E.G. Coddling, Anal. Chem., 45, 1491 (1973).
25. K.W. Jackson, K.M. Aldous and D.G. Mitchell, Spectrosc. Letters, 6, 315 (1973).
26. D.O. Knapp, N. Omenetto, L.P. Hunt and F.W. Plankey, Anal. Chim. Acta, 69, 455 (1974).
27. R.E. Santini, M.J. Milano and H.L. Pardue, Anal. Chem., 45, 915A (1973).
28. R.K. Winge, V.A. Fassel, R.N. Kniseley and W.L. Sutherland, Paper No. 433 at Pittsburgh Conference on Analytical Chemistry and Applied Spectroscopy, 1974.
29. P.R. Griffiths, Anal. Chem., 7, 645A (1974).
30. M.D. Low, J. Chem. Ed., 47, A163 (1970).
31. M.D. Low, J. Chem. Ed., 47, A255 (1970).
32. M.D. Low, J. Chem. Ed., 47, A349 (1970).
33. M.D. Low, J. Chem. Ed., 47, A415 (1970).
34. Unpublished work in the University of Florida chemistry laboratory, 1973.
35. R.N. Ibbett, D. Aspinall and J.R. Grainger, Appl. Opt., 7, 1089 (1968).
36. J.A. Decker and M.O. Harwit, Appl. Opt., 7, 2205 (1968).
37. E.D. Nelson and M.L. Fredman, J. Opt. Soc. Amer., 60, 1665 (1970).
38. P. Fellgett, J. Phys. Radium, 19, 187 (1958).
39. L. Mertz, "Transformations in Optics," John Wiley and Sons, Inc., New York, 1965, pp. 7-13.

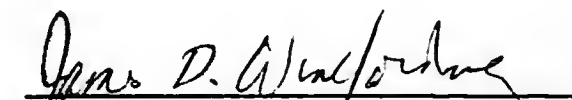
40. N. Omenetto and G. Rossi, Anal. Chem., 40, 195 (1968).
41. N. Omenetto and G. Rossi, Spectrochim. Acta, 24B, 95 (1969).
42. N. Omenetto and G. Rossi, Anal. Chim. Acta, 40, 195 (1968).
43. R. Smith, R.C. Elser and J.D. Winefordner, Anal. Chim. Acta, 48, 35 (1969).
44. R.F. Browner and J.D. Winefordner, Spectrochim. Acta, 28B, 263 (1973).
45. R.M. Dagnall, G.F. Kirkbright, T.S. West and R. Wood, Anal. Chem., 42, 1029 (1970).
46. L.M. Fraser and J.D. Winefordner, Anal. Chem., 44, 1444 (1972).
47. Unpublished work in the University of Florida chemistry laboratory, 1973.
48. G.B. Marshall and T.S. West, Anal. Chim. Acta, 51, 179 (1970).
49. B.M. Patel, R.F. Browner and J.D. Winefordner, Anal. Chem., 44, 2272 (1972).
50. C. Veillon, J.M. Mansfield, M.L. Parsons and J.D. Winefordner, Anal. Chem., 38, 204 (1966).
51. D.W. Ellis and D.R. Demers, Anal. Chem., 38, 1943 (1966).
52. R.M. Dagnall, K.C. Thompson and T.S. West, Anal. Chim. Acta, 36, 269 (1966).
53. M.P. Bratzel, R.M. Dagnall and J.D. Winefordner, Anal. Chim. Acta, 52, 157 (1970).
54. T.C. Rains, M.S. Epstein and O. Menis, Anal. Chem., 46, 207 (1974).
55. K.M. Aldous, R.F. Browner, R.M. Dagnall and T.S. West, Anal. Chem., 42, 939 (1970).
56. J.A. Decker, Anal. Chem., 44, 127A (1972).
57. J.W. Cooley and J.W. Tukey, Math. Comput., 19, 297 (1965).
58. R.W.B. Pearse, A.G. Gaydon, "The Identification of Molecular Spectra," 3rd Edition, Chapman & Hall Ltd., London, 1965.
59. P.J. Th. Zeegers and J.D. Winefordner, Spectrochim. Acta, 26B, 181 (1971).

BIOGRAPHICAL SKETCH


Francis William Plankey, Jr., was born in Malden, Massachusetts on February 28, 1945. He attended schools in Lynnfield, Massachusetts and graduated from high school there in June 1962. He attended Tufts University in Medford, Massachusetts before entering the United States Army in 1965. After his honorable discharge from the service, he resumed his studies at the University of Massachusetts at Amherst. In 1971, he graduated magna cum laude with a Bachelor of Science degree in chemistry and that same year, he started graduate study at the University of Florida.

He is married to the former Mary Barbara Martin of Birmingham, Michigan, and is the father of two boys, Michael and Timothy.

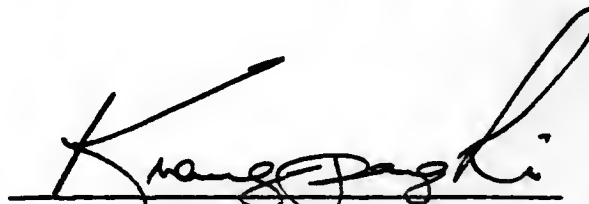
I certify that I have read this study and that in my opinion it conforms to acceptable standards of scholarly presentation and is fully adequate, in scope and quality, as a dissertation for the degree of Doctor of Philosophy.


James D. Winefordner, Chairman
Professor of Chemistry

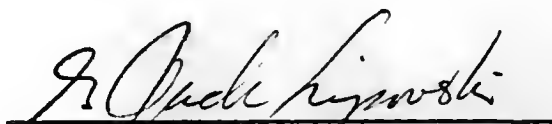
I certify that I have read this study and that in my opinion it conforms to acceptable standards of scholarly presentation and is fully adequate, in scope and quality, as a dissertation for the degree of Doctor of Philosophy.


Roger G. Bates
Professor of Chemistry

I certify that I have read this study and that in my opinion it conforms to acceptable standards of scholarly presentation and is fully adequate, in scope and quality, as a dissertation for the degree of Doctor of Philosophy.


Kuang Pang Li
Assistant Professor of Chemistry

I certify that I have read this study and that in my opinion it conforms to acceptable standards of scholarly presentation and is fully adequate, in scope and quality, as a dissertation for the degree of Doctor of Philosophy.

A handwritten signature in cursive script, reading "G. Jack Lipovski", written over a horizontal line.

G. Jack Lipovski
Associate Professor of Electrical
Engineering

This dissertation was submitted to the Graduate Faculty of the Department of Chemistry in the College of Arts and Sciences and to the Graduate Council, and was accepted as partial fulfillment of the requirements for the degree of Doctor of Philosophy.

August, 1974

Dean, Graduate School

